

Investigating Manganese Oxidation by *Aurantimonas manganoxydans* SI85-9A1

By

Nicholas Caputo

B.S. in Chemistry, Colorado School of Mines

A THESIS

Presented to the Institute of Environmental Health,
Division of Environmental and Biomolecular Systems

and the Oregon Health & Science University

School of Medicine

in partial fulfillment of

the requirements for the degree of

Master of Science

June 2011

Division of Environmental & Biomolecular Systems

School of Medicine

Oregon Health & Science University

Certificate of Approval

This is certify that the Master's thesis of

Nicholas Caputo

has been approved

Dr. Bradley Tebo
Thesis Research Advisor
Professor, OHSU

Dr. James W. Whittaker
Thesis Committee Chair
Professor, OHSU

Dr. Arthur Glasfeld
Department of Chemistry
Professor, Reed College

Table of Contents

Certificate of Approval.....	ii
Table of Contents.....	iii
List of Tables	v
List of Figures	i
List of Equations.....	ii
Acknowledgments.....	iii
Abstract.....	v
Chapter 1: Introduction of the Biogeochemistry of Manganese.....	1
Importance of manganese in the environment.....	1
Mn(II) oxidation by microorganisms.....	3
Purpose of this thesis	7
Chapter 2: Characterization of Mn(II) oxidizing Peroxidase A	9
Introduction.....	9
Methods and Materials.....	11
Results and Discussion	18
Summary	36
Chapter 3: Development of a genetic system for <i>A. manganoxydans</i> SI85-9A1	38
Introduction.....	38
Methods and Materials.....	40
Results and Discussion	48
Summary	61
Chapter 4: The Mechanism of Mn(II) oxidation <i>in vivo</i> and <i>in vitro</i>	63
Introduction.....	63
Methods and Materials.....	68
Results and Discussion	72
Summary	80
Chapter 5: Summary and Future Directions.....	83
References	86
Appendix A: Expression of Mn(II) oxidizing Proteins.....	93
Introduction.....	93
Methods and Materials.....	93
Results and Discussion	100
Summary	103
Appendix B: Tandem MS Data.....	105

Introduction.....	105
Results.....	105
Biographical Sketch.....	120

List of Tables

Table 1: Complexity of proteins in each stage of purification.....	21
Table 2: Top four proteins by most assigned spectra per group	23
Table 3: Purification table for MopA purification	24
Table 4: Amino Acid composition of Type 1 secretion signal	29
Table 5: Gram negative bacteria with RTX peroxidases	32
Table 6: Strains, plasmids, and primers used in Chapter 3.....	41
Table 7: PCR reaction conditions.....	47
Table 8: Antibiotic MIC for <i>A. manganoxydans</i> SI85-9A1	49
Table 9: Properties of proteins found near MopA and other accessory proteins	58
Table 10: Qualitative Mn(II) oxidation and cell density of EMS mutants	60
Table 11: Strains, plasmids and primers used in Appendix A	94
Table 12: PCR conditions used in Appendix A	96
Table 13: Variables tested for elution of Mop from chitin resin.....	102
Table 14: Proteins identified after each stage of purification	106
Table 15: Peptide sequences top five identified proteins from LBOM protein matrix ...	108
Table 16: Peptide sequences top five identified proteins after IEX purification stage ...	111
Table 17: Peptide sequences top five identified proteins after HIC purification stage ...	114
Table 18: Peptide sequences top five identified proteins after SEC purification stage...	116

List of Figures

Figure 1: SDS-PAGE gel of MopA purification showing enrichment of protein bands...	19
Figure 2: Localization of proteins identified using MS/MS	21
Figure 3: Mn(II) oxidation inhibition by cyanide	26
Figure 4: Native PAGE activity correlation gel.....	27
Figure 5: MopA predicted 3 ^o structure based on 1 ^o sequence	28
Figure 6: Growth of <i>A. manganoxydans</i> SI85-9A1 in M and K-media.....	50
Figure 7: Restreak plate of pJH1 conjugants and contaminant.....	53
Figure 8: Plasmid DNA isolated from the six conjugants	55
Figure 9: PCR screen to prove the identity of conjugants.	55
Figure 10: Putative 'Moperon'	56
Figure 11: <i>In vitro</i> Mn(II→IV) oxidation disruption.....	73
Figure 12: <i>In vitro</i> Mn(II→III) oxidation disruption.....	74
Figure 13: <i>In vitro</i> Mn(III→IV) oxidation disruption	75
Figure 14: <i>In vitro</i> Mn(III→IV) oxidation disruption; 10x [Cat] over Figure 13	76
Figure 15: <i>In vitro</i> Mn(II→IV) oxidation disruption.....	77
Figure 16: Time course of Mn(II) oxidation <i>in vivo</i>	78
Figure 17: Effect of xanthine concentration on <i>in vivo</i> Mn(II) oxidation	80
Figure 18: Purification of MoxA using immobilized metal affinity chromatography	101
Figure 19: Western blot of purified MoxA	102

List of Equations

Equation 1: Overall Mn(II→IV) oxidation	2
Equation 2: Mechanism catalyzed by peroxidases.....	7
Equation 3: Sequential one electron reductions forming reactive oxygen species	65
Equation 4: Reaction catalyzed by superoxide dismutases.....	65
Equation 5: Reaction catalyzed by catalases.....	66
Equation 6: Possible Mn(II→III) oxidation	66
Equation 7: Possible reaction catalyzed by MopA for Mn(III→IV) oxidation <i>in vitro</i>	81
Equation 8: Possible Mn(II→IV) oxidation.....	82

Acknowledgments

First, I would like to thank Dr. Brad Tebo for his support for my graduate studies. He gave me the financial backing and scientific freedom to pursue my own path and figure out new problems as they presented themselves. He has taught me how to look at the world objectively and learn from everything I see so I can make it better through research and action.

I would also like to acknowledge Dr. Craig Anderson for his initial help and mentorship when I first entered the lab of Dr. Tebo. Through his guidance, I got my start on this project and learned what the main problems were in this research. Dr. Kati Geszvain has also helped me with analysis of data, guided some of my research, and provided critical reviews.

Additionally I would like to give my thanks to Drs. Jim and Mei Whittaker. I got my start at OHSU with them and they were instrumental in helping me learn the scientific method and key skills that allowed me to perform my work with an eye for detail. Under their eye, I started to figure out what I wanted out of my education and how I could go and get it.

I would also like to thank everyone else associated with the Tebo/Haygood lab and OHSU, especially Nancy Christie, Carolyn Sheehan and Mari Garcia. Nancy has always helped me with anything I needed and made sure I was well taken care of. Carolyn helped me with everything I needed to keep my research moving forward and routinely dropped her own work to aid me. Mari has been extremely helpful setting things up in lab so I could move swiftly and immediately on my work. Everyone else in the lab

has been extremely helpful in helping me think about my research and trying to fit it all together. Without their help, I do not think I would have been able to get through this.

Finally, I would like to thank my friends and family for their support during my time at OHSU. My mother, father, and sister have helped me stay strong through the hard times and asked me key questions when needed. They have always encouraged me to work hard at everything I have done and are one of the main reasons I chose to go to graduate school. With their help, I was able to keep my head on straight and work hard for this degree. My community of friends in Portland has also been helpful in giving me an outlet from school and keeping me straight headed in the good times and the bad.

This research was made possible by grant number P42ES010337 from the National Institute of Environmental Health Sciences (NIEHS) and the Oregon Opportunity fund. Mass spectrometry data was generated by the Oregon Health and Science University Proteomics Shared Resource (OHSU-PSR) funded by the Oregon Opportunity Fund and National Institute of Health (NIH) center grants 5P30CA069533 and 5P30EY010572.

Abstract

Investigating Manganese oxidation by *Aurantimonas manganoxydans* SI85-9A1

Nicholas Caputo, B.S.

Master of Science

Institute of Environmental Health, Division of Environmental and Biomolecular Systems

Oregon Health & Science University

School of Medicine

June 2011

Thesis Advisor: Bradley Tebo

Since manganese is the second most abundant redox active transition metal after iron in the crust of the Earth, it has a large significance in terms of biogeochemical cycling. The bacteria that oxidize manganese are ubiquitous in many ecosystems, but the cellular function of oxidation is currently unknown. The enzymes within the bacteria that perform this chemistry have also been elusive in their identification. A new class of Mn(II) oxidizing peroxidase (MopA) has been discovered in *Aurantimonas manganoxydans* SI85-9A1, the first such peroxidases found in bacteria. Chemical assays of the loosely bound outer membrane proteins of *A. manganoxydans* SI85-9A1 suggest a

heme peroxidase is involved with Mn(II) oxidation, although its exact role is not known. Functional assays and structural predictions provide some interesting insights into its possible use in Mn(II) oxidation as related to similar proteins. Through tri-parental mating with an *E. coli* donor, it was possible to incorporate the plasmid pJH1 into *A. manganoxydans* SI85-9A1. This is the first step in development of a genetic system and is the first instance of *A. manganoxydans* SI85-9A1 being able to stably incorporate plasmids of any kind. The use of superoxide dismutase and catalase in mechanistic studies reveals that superoxide is involved in Mn(II→III) oxidation and hydrogen peroxide is involved in Mn(III→IV) oxidation. These results all hint at the involvement of various forms of oxygen in the oxidation of manganese and point to a complex of proteins being responsible for overall Mn(II) oxidation.

Chapter 1: Introduction of the Biogeochemistry of Manganese

Importance of manganese in the environment

Manganese is one of the more important transition metals found in the environment. In terms of redox active transition metals, manganese is second only to iron in abundance in the Earth's crust (Sigel and Sigel, 1999). Thus, it is relatively ubiquitous and plays key roles in biogeochemical cycling of many toxic metals such as lead, cadmium, mercury, arsenic, cobalt, zinc, plutonium, and uranium; as well as recalcitrant organic molecules such as humic acid and lignin (Tebo et al., 2004). In nature, manganese is found in one of three oxidation states: Mn(II), Mn(III), or Mn(IV). Mn(II) is an aqueous species that participates in many biogeochemical processes and has been found as high as millimolar concentrations (Tebo et al., 2005). It is oxidized in biogeochemical processes and is an essential nutrient for all life, being incorporated into enzymes such as superoxide dismutase, type II catalase, and the oxygen evolving photosystem complex II of photosynthetic organisms (Sigel and Sigel, 1999).

Mn(IV) is found as insoluble oxides that appear black to brown in color. Aside from oxygen, Mn(IV) oxides are the strongest oxidants in the environment. They are also strong sorbants, which, along with their oxidative capabilities, leads to their strong role in biogeochemical cycling. They are able to react with many kinds of heavy metals, sometimes oxidizing them to insoluble forms that are then removed from the aqueous system. In addition to redox processes, Mn(IV) oxides are able to sorb metals and transport them out of solution or into other redox gradients where the toxic metals can be transformed through additional redox processes (Tebo et al., 2005). The equilibrium between Mn(II) and Mn(IV) depends upon the conditions of the system. Under oxidizing conditions (high Eh/pH), Mn(IV) is favored; under reducing conditions (low Eh/pH) Mn(II) is favored. At biologically relevant conditions, Mn(II→IV) oxidation is an exergonic reaction, thus it is favored to happen under conditions favorable for life and may be a possible energy source (Tebo et al., 2004). Equation 1 depicts the aerobic oxidation of Mn(II) to form Mn(IV).

Equation 1: Overall Mn(II→IV) oxidation



The third, although highly unstable, oxidation state of manganese is Mn(III). Upon formation, the Mn(III) ion will spontaneously disproportionate to Mn(II) and Mn(IV). It can be stabilized with inorganic ligands such as pyrophosphate (Tebo et al., 2007; Madison et al., 2011) or organic ligands such as bacterial siderophores (Duckworth and Sposito, 2005). Mn(III) is a strong oxidant that will react with most things it meets. In spite of this instability, Mn(III) is readily incorporated into Mn oxides, forming Mn(III,IV) oxides. These Mn(III,IV) oxides (from now on collectively referred to as Mn

Oxides) are found in such environments as basalt glasses on the sea floor, hydrothermal vents, midocean ridge spreading centers, ferromanganese nodules, redox interfaces, desert varnishes, river/stream sediments, and water pipes (Tebo et al., 2005).

Mn(II) oxidation by microorganisms

Mn(II) oxidizing organisms are widespread, although the function of Mn(II) oxidation in the cell is unknown. These organisms are mainly bacteria and fungi, catalyzing the rate of Mn oxide formation at circumneutral pH by 4-5 orders of magnitude (Nealson et al., 1988). It is thought that bacteria could utilize Mn(II) oxidation to allow them to live a chemolithoautotrophic lifestyle. Mn oxides may also serve as a method of protection through its oxidative power or serve as an electron sink for times when no others are available. Various Mn(II) oxidizing enzymes have been found that perform the oxidation chemistry within the cell. These proteins have been found to be multicopper oxidases (MCOs) in bacteria (Tebo et al., 2005) and peroxidases in fungi, although MCOs may also be important in fungi as well (Schlosser and Hofer, 2002). Several of the more well characterized Mn(II) oxidizing organisms and proteins are detailed below.

***Aurantimonas manganoxydans* SI85-9A1**

The marine Mn(II) oxidizing α -proteobacterium *A. manganoxydans* SI85-9A1 is a Gram-negative rod. It was isolated at the oxic/anoxic interface of Saanich Inlet off the coast of Victoria, British Columbia at a depth of 120 m. PCR screening has shown the presence of ribulose-1,5-bisphosphate carboxylase/oxygenase (RuBisCO) within the genome, meaning that *A. manganoxydans* SI85-9A1 may be able to oxidize Mn(II) autotrophically. However, *A. manganoxydans* SI85-9A1 has never been successfully

grown autotrophically, even though the RuBisCO gene was active when cloned into *E. coli* (Caspi et al., 1996). The genome sequence reveals that *A. manganoxydans* SI85-9A1 contains genes necessary for normal respiratory metabolism. In addition, *A. manganoxydans* SI85-9A1 has the potential to utilize a variety of substrates as electron donors including C₁ and inorganic S-compounds, and carbon dioxide. The role of Mn(II) oxidation may drive this organisms metabolism by supporting a chemolithoautotrophic lifestyle wherein *A. manganoxydans* SI85-9A1 gains electrons as energy to power the cell (Dick, Podell, et al., 2008). Initial work by Caspi (1996) on developing a genetic system in *A. manganoxydans* SI85-9A1 focused on determining antibiotic minimum inhibitory concentrations (MICs) for growth on solid media, optimization of electroporation conditions, and conjugation to introduce plasmids into the cell. These attempts at introducing plasmids failed, but yielded information useful in beginning the current study. In a non-genetic study, manganese oxidizing peroxidase A (MopA) was identified using mass spectrometry from the loosely bound outer membrane proteins (LBOM) of *A. manganoxydans* SI85-9A1. This protein is a calcium binding heme peroxidase that is able to use oxygen to oxidize Mn(II) (Anderson, Johnson, et al., 2009). This thesis continues from where that paper left off.

***Pseudomonas* species**

Pseudomonas species are Gram-negative rods of γ -proteobacterial origin. In *Pseudomonas* MnB1 (now *P. putida* GB-1) the Mn(II) oxidase was localized to the intracellular matrix, found to be expressed during stationary growth, and expression of the Mn(II) oxidase was not dependent upon the concentration of Mn(II) (Jung and Schweisfurth, 1979). The Mn(II) oxidase from *P. fluorescens* GB-1 (now *P. putida* GB-

1) was partially purified through biochemical chromatography. It was isolated from whole cell soluble protein extracts, purified by multi-stage chromatography, and characterized by *in vitro* assays, although the proteins responsible for Mn(II) oxidation were not identified (Okazaki et al., 1997). Additionally, in *P. putida* GB-1, mutagenesis showed that an MCO termed CumA may be involved in Mn(II) oxidation and *P. putida* GB-1 also showed increased oxidation upon addition of Cu²⁺ (Brouwers et al., 1999). CumA was later shown not to be required for Mn(II) oxidation and the true cause was traced to a mutation in a two component regulatory system (Geszvain and Tebo, 2009) with an MCO different than CumA involved in Mn(II) oxidation. Further transposon insertion mutagenesis studies identified other metabolic genes associated with Mn(II) oxidation. These include genes involved with biogenesis of *c*-type cytochromes, tricarboxylic acid (TCA) cycle components, and tryptophan biosynthesis. Complementation of mutants defective in cytochrome *c* biogenesis resulted in restored Mn(II) oxidation (Caspi et al., 1998). Additional genetic studies have linked the type II related general secretory pathway (Gsp) protein secretion system to Mn(II) oxidation as the secretion pathway for the Mn(II) oxidase (De Vrind et al., 2003). Finally, flagellar synthesis regulation genes and structural genes have been linked to Mn(II) oxidation, showing perhaps flagella synthesis and Mn(II) oxidation are regulated by a similar response (Geszvain et al., 2011).

***Bacillus* SG-1**

The Mn(II) oxidase from *Bacillus* strain SG-1 has been directly identified as an MCO named MnxG. *Bacillus* strain SG-1 was shown by transposon insertion mutagenesis to have a putative operon (*mnxA* to *mnxG*) required for Mn(II) oxidation,

with the gene *mnxG* encoding an MCO predicted to be the Mn(II) oxidase (van Waasbergen et al., 1996). *Bacillus* will only perform Mn(II) oxidation when in the spore state and the Mn(II) oxidase activity was localized to the exosporium (Dick, Torpey, et al., 2008). A multi-stage purification strategy was applied, and the Mn(II) oxidase identified from a Mn(II) oxidizing band from an in gel Mn(II) oxidation activity assay (Dick, Torpey, et al., 2008). There is indication that it is part of a complex of proteins involved in Mn(II) oxidation because another protein from the *mnx* operon, MnxF, was found in the band as well (Dick, Torpey, et al., 2008).

Fungi

The first Mn(II) oxidase was found in a lignin degrading white rot basidiomycete, *Phanerochaete chrysosporium*. The protein was identified as a heme containing Mn(II) oxidizing peroxidase (MnP) and it has been extensively characterized through activity measurements and crystal structures (Sundaramoorthy et al., 2010). MnPs couple the oxidation of two Mn(II) to two Mn(III) with the concomitant reduction of one molecule of hydrogen peroxide (Sundaramoorthy et al., 2005). The Mn(III) produced by this reaction is chelated by organic acids and diffuses from the cell to interact with lignin, breaking them down for cell metabolism (Perez and Jeffries, 1992). MnPs also bind Ca^{2+} that helps stabilize the heme pocket (Sutherland et al., 1997).

Heme peroxidases are single heme containing proteins that catalyze the heterolytic reduction of hydrogen peroxide to water, in three sequential steps. They usually perform this chemistry in conjunction with the oxidation of another molecule. This accessory molecule can be either organic or inorganic, depending on the

requirements of the organism. The reaction catalyzed by peroxidases can be seen in Equation 2.

Equation 2: Mechanism catalyzed by peroxidases
Reduced: reduced reactant; oxidized: oxidized product



Mn(II) oxidizing peroxidases have been found in fungi that catalyze the oxidation of Mn(II→III). These peroxidases work by initially reacting with hydrogen peroxide in a two electron oxidation of the iron-heme reactive site to form the oxidized intermediate compound I. Compound I reacts with one molecule of a reactant to form compound II, which then reacts with another molecule of reactant. These two one-electron transfer steps constitute the catalytic cycle of peroxidases. Mn(II) oxidizing peroxidases work in the same way, with Mn(II) as the reduced reactant and Mn(III) as the oxidized product. More detail on additional structural and functional details of MnPs will be given below and in Chapter 2.

Purpose of this thesis

Mn(II) oxidation in fungi plays an important role for the cell to access refractory organic material such as lignin and other humic substances. The benefits of Mn(II) oxidation to bacteria are less well known. The questions addressed in this thesis are primarily: What is the Mn(II) oxidase in *A. manganoxydans* SI85-9A1? What is the role of reactive oxygen species in Mn(II) oxidation in this organism? Can *A. manganoxydans* SI85-9A1 be genetically manipulated to give us clues to Mn(II) oxidases and other metabolic processes affected by Mn(II) oxidation?

Chapter 2 complements the previously published work (Anderson, Johnson, et al., 2009) identifying MopA as the putative Mn(II) oxidase. Activity assays that relate the peroxidase activity to Mn(II) oxidation will be discussed and possible structure will be analyzed through examination of its primary sequence. The details of the purification strategy will be discussed through examination of the mass spectral data.

Chapter 3 details work done towards developing a genetic system for *A. manganoxydans* SI85-9A1. Several methods of plasmid transfer into *A. manganoxydans* SI85-9A1 have been developed, forming the basis for utilizing genetic techniques to allow manipulation of this organism. These will be discussed along with what is necessary for future mutagenic studies.

Finally, Chapter 4 will describe analysis of the reaction mechanism of Mn(II) oxidation in *A. manganoxydans* SI85-9A1. Superoxide dismutase and catalase were added to both loosely bound outer membrane protein isolates and ascorbate washed whole cell *A. manganoxydans* SI85-9A1 to try to disrupt Mn(II) oxidation. These experiments were performed to determine the role of superoxide and hydrogen peroxide in the two half reactions of Mn(II) oxidation.

Chapter 2: Characterization of Mn(II) oxidizing Peroxidase A

Introduction

Mn(II) oxidases have often been identified by genetic screening of organisms by random and directed mutagenesis. The power of genetic screening cannot be denied, but an organism has to be amenable to genetic manipulation for it to work successfully. *A. manganoxydans* SI85-9A1 has proven to be difficult to manipulate genetically (Caspi, 1996), thus a different approach must be followed in order to examine the Mn(II) oxidase. Purification of the Mn(II) oxidase from *A. manganoxydans* SI85-9A1 will allow us to study the reaction mechanism in more detail and begin to understand the physiological role of Mn(II) oxidation. Biochemical chromatography is a powerful technique that allows us to separate biomolecules by exploiting various properties of the proteins of interest. When coupled with a specific activity assay, it becomes possible to do multiple stages of purification to obtain the purest possible oxidase. The use of tandem mass spectrometry (MS/MS) followed by peptide mapping back to an *in silico* digested

peptide map from *A. manganoxydans* SI85-9A1 allows identification of proteins within the matrix of fragmented peptides. Once protein identity is found, activity assays specific for that type of enzyme can correlate protein activity to Mn(II) oxidation activity and will help validate MS/MS results. Primary structure analysis can identify important domains that may give clues to protein function and provide jumping off points for future experimentation.

The primary sequence of a protein can give a wealth of information. The Mn(II) oxidase of *A. manganoxydans* SI85-9A1 has been identified as Mn(II) oxidation peroxidase A (MopA). MopA has already been described as having heme peroxidase domains, repeat-in-toxin (RTX) Ca²⁺ binding regions (Anderson, Johnson, et al., 2009), and amino acid sequence database searching suggests that it is secreted by a type 1 secretion apparatus (data not published). Mn(II) oxidizing heme peroxidases have already been described, but the heme peroxidase domains found in MopA belong to a different group of peroxidases: the animal heme peroxidase superfamily. These domains are found in prokaryotes and eukaryotes, providing protective or biosynthetic roles for the cell (Loughran et al., 2008). RTX toxins have multiple activities including formation of a protective S-layer, plant root nodulation, bacteriocidal proteins (bacteriocins), lipases causing eukaryotic membrane damage, proteases affecting eukaryotic membrane proteins, and general eukaryotic cytotoxins (pore-formation by actin cross-linking) (Linhartová et al., 2010). They range in size from 40 to >600 kDa, are all secreted via type 1 secretion (Satchell, 2007), contain between 6 and 40 Ca²⁺ binding repeats (Lally et al., 1999), and generally have an isoelectric point (pI) between 4 and 6 (Linhartová et al., 2010). The type 1 secretion signal has been found to occur in approximately the final 50-

60 amino acids of type 1 secreted proteins and is a non-cleaved signal recognized by the inner membrane associated ABC transporter and translocated to the extracellular matrix in a one-step mechanism (Delepelaire, 2004).

The purpose of this chapter is to describe the characterization of the newest class of Mn(II) oxidizing proteins, the bacterial Mn(II) oxidizing peroxidase. This protein is one of the first such Mn(II) oxidizing proteins identified in prokaryotes and has been termed MopA (Anderson, Johnson, et al., 2009). This chapter will cover identification of MopA from four stages of orthogonal chromatography and analysis of the resulting Mn(II) oxidizing proteome. Assays to correlate Mn(II) oxidation and heme peroxidase activity will also be covered, some of which were published in Anderson, Johnson, et al. (2009). Finally, the protein sequence will be analyzed in an effort to assign possible physiological function to MopA.

Methods and Materials

Growth Conditions

A. manganoxydans SI85-9A1 was grown in six 1 L batches in 2.8 L baffled Fernbach flasks at room temperature at 150-200 RPM in M-medium (Tebo et al., 2007). M-medium is a minimal nutrient medium made with autoclaved 1x artificial seawater (ASW; 100 mM MgSO₄, 20 mM CaCl₂, 600 mM NaCl, 20 mM KCl), 0.05 g L⁻¹ Bacto yeast extract and 0.05 g L⁻¹ Bacto peptone (Fisher Scientific, USA). The following are added to the above post autoclaving and are filter sterilized (0.2 μm) immediately prior to addition to the medium: 20 mM HEPES pH 7.8 (1 M initial), 2 mM KHCO₃ (1 M initial), 100 μM MnCl₂ (1 M initial), and 3 mg ml⁻¹ ferric ammonium citrate (15 mg ml⁻¹ initial). Both MnCl₂ and ferric ammonium citrate were freshly prepared prior to addition. As

carbon sources, 10 mM glycerol (5 M initial) and 10 mM sodium formate (5 M initial) were added to the base M-medium, both filter sterilized (0.2 μm) immediately prior to addition. As an inoculum, a 5 ml overnight K-medium (see Chapter 3) culture is prepared from a single Mn(II) oxidizing colony grown on an M-media plate. From this overnight culture, 100 μl , is used to inoculate each flask. For solid M-medium, 15 g L⁻¹ noble agar is used.

Protein Isolation

Mn(II) oxidation activity has been localized to the loosely bound outer membrane (LBOM) fraction (Anderson, Johnson, et al., 2009). To obtain this protein fraction, 6 L of actively oxidizing *A. manganoxydans* SI85-9A1 was collected into one pellet (approximately 4-6 g) at 8,000 rotations per minute (RPM) for 10 minutes using a Sorvall RC5-B centrifuge with a Fiberlite F10-6x500y fixed angle rotor at 4°C. Once all of the *A. manganoxydans* SI85-9A1 was collected into one pellet, it was resuspended in 100 ml of a high salt Tris buffer (100 mM Tris pH 7.5, 1 M KCl) and ascorbate was added to 200 μM in order to reduce all Mn oxides. This salt/cell solution was stirred vigorously for 4 hours at 4°C. The cells were pelleted again and the supernatant was collected and filtered to remove residual cells. The supernatant was then concentrated to a volume of 5-15 ml using a 400 ml Amicon stirred ultraconcentration cell fitted with a 10 kDa MWCO membrane (Millipore Ultrafiltration membranes, Millipore, USA). This ultraconcentrated fraction is considered the loosely bound outer membrane (LBOM) protein fraction. The LBOM fraction was dialyzed in 20 mM HEPES buffer pH 7.8 using 10 kDa MWCO dialysis membranes. Dialysis proceeded in three phases of 4 L in 20 mM 4-(2-hydroxyethyl)-1-piperazineethanesulfonic acid (HEPES) dialysis buffer as follows:

overnight at 4°C, 2 hours at room temperature, and 3 hours at room temperature; all with ~25 RPM stirring. The final, dialyzed fraction was concentrated using a 10 kDa cutoff spin column (Amicon Ultra-4 or -15) to ~1 ml and stored at 4°C until use. Protein concentration was measured using the standard Bradford Assay (Pierce, USA).

Fast Protein Liquid Chromatography

Purification of the Mn(II) oxidase was performed at 4°C using fast protein liquid chromatography (FPLC) from ÄKTA Systems (GE Life Sciences, USA), fitted with GE Healthcare chromatography columns. Purification utilized three orthogonal types of protein chromatography to isolate the Mn(II) oxidase. The dialyzed LBOM proteins were initially separated by ion exchange chromatography (IEX) using a 5 ml HiTrap Q fast flow anion exchange column with 20 mM Tris buffer pH 8.5 and an increasing 0 to 1 M NaCl linear elution gradient. The elution was fractionated into 1.6 ml fractions, with each being tested for Mn(II) oxidation activity by adding 10 µl of 1 mM MnCl₂ to 90 µl of protein fraction. This was left to incubate overnight and 100 µl Leucoberberlin Blue reagent (LBB: 0.4% w/v LBB solid, 45 mM acetic acid) was added to discern which fraction was active for Mn(II) oxidation. Active fractions were pooled and concentrated to ~1 ml using Amicon Ultra-4 or -15 spin columns. The second stage of purification consisted of hydrophobic interaction chromatography (HIC) using a 5 ml HiTrap phenyl high performance (HP) column. To prepare the sample for purification, 3 M NH₄SO₄ was added to the active fraction until a concentration of 1.7 M NH₄SO₄ was reached. The buffer was 20 mM HEPES pH 7.8 and a decreasing linear elution gradient was used (1.7 to 0 M NH₄SO₄). After another round of testing for activity, pooling the fractions, and concentration the proteins were subjected to a final purification of size exclusion

chromatography (SEC). The proteins were separated using a 120 ml HiPrep 16/60 Sephacryl S-200 high-resolution column with 20 mM HEPES pH 7.8 and 150 mM NaCl. The final fractions were again tested for activity, active fractions pooled, and concentrated. Samples from all steps were saved and stored at 4°C for further analysis.

Polyacrylamide Gel Electrophoresis

Reducing Conditions

The standard Laemmli buffer system (Laemmli, 1970) was used for sodium dodecyl sulfate polyacrylamide gel electrophoresis (SDS-PAGE). SDS-PAGE was performed in a BioRad Mini Protean Electrophoresis Cell using boiling to denature proteins (98°C for 10 minutes) and dithiothreitol (DTT) as a reducing agent. Standard recipes based on the Laemmli conditions were followed for the running buffer, sample buffer, and gel formulations (BioRad Mini-PROTEAN 3 instruction booklet), and precast gels were used as well (Mini-PROTEAN precast gels Tris-Tricine 4-20%). Gels were run with a molecular weight marker (2-5 µl; PageRuler Plus, Fermentas, US) for 200 V gel⁻¹ (handmade) or 20 mA gel⁻¹ (precast) until the dye front reached the bottom of the gel (50-70 minutes, depending upon the gel). These were then stained using Coomassie blue staining (Imperial Protein Stain, Pierce, US) or silver stained (Silver Snap II kit, Pierce, US). Imaging was performed by scanning the gels using a standard computer scanner (Canon CanoScan LiDE 500F).

Native Conditions

Native gels were prepared according to published instructions (BioRad Miniprotean 3 instruction booklet), and neither SDS, boiling, nor DTT were used in preparation. These gels were stained using a Mn(II) activity assay, a heme peroxidase

activity assay (both assays described below), or silver stained (SilverSnap II kit, Pierce, US).

Protein Activity Assays

Mn(II) oxidation assay

The *in vitro* Mn(II) oxidation activity assay tests for the presence of a Mn(II) oxidase in a mixture of proteins (Tebo et al., 2007). It has the ability to be scaled to various volumes and for the standard *in vitro* assay, 100 $\mu\text{g ml}^{-1}$ protein mixture was used in 20 mM HEPES pH 7.8. Mn(II) was added to 100 μM and water to bring mix to desired volume. Mn(II) oxidation assays proceeded overnight at which point LBB was mixed with the assay sample in a 1:5 (sample:LBB) volume ratio. This was allowed to react in the dark for 10-15 minutes, and read in a spectrophotometer at 618 nm.

Cyanide inhibition assay

A normal *in vitro* Mn(II) oxidation assay was performed with potassium cyanide added from 1 μM to 10 mM. These were performed in 50 mM HEPES pH 7.8 and precautions were taken to minimize potential cyanide exposure due to acidification of the assay from LBB (i.e lab coat, goggles, and the assay was performed in a fume hood).

Heme peroxidase assay

Native PAGE was performed as described previously. Staining was performed according to previously published protocols (Thomas et al., 1976; Hagan and Mobley, 2009). Immediately prior to use, a 6.3 mM (15 mg ml^{-1}) solution of 3,3',5,5'-tetramethylbenzidine (TMBZ; Fisher, USA) was prepared in methanol and cooled to 4°C once the TMBZ was fully dissolved. This was mixed with prechilled 250 mM sodium acetate (NaAc; pH 5.0) at a ratio of 3 parts TMBZ solution to 7 parts NaAc buffer. After

a brief wash with water, the gel was allowed to equilibrate in the 3:7 solution for 1.5 hours at 4°C and covered from light. Hydrogen peroxide was then added to a final concentration of 30 mM, and the bands were allowed to develop for 30 minutes (light-blue bands were seen almost immediately after the addition of hydrogen peroxide). The gel was imaged without further clarification of the background. The bands were related to native PAGE silver-stained activity gels as described above.

Protein Tandem Mass Spectrometry and peptide data analysis

Tandem mass spectrometry (MS/MS) was used to probe the Mn(II) oxidizing fractions from the purification. Protein concentration was determined using the Bradford Assay (Pierce, US) and ~10 µg of protein was dried in a Speedvac (Savant). The samples were then digested and analyzed at the OHSU Proteomics Shared Resource (PSR). To each dried sample, 10 µl digestion buffer (8 M urea, 1 M Tris pH 8.5, 8 mM CaCl₂, 0.2 M methylamine) was added and vortexed to mix. To this solution, 1 µl of 0.2 M dithiothreitol (DTT) was added and the entire mix was incubated at 50°C for 15 minutes. After the sample was allowed to cool, 1 µl of 0.5 M iodoacetamide (IAA) was added, the solution was vortexed, then incubated in the dark at room temperature for 15 minutes. An additional 2 µl of DTT was added followed by vortexing and incubation at room temperature for 15 minutes. Enough trypsin was then added to ensure a 1:25 enzyme-to-substrate ratio in the solution along with water to achieve a final volume of 40 µl. This entire solution was incubated overnight at 37°C. The digestion was stopped the next morning by addition of 88% formic acid. Samples were either run immediately or frozen at -20°C until analysis. A Thermo Finnegan linear trap quadrupole (LTQ) LC-MS/MS instrument was used for analysis.

Tandem mass spectra were extracted by Mascot (Matrix Science, London, United Kingdom). All MS/MS samples were analyzed using Sequest (ThermoFinnigan, San Jose, CA; version 27, rev. 12). Sequest was set up to search NCBI assuming the digestion enzyme non-specific. Sequest was searched with a fragment ion mass tolerance of 1.00 Da and a parent ion tolerance of 2.5 Da. Iodoacetamide derivative of cysteine was specified in Sequest as a fixed modification. Oxidation of methionine was specified in Sequest as a variable modification.

Scaffold (version Scaffold_3.0.9.1, Proteome Software Inc., Portland, OR) was used to validate MS/MS based peptide and protein identifications. Peptide identifications were accepted if they could be established at greater than 80.0% probability as specified by the Peptide Prophet algorithm (Keller et al., 2002). Protein identifications were accepted if they could be established at greater than 99.0% probability and contained at least 3 identified peptides. Protein probabilities were assigned by the Protein Prophet algorithm (Nesvizhskii et al., 2007). Proteins that contained similar peptides and could not be differentiated based on MS/MS analysis alone were grouped to satisfy the principles of parsimony.

Bioinformatics

Protein data access for use with large numbers of proteins was performed through the Protein Information Resource (PIR; <http://pir.georgetown.edu/iproclass/>) batch retrieval interface. Protein localization was performed using data retrieved from the PIR and analyzed using PSORTb v3.0 (<http://www.psort.org/>). Manual curation of the data was performed to associate the localization determined by PSORTb to the protein list

retrieved from Scaffold. PROSITE (<http://expasy.org/prosite/>) was used to examine the domains of the protein by examination of the primary sequence.

Results and Discussion

Purification of MopA

This study is a continuation of previous work showing that MopA is present in the loosely bound outer membrane (LBOM) proteins, as found through the use of a high salt wash of Mn oxide free cells that interrupts peripheral membrane protein interactions with the cell wall. MopA was also identified as the major protein component of a purified fraction in tandem MS experiments (Anderson, Johnson, et al., 2009). MopA is a heme-containing peroxidase with two functional peroxidase domains and multiple Ca²⁺ binding regions. The isolation and purification of MopA was repeated, this time with the goal of collecting samples at each step of purification and subjecting them to tandem MS, activity assays, and SDS-PAGE to look for purity. In this way, a putative Mn(II) oxidation proteome could be identified from the LBOM of *A. manganoxydans* SI85-9A1. Approximately 10 µg of protein was saved from each fraction for analysis by tandem mass spectrometry. The goal was to see how the protein profile changes through purification and to examine which proteins persist through the purification stages while other proteins are discarded. When equal amounts of protein from each stage of purification were run on a reducing SDS-PAGE gel, several of the same bands stay throughout the purification (Figure 1). Since the predicted molecular weight of MopA is ~347 kDa, the protein would not run very far into the gel, as seen by the band at the very top of the gel. The rest of the proteins may be impurities in the purification scheme or they may be breakdown products of MopA (discussed below).

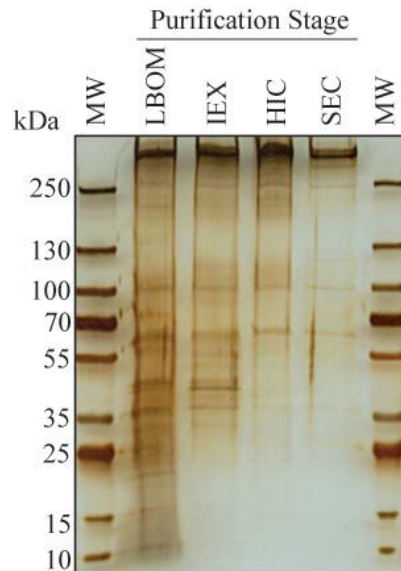


Figure 1: SDS-PAGE gel of MopA purification showing enrichment of protein bands
LBOM: loosely bound outer membrane proteins; IEX: post ion exchange proteins; HIC: post hydrophobic interaction chromatography proteins; SEC: post size exclusion chromatography proteins

MS/MS of purification stages

MS/MS of the protein samples showed which proteins are present as the purification proceeds. The complexity of the samples is reduced as the purification proceeds from LBOM→IEX→HIC→SEC, seen in Table 1. The data were broken down into five basic protein groups. The heme peroxidase group consists of the previously identified MopA protein, along with another protein from the ‘Moperon’ (discussed in Chapter 3) that contains a heme peroxidase-binding region and may be associated with MopA. MopA is localized extracellularly and is a peripheral outer membrane protein (discussed in more detail later). The ATP binding cassette (ABC) transporter group of proteins consists of inner and outer membrane bound proteins that recognize an amino acid signal sequence of an unfolded protein. In Gram-negative bacteria, ABC transporters carry out transport across the inner membrane, periplasm and outer membrane in one step with the hydrolysis of ATP. The transport apparatus consists of the inner membrane

bound ATP binding cassette (ABC) transport protein, periplasmic adapter proteins that link the ABC transporter to the TolC outer membrane transporter (more detail on type 1 secretion in Chapter 3) (Eitinger et al., 2011). Both the ABC transport proteins and periplasmic adapter proteins were identified in the LBOM protein fraction. The tripartite ATP-independent periplasmic (TRAP) transporter group is a secondary transporter system, transporting a substrate from the periplasm to the cytoplasm along with another substrate utilizing the energy stored in concentration gradients. The TRAP complex consists of two inner membrane bound domains that act as transporter and a soluble periplasmic protein that binds a specific substrate and shuttles it to the bound transporter domains (Mulligan et al., 2011). All three portions of the TRAP transporter proteins were identified in the LBOM protein mixture. The flagella group proteins consisted of proteins associated with flagellar bodies and type 3 secretion. These proteins are ubiquitous outer membrane proteins and consist of the membrane integrated basal body complex, a rotary motor powered by H^+ concentration gradients, the signal sensing switch complex, the hook complex that allows multiple flagella to move together, and the filament complex that translates the rotary motion into physical movement (Macnab, 2003). The group termed 'other' consists of proteins that are metabolic in nature and may be localized in the cytoplasm, periplasm, or are membrane bound. The function of these proteins include glycolytic enzymes (enolase), antioxidant enzymes (catalase), and DNA binding proteins (Holiday junction DNA helicase); among others.

Table 1: Complexity of proteins in each stage of purification

Protein Group	Purification Stage							
	LBOM		IEX		HIC		SEC	
	Total # Individual Proteins	Total # Assigned Spectra	Total # Individual Proteins	Total # Assigned Spectra	Total # Individual Proteins	Total # Assigned Spectra	Total # Individual Proteins	Total # Assigned Spectra
Heme Peroxidases ABC Family TRAP	2	966	1	538	2	1075	1	198
Family Flagella Associated	20	307	14	220	2	8	0	0
Other	5	61	6	73	1	8	0	0
	9	148	7	121	5	82	2	10
	18	281	14	122	16	119	4	31
Total	54	1763	42	1074	26	1292	7	239

The majority of the proteins identified by MS/MS through all the fractions (79 proteins) are cytoplasmic or periplasmic, as shown in Figure 2. This shows that there may be cell lysis occurring during the buffered high salt wash step that separates the proteins from the cells. This vigorous step may lyse cells, thereby releasing cytoplasmic and membrane components into the LBOM protein fraction. This is probably unavoidable since cell may always lyse during protein extract preparation no matter what care is taken.

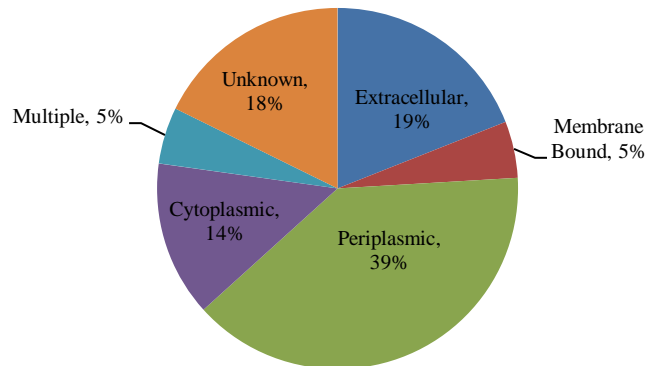


Figure 2: Localization of proteins identified using MS/MS

Evidence of two additional interesting proteins was found in this data. The first is annotated as a possible hemolysin-type Ca^{2+} binding region (ZP_01225896). This protein is also found associated with MopA in the genome, as it is found just upstream of MopA and may be coexpressed (discussed in more detail in Chapter 3). This protein has also been localized to the extracellular space of the cell but it is not known whether it associates with MopA or what its activity is. It was found only in the LBOM and HIC stages of the purification. It may be present in the other stages of purification, but may not have been detected. Another interesting protein to note is a putative multicopper oxidase (ZP_01225909). This multicopper oxidase (MCO) is found to be a homologue of a similar MCO in *Pseudomonas putida* GB-1 that has been genetically identified as essential for Mn(II) oxidation (Kati Gesvzain, personal communication) as well as MCOs in Mn(II) oxidizing *Leptothrix* species.

Of the proteins identified in each stage of purification, only MopA showed any significant presence. It is the predominant protein in the LBOM protein layers of the cell, since it is one of the only identified proteins shown to be localized to the extracellular matrix of the cell (the other being the hemolysin calcium binding region). Table 2 displays the top four proteins by number of assigned spectra per stage of purification. In both the LBOM and IEX stage of the purification, MopA is shown to be roughly 50% of the fraction, while in the HIC and SEC stages MopA becomes a larger fraction of the protein mixture. The number of assigned spectra is at least an order of magnitude greater for MopA over the next most abundant protein in all stages, showing that MopA contributed more peptides to the identification matrix than the others.

Table 2: Top four proteins by most assigned spectra per group

Identified Protein	NCBI Accession #	MW	# Assigned Spectra	% Coverage	% of Fraction	Category
LBOM						
putative hemolysin-type calcium-binding peroxidase protein	ZP_01225898	347 kDa	934	45%	52.98%	H
lysine-arginine-ornithine-binding periplasmic protein	ZP_01227459	36 kDa	79	74%	4.48%	O
periplasmic phosphate-binding protein, ABC-type transporter	ZP_01226847	37 kDa	58	62%	3.29%	A
glutamine synthetase I	ZP_01227554	52 kDa	49	56%	2.78%	O
IEX						
putative hemolysin-type calcium-binding peroxidase protein	ZP_01225898	347 kDa	538	35%	50.09%	H
ABC-type sugar transport system, periplasmic component	ZP_01228804	65 kDa	51	45%	4.75%	A
ABC-type branched-chain amino acid transport systems	ZP_01228814	39 kDa	46	45%	4.28%	A
twin-arginine translocation pathway signal	ZP_01228741	72 kDa	40	25%	3.72%	O
HIC						
putative hemolysin-type calcium-binding peroxidase protein	ZP_01225898	347 kDa	1045	44%	80.88%	H
possible hemolysin-type calcium-binding region	ZP_01225896	87 kDa	30	21%	2.32%	H
glutamine synthetase I	ZP_01227554	52 kDa	25	39%	1.93%	O
flagellin protein	ZP_01226297	31 kDa	22	31%	1.70%	F
GF						
putative hemolysin-type calcium-binding peroxidase protein	ZP_01225898	347 kDa	198	23%	82.85%	H
putative gluconolactonase	ZP_01227614	41 kDa	17	38%	7.11%	O
carbon monoxide dehydrogenase, medium subunit	ZP_01227911	28 kDa	7	25%	2.93%	O
flagellin protein	ZP_01226297	31 kDa	6	19%	2.51%	F

H = Heme Peroxidase group; A = ABC transporter group; T = TRAP transporter group; F = Flagella associated group; O = Other protein group

A role for MCOs in *A. manganoxydans* SI85-9A1 Mn(II) oxidation still cannot be ruled out due to the presence of an MCO within the MS/MS results. This protein shows homology to MCOs found in other Mn(II) oxidizing prokaryotes, in particular, an MCO (YP_001668898) found in *Pseudomonas putida* GB-1. They share 88% homology at the protein level and the *P. putida* MCO has been found to be important for Mn(II) oxidation. The identification of the putative MCO (ZP_01225909) in the first three stages of purification may show that this protein is a part of a complex with MopA required for Mn(II) oxidation to occur. Even though it was not identified in the active fraction after SEC, this does not mean it was not present. It may have simply not been in high enough

abundance for identification. The purification stages are not performed under denaturing conditions so complexes of proteins may be able to stay together through the stages.

These two proteins may act synergistically in Mn(II) oxidation, with one protein providing the other with reactants necessary for Mn(II) oxidation.

Functional Assays

In vitro Mn(II) oxidation and purity of the Mn(II) oxidase

The purity of the protein matrix from beginning to end was analyzed using the standard *in vitro* Mn(II) oxidation assay. This assay measures the amount of Mn oxides produced by the sample when mixed with Mn(II) and allowed to react overnight. After the reaction period, the sample is mixed with the Leucoberberlin Blue reagent (LBB, see materials and methods of this chapter for formulation), a blue color develops that can be analyzed by UV/Visible spectrophotometry.

Table 3 shows that the purity increased as purification proceeded and that each stage increased the overall purity of MopA. The percent yield of this purification scheme is low, showing that there may be optimization needed in order to get the most MopA out of the LBOM proteins.

Table 3: Purification table for MopA purification

Step	Volume (ml)	Total Protein (mg)	Total Activity (U*)	Sp Act (U mg ⁻¹)	% Yield	Fold Purification
LBOM Proteins	1.500	0.381	1,503	3,946	100	1.0
IEX (Q FF)	0.500	0.058	319.6	5,510	21	1.4
HIC (Phenyl FF)	0.200	0.015	183.5	12,240	12	3.1
SEC (S-200)	0.100	0.004	62.29	15,570	4	3.9

1 U = nmol MnO₂ hour⁻¹

In vitro cyanide inhibition

A standard *in vitro* Mn(II) oxidation assay was performed with the addition of cyanide to determine how a known heme inhibitor affects Mn(II) oxidation. In

hemoglobin, myoglobin and cytochrome *c* oxidases cyanide binds the heme prosthetic group. It specifically binds to the ferrous iron in the same pocket that dioxygen would bind. Toxicity to the organism occurs because oxygen is unable to be used as a terminal electron acceptor during respiration (Cummings, 2004). The same principle should be able to be exploited in Mn(II) oxidation, where hydrogen peroxide is again reduced by the protein. Mn(II) oxidation was barely affected at low concentrations of cyanide (0.001-0.1mM) but was decreased by half at ~0.7mM cyanide and virtually eliminated at 1mM cyanide. This shows that the predominant mode for Mn(II) oxidation may occur through the heme groups located in the peroxidase domains of MopA. This inhibition of MopA by cyanide was approximately 70 times higher than cyanide inhibition of rat cytochrome *c* oxidase ($13.2 \pm 1.8 \mu\text{M}$). This would go to show that the LBOM preparation from *A. manganoxydans* SI85-9A1 is relatively resistant to cyanide. The fact that cyanide does inhibit, but at a high concentration may suggest metabolic involvement. The cyanide may be affecting other proteins within the system that are involved in Mn(II) oxidation but are not MopA. This is plausible because a variety of proteins are found in the LBOM protein preparation and may contribute to Mn(II) oxidation.

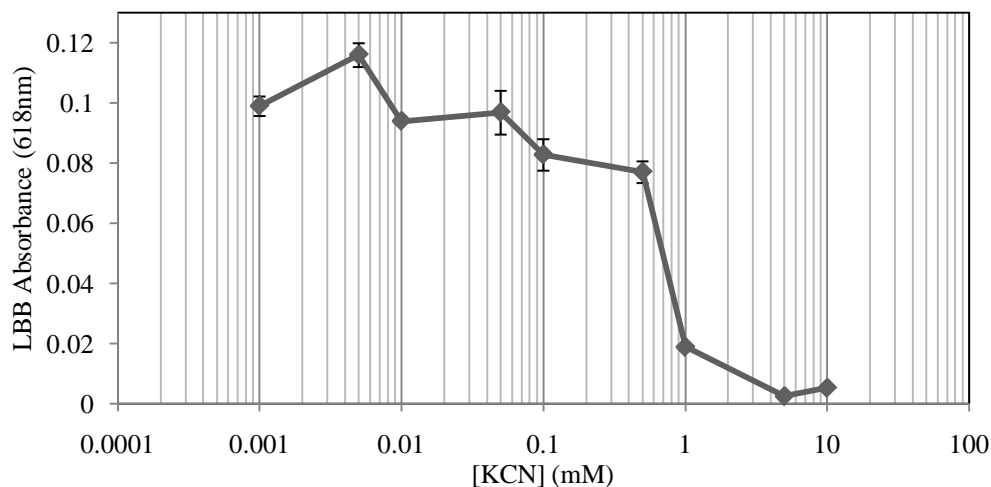


Figure 3: Mn(II) oxidation inhibition by cyanide

In gel heme activity

In order to visually correlate Mn(II) oxidation with heme activity, native PAGE was utilized to perform multiple activity assays in parallel and identify Mn(II) oxidizing components using multiple activity stains. To test for the presence of a heme peroxidase, 3,3',5,3'-tetramethylbenzidine (TMBZ) is used and will turn blue in the presence of a peroxidase protein and hydrogen peroxide (Thomas et al., 1976; Hagan and Mobley, 2009). Three aliquots of equal amounts of LBOM were run in a single native PAGE gel. After separating the proteins by 1-dimensional PAGE, they were cut into three equal gel strips. Each strip was then subjected to a different procedure. The first set was silver stained to show the total proteins present in the LBOM proteins. As can be seen in Figure 4, there are several bands found within the LBOM, possibly belonging to MopA or to different proteins (Ag-stain lane). The second strip was subjected to an in gel Mn(II) oxidation assay and allowed to react overnight (Mn(II) Ox Activity lanes). After incubation, thick brown bands were seen in the gel visible to the naked eye (-LBB lane). When LBB was added to the gel, these brown bands turned blue, showing that they were

Mn oxides (+LBB lane). The final strip was subjected to the heme peroxidase activity assay using TMBZ (denoted ‘Heme-stain’ in Figure 4). Upon addition of hydrogen peroxide, blue bands begin to appear wherever TMBZ is being oxidized by the active peroxidase protein. As can be seen in Figure 4, the blue bands correlate exactly with Mn(II) oxidation and different protein bands within the gel. This provides additional evidence that MopA, a heme containing peroxidase, is involved in Mn(II) oxidation and may be the principle player in Mn(II) oxidation within *A. manganoxydans* SI85-9A1. It should be noted that all of the heme-stain bands aligned with Mn(II) oxidizing bands, Figure 4 is a lower resolution image (original image data was lost due to a hard drive failure) and does not show the lighter bands well in the Mn(II) oxidizing activity bands (~130kDa in -LBB and +LBB lanes).

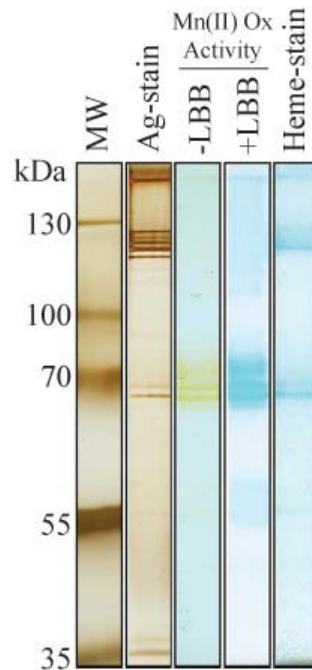


Figure 4: Native PAGE activity correlation gel

Possible function from Structural Prediction tools

Figure 5 depicts the important structural features predicted by the primary sequence of MopA. These features were predicted from the primary amino acid sequence and the image is based on the output from PROSITE (<http://expasy.org/prosite/>). In addition to the major domains discussed below, sites that are more common among proteins were identified relating to post translational modification. Sites were identified throughout the proteins for N-myristoylation (although only a eukaryotic and viral phenomenon (Farazi et al., 2001)), N-glycosylation, phosphorylation, and cell attachment. These predicted sites may help the protein become fully active in the extracellular matrix and may help keep it associated with the cell. The major domains predicted for the rest of the protein includes the type 1 secretion signal, Ca²⁺ binding regions related to repeat-in-toxin (RTX) regions, and animal heme-binding peroxidase domains.



Figure 5: MopA predicted 3^o structure based on 1^o sequence
Based on Prosite and CDD; Blue: animal heme peroxidase domains; orange: RTX/Ca²⁺ binding domains; green: type 1 secretion signal

Type I secretion signal

In the *A. manganoxydans* SI85-9A1 genome, MopA is annotated as a hemolysin-type protein, meaning that it could have similar properties as hemolysin (HlyA) from *E. coli*. HlyA is secreted by a type 1 secretion signal in its C-terminus and MopA contains a similar C-terminal signal. Although there seems to be no real defined sequence specificity for type 1 secretion signals, the signal region has been found to be rich in leucine (L), aspartate (D), alanine (A), valine (V), threonine (T), serine (S), isoleucine (I)

and phenylalanine (F) yet poor in lysine (K), histidine (H), proline (P), methionine (M), tryptophan (W), and cysteine (C). The C-terminal 50 amino acids of MopA were analyzed using the ProtParam tool on the ExPASy Proteomics server (<http://expasy.org/tools/protparam.html>) to examine its amino acid composition. Table 4 shows that the 50 terminal amino acids of MopA are indeed rich in certain amino acids and poor in others. The presence of high levels of glycine (G) shown in Table 4 is not surprising, as this region also has been identified as a Ca²⁺ binding region, which are glycine rich regions in the form of G-G-X-G-(N/D)-D-X-(L/I/F)-X (Linhartová et al., 2010), also identified in the C-terminal amino acids of MopA. Type 1 secretion and its components as related to MopA will be discussed in more detail in Chapter 3.

Table 4: Amino Acid composition of Type 1 secretion signal

Rich		Poor		Other	
AA	#	AA	#	AA	#
alanine	6	histidine	2	glycine	14
threonine	6	cysteine*	0	glutamine	6
aspartate	5	methionine	0	glutamate	6
valine	5	proline	0	arginine	4
leucine	5	tryptophan	0	asparagine	0
isoleucine	2			tyrosine	0
phenylalanine	2			pyrolysine	0
serine	2			selenocysteine	0

*no Cysteine in MopA

Repeats-in-toxin (RTX) toxin exoproteins

The plausible structural considerations raised by the presence of Ca²⁺ binding motifs (orange in Figure 5) within MopA can be described by examining known RTX toxin structures. The most common type of Ca²⁺ binding domain in proteins is the calmodulin (EF-hand) domain. It binds Ca²⁺ and causes a unique structural change that aids protein function (Gifford et al., 2007). RTX domains bind Ca²⁺ in a different way but still cause a conformational change within the overall protein that helps initiate or maintain protein function. RTX Ca²⁺ binding regions are comprised of nonapeptide

repeats in the form of G-G-X-G-(N/D)-D-X-(L/I/F/V/W/Y)-X, and usually occur in glycine and aspartate rich regions of the proteins (composite of: Satchell, 2007; Linhartová et al., 2010). They can comprise up to 25% of the 1^o sequence of RTX proteins (Satchell, 2007). When calcium binds to these repeats, an interesting 2^o structure forms: the parallel β -helix or parallel β -roll. In this structure, the first six residues of the motif bind Ca²⁺ in a turn and a short β -strand is formed with the remaining three. When multiple motifs are stacked on top of each other, a right-handed helix is formed with parallel β -strands and Ca²⁺ bound in consecutive turns. In sum, Ca²⁺ binding causes the RTX protein to become active and perform its metabolic function (Linhartová et al., 2010). MopA has many such repeats. PROSITE identified 10 individual Ca²⁺ binding repeats from MopA (identified by PROSITE method PS00330: pattern D-X-(L/I)-X-X-X-X-G-X-D-X-(L/I)-X-G-G-X-X-X-D). Upon closer manual inspection by the author, these repeats could be pieced together to form five sets of varying length (from 18-45 amino acids long). When the more simple sequence from Satchell (2007) and Linhartová et al. (2010) [G-G-X-G-(N/D)-D-X-(L/I/F/V/W/Y)-X] was manually searched for within the sequence, many more such repeats came up (~40), concentrated between the peroxidase domains as well as in the C-terminal tail region. These regions were glycine and aspartate rich regions of the protein (as shown by PROSITE and consisted of ~850 amino acids or 26% of the protein). These repeats may allow MopA to become active upon binding Ca²⁺, which has been shown since the addition of Ca²⁺ to the standard Mn(II) oxidation assay increased oxidation by 4.26-fold (Anderson, Johnson, et al., 2009).

The presence of the RTX Ca^{2+} binding repeats raises an interesting question as to the function of MopA. As described previously, proteins belonging to the RTX toxin group have a multitude of functions, all of which are designed to protect the cell (Linhartová et al., 2010). The relationship of MopA to this class of toxins is unclear since it is unknown what role Mn(II) oxidation plays for the cell. MopA has a molecular weight of 347 kDa and a theoretical pI of 4.03, closely matching that predicted for most RTX toxins (ExpASy ProtParam tool; <http://expasy.org/tools/protparam.html>). Other peroxidase proteins have been identified as RTX exoproteins by using RPS-BLAST ver 2.2.20 and comparing it to CDD version 2.16 (Linhartová et al., 2010). Table 5 lists the proteins and organisms with these RTX peroxidases. The fact that these peroxidases are extracellular may provide the cells with a layer of protection from reactive oxygen species, may allow the cell access to nutrients that are generally not available inside the cell, or provide cell defense from predators. These may be the case for MopA in *A. manganoxydans* SI85-9A1.

Table 5: Gram negative bacteria with RTX peroxidases

Accession	Bacteria name	Protein annotation	Length (aa)	pI
YP_001514679.1	Acaryochloris marina MBIC11017	peroxidase family protein	788	4.08
YP_002488925.1	Arthrobacter chlorophenicus A6	Animal heme peroxidase	1712	4.08
YP_830737.1	Arthrobacter sp. FB24	heme peroxidase	1625	4.10
YP_001791329.1	Leptothrix cholodnii SP- 6*	heme peroxidase	1650	3.81
YP_673356.1	Mesorhizobium sp. BNC1	heme peroxidase	2950	3.71
YP_002418988.1	Methylobacterium	Animal heme peroxidase	2342	3.92
YP_002423527.1	chloromethanicum CM4	Animal heme peroxidase	2342	3.92
YP_002420757.1	Methylobacterium	Animal heme peroxidase	3587	3.90
YP_001639132.1	extorquens PA1	heme peroxidase	3587	3.90
YP_001657980.1	Microcystis aeruginosa NIES-843	hypothetical protein MAE_29660	1289	4.44
YP_001268466.1	Pseudomonas putida F1*	heme peroxidase	3619	3.84
YP_001669581.1	Pseudomonas putida GB-1*	heme peroxidase	3608	3.87
NP_744706.1	Pseudomonas putida KT2440*	heme peroxidase	3619	3.85
YP_779943.1	Rhodopseudomonas palustris BisA53	heme peroxidase	3113	3.80
YP_568698.1	Rhodopseudomonas palustris BisB5	heme peroxidase	3094	3.83
YP_723199.1	Trichodesmium erythraeum IMS101	hemolysin-type calcium-binding region	678	3.98

*: Mn(II) oxidizing organism

Adapted from (Linhartová et al., 2010)

Extracellular reactive oxygen species may form in excess at high overall cell densities relative to the organism studied (Imlay, 2008). Cells become leaky with ROS and it has been shown that intracellular ROS can cause a variety of cell damage. ROS have also been used as a defense mechanism in white blood cells against invading cells (Imlay, 2008). These processes may be occurring in stationary phase and the cell may need to protect itself in order to continue living. Mn(II) may be utilized in this fashion because it may not be used for any other process and is readily available. Mn(II) has been shown to be important for the lifestyle of *Deinococcus radiodurans*. In *D. radiodurans*, growth is dependent on Mn(II) concentration when grown under ionizing radiation. The Mn(II) is associated with orthophosphate and peptides and provides a layer of protection from hydroxyl radicals by reaction with them instead of the protein (Daly et al., 2004,

2010; Slade and Radman, 2011). Chelated Mn has also been found to act as a superoxide dismutase mimic even when not associated with proteins (Archibald and Fridovich, 1981, 1982a, 1982b). These examples show how free Mn(II) can be coupled in a controlled fashion to the detoxification of ROS. By coupling Mn(II) oxidation to hydrogen peroxide reduction through a peroxidase, this power is controlled even more and may allow the cell to survive in harsher environments.

Nutrient limitation may be another reason for extracellular production of peroxidases. During exponential phase, more readily acceptable electron donors are used up, leaving nutrients like Mn(II) to be used during stationary phase. By coupling oxidation of Mn(II) to the oxidation of hydrogen peroxide or another molecule, the cell would be able to utilize the electrons from Mn(II) oxidation as an energy source to build ATP. It is also possible that these peroxidases are used in the same manner as they are used in fungi, since fungi use Mn(III) to breakdown recalcitrant humic substances into usable organic molecules that the cell can take in to use as a carbon source.

The possibility of defense is another intriguing possibility. Mn(III) has been shown in fungi to be utilized as a powerful oxidant to breakdown recalcitrant humic substances. Since Mn(III) is very reactive, it is plausible that it could be used as an antimicrobial agent. Mn(III) has been seen in pyrophosphate capture experiments during the oxidation of Mn(II→IV) (Webb et al., 2005; Anderson et al., 2009). The cells may produce excess amounts of Mn(III) in an effort to protect itself during a nutrient limited period by allowing the Mn(III) to react with the proteins and extracellular matrix of competing cells, damaging the cells and causing them to not be able to compete for nutrients as well. This may give a competitive advantage to *A. manganoxydans* SI85-9A1

and allow it to out compete other organisms since *A. manganoxydans* SI85-9A1 grows slowly and to a low cell density relative to other organisms.

One final note is that the expression of some RTX exoproteins type 1 secretion components is governed by the stage of growth. This has been found for multifunctional autoprocessing RTX (MARTX) toxins where expression of the secretion apparatus is regulated by a suppression mechanism and is only lifted when the cells reach stationary phase (Boardman et al., 2007). This may too be the case with MopA, since Mn(II) oxidation in general has been shown to be a stationary-phase phenomenon, is blocked by the presence of rich media, and Mn(II) oxidases are expressed even without the presence of Mn(II) (Jung and Schweisfurth, 1979). The expression machinery for MopA may be repressed during exponential phase growth, but when stationary phase growth is reached, transcriptional repression may be released and MopA would be secreted. This could be in response to nutrient limitation that would increase the need for alternative energy sources or cellular protection, as described above.

Comparison to Fungal Mn(II) Peroxidases

In contrast to fungal Mn(II) peroxidases, MopA belongs to a completely different class of peroxidase. As shown in the PeroxiBase and PROSITE, secreted fungal peroxidases are classified under the non-animal plant peroxidase superfamily as type II secreted fungal peroxidases (<http://peroxibase.toulouse.inra.fr/classes.php> and <http://www.expasy.ch/cgi-bin/nicedoc.pl?PS50292>). MopA has been annotated as belonging to the animal heme peroxidase superfamily. This superfamily contains myeloperoxidase, lactoperoxidase, eosinophil peroxidase and thyroid peroxidase. The first three play a role in immunity and antimicrobial activity while thyroid peroxidase

helps in the biosynthesis of thyroid hormones (Loughran et al., 2008). The purpose of animal heme peroxidases within bacteria is relatively unknown and MopA is one of the first characterized proteins of this group. It is interesting to note that these animal peroxidases arose separately from the plant peroxidases since they differ on the 1^o, 2^o, and 3^o levels of protein structure (Taurog, 1999). This may show a sort of convergent evolution for the need of Mn(II) oxidation between different groups of organisms.

Mn(II) oxidizing peroxidases (MnP) have been studied in fungi for a long time and much is known about their structure and function (Sundaramoorthy et al., 2010). Experiments have not been performed yet to test whether *A. manganoxydans* SI85-9A1 is able to oxidize humic substances, but it has been shown in bacteria that Mn(III) is an intermediate in the oxidation of Mn(II) (Webb et al., 2005; Anderson, Johnson, et al., 2009). It has also been shown in fungi that MnPs and MCOs can work synergistically, with MnPs using H₂O₂ produced by MCO mediated Mn(II) oxidation (Schlosser and Hofer, 2002). MopA may be able to act under a similar mechanism. The presence of an MCO through the MS/MS data is interesting because it could mean that MopA and the MCO are coupled in some sort of a Mn(II) oxidizing complex, with one protein possibly providing the oxidizing power to the other protein. The MCO gene is also located just upstream of MopA in the *A. manganoxydans* SI85-9A1 genome, suggesting they may be under similar genetic regulation. MnPs bind Ca²⁺ as well: the Ca²⁺ ions bind proximal and distal to the heme prosthetic group and help stabilize the entire heme environment (Sutherland et al., 1997). The Ca²⁺ binding in MopA may be a general structural component rather than functional, although the lack of a crystal structure cannot rule out the interaction of Ca²⁺ with the heme environment and Mn(II). MopA does not contain

any disulfide bonds (no cysteine at all) whereas MnP contains five such linkages that help provide protein stability (Reading and Aust, 2001). These comparisons highlight the interesting similarities and differences between MopA and MnPs and provide a jumping off point for future research.

Summary

The results presented here show the necessity of MopA in Mn(II) oxidation and shed light onto some structural features. First, Mn(II) oxidation activity was followed from a rough mixture of loosely bound outer membrane proteins through ion exchange, hydrophobic interaction and size exclusion chromatography. MopA was found in the final, active fraction and identified by LC-MS/MS through the stages as the predominant protein. Second, Mn(II) oxidation activity was quenched with the addition of cyanide, a potent heme protein inhibitor. This cessation of Mn(II) oxidation could be attributed to the inactivation of MopA. Third, Mn(II) oxidation activity was correlated to protein content and peroxidase activity in Native PAGE. This correlation shows that the protein is at least part of a complex of proteins involved in Mn(II) oxidation. Finally, examination of the amino acid sequence has shed some light on the possible overall function of the protein. MopA is likely secreted in one step by the type 1 secretion apparatus to the outer membrane of the cell as an unfolded protein. The relationship of MopA RTX toxins and similar proteins may give a clue to their mode of activity and activation. The final relationship to MnPs found in fungi is another interesting feature, as this is the first Mn(II) oxidizing peroxidase identified in prokaryotes. MopA seems to be a completely different protein than MnP even though they have come to perform the same function. MopA is a necessary component of Mn(II) oxidation in *A.*

manganoxydans SI85-9A1, even though MopA homologues may not be necessary for Mn(II) oxidation in other organisms: *P. putida* GB-1 in frame deletions of its *mopA* homolog still oxidize Mn(II). This may suggest that Mn(II) oxidation is different in each Mn(II) oxidizing organism.

Chapter 3: Development of a genetic system for *A.*

***manganoxydans* SI85-9A1**

Introduction

In order to gain a more complete understanding of Mn(II) oxidation in *A. manganoxydans* SI85-9A1, a genetic manipulation system needs to be developed. This would allow elucidation of all the genes and proteins involved in the chemistry of Mn(II) oxidation. Organisms from diverse habitats have been notoriously difficult to genetically modify due to the conditions in which they survive. In spite of this, various techniques have been developed to work with these organisms so they can be probed using genetic tools. An understanding of the genetics of *A. manganoxydans* SI85-9A1 is made easier because 1) the genome is already known, allowing easy verification of mutated genes; and 2) a partial proteome of Mn(II) oxidation is known that has shown MopA to be a Mn(II) oxidase.

Various marine and/or Mn(II) oxidizing organisms have been studied using genetic techniques. The open ocean dwelling *Synechococcus* was found to incorporate a

select set of plasmids (Brahamsha, 1996). The *Roseobacter* clade is a group of Gram-negative marine organisms closely related to *A. manganoxydans* SI85-9A1 and they comprise up to 85% of marine bacterial communities, performing much of the associated chemistry. They have been found to be amenable to conjugation and electroporation, but chemical competency procedures failed to achieve any results (Piekarski et al., 2009). As discussed earlier, in terms of Mn(II) oxidizing organisms, there have been many attempts using genetic tools to determine both the Mn(II) oxidase and physiological function of the Mn(II) oxidase. One confirmed and several putative Mn(II) oxidases have been identified through genetic tools that belong to the multicopper oxidase (MCO) family of enzymes (discussed earlier).

The ability to genetically manipulate *A. manganoxydans* SI85-9A1 would allow us to associate metabolic functions to Mn(II) oxidation and help determine the function of Mn(II) oxidation for the organism. Several initial steps need to be performed in order to formulate the genetic toolkit. First, the antibiotic susceptibility of *A. manganoxydans* SI85-9A1 was determined in order to determine useful selective markers. Second, growth of *A. manganoxydans* SI85-9A1 in various media was investigated to determine when *A. manganoxydans* SI85-9A1 is rapidly dividing. Third, methods of plasmid transfer into *A. manganoxydans* SI85-9A1 were examined. Several methods of transformation and conjugation were tried since *A. manganoxydans* SI85-9A1 has been shown to be recalcitrant to traditional plasmid transfer methods (Caspi, 1996). Multiple plasmids were also examined in order to find one or many plasmids that *A. manganoxydans* SI85-9A1 will accept. Finally, genes located near *mopA* were examined in order to provide

potential targets for mutagenesis and to understand the pathway of possible MopA secretion.

Methods and Materials

Growth conditions, strains, and plasmids

Strains and plasmids are summarized in Table 6. *A. manganoxydans* SI85-9A1 was incubated in M- or K-medium at room temperature with and 150-200 RPM, in flask sizes as needed by the experiment (Tebo et al., 2007). M-medium is a minimal nutrient medium made with autoclaved 1x artificial seawater (ASW; 100 mM MgSO₄, 20 mM CaCl₂, 600 mM NaCl, 20 mM KCl), 0.05 g L⁻¹ Bacto yeast extract and 0.05 g L⁻¹ Bacto peptone (Fisher Scientific, USA). The following are added to the above post autoclaving and are filter sterilized (0.2 μm) immediately prior to addition to the medium: 20 mM HEPES pH 7.8 (1 M initial), 2 mM KHCO₃ (1 M initial), 100 μM MnCl₂ (1 M initial), and 3 mg ml⁻¹ ferric ammonium citrate (15 mg ml⁻¹ initial). Both MnCl₂ and ferric ammonium citrate were freshly prepared prior to addition. As carbon sources, 10 mM glycerol and 10 mM sodium formate were added to the base M-medium, both filter sterilized (0.2 μm) immediately prior to addition. K-medium is a richer medium and is made in a similar manner as M-medium but with the following differences: 0.5 g L⁻¹ Bacto yeast extract, 2 g L⁻¹ Bacto peptone (Fisher Scientific, USA), and without KHCO₃. As an inoculum, a 5 ml overnight K-medium culture is prepared from a single Mn(II) oxidizing colony grown on an M-media plate. From this overnight culture, 100 μl, is used to inoculate each flask. *Escherichia coli* is grown in Luria Broth (LB; 10 g L⁻¹ Bacto Tryptone, 5 g L⁻¹ Bacto yeast extract, 10 g L⁻¹ NaCl (Fisher, US)) at 37°C supplemented

with antibiotics as necessary. For solid media, 15 g L⁻¹ granulated (K-medium and LB) or noble (M-medium) agar is used.

Table 6: Strains, plasmids, and primers used in Chapter 3

Strain, plasmid, or primer	Description	Reference
Strain:		
<i>A manganoxydans</i> SI85-9A1	Mn(II) oxidizing α -proteobacterium	(Anderson, Dick, et al., 2009)
<i>Escherichia coli:</i>		
Tam1	mcrA Δ (mrr-hsdRMS-mcrBC) Φ 80lacZ Δ M15 Δ lacX74 recA1 araD139 Δ (ara-leu)7697 galU galK rpsL endA1 nupG	RapidTrans, Active Motif, USA
ER2566	F' proA+B+ lacIqzzf::Tn10(TetR)/ fhuA2 lacZ::T7 gene1 [lon] ompT gal sulA11 R(mcr-73::miniTn10--TetS)2 [dcm] R(zgb-210::Tn10--TetS) endA1 Δ (mcrC-mrr)114::IS10	New England Biolabs, USA
S17 λ -pir	Tp' Sm' <i>hsdR pro recA</i> RP4-2-Tc::Mu-Km::Tn7 in chromosome; S17-1 lysogenized with lambda pir bacteriophage	(de Lorenzo et al., 1990)
DH5 α	fhuA2 Δ (argF-lacZ)U169 phoA glnV44 Φ 80 Δ (lacZ)M15 gyrA96 recA1 relA1 endA1 thi-1 hsdR17	Bethesda Research Laboratories, USA
<i>Pseudomonas putida</i> GB1	Mn(II) oxidizing strain used as PCR DNA bacterial control	
Plasmid:		
pRK2013	Helper plasmid for conjugation; Km	(Figurski and Helinski, 1979)
pUCP22	<i>E. coli</i> - <i>Pseudomonas</i> shuttle vector; Ap, Gm	(West et al., 1994)
pBBR1MCS-2	Broad host range cloning vector, lacZ α ; Km	(Kovach et al., 1994, 1995)
pBBR1MCS-5	Broad host range cloning vector, lacZ α ; Gm	(Kovach et al., 1994, 1995)
pRK290::Tn5	Carries Tn5 for transposon mutagenesis; Km	(Parales and Harwood, 1993)
pRL27	Carries Tn5 for transposon mutagenesis; Km	(Larsen et al., 2002)
pEX18Gm	Suicide vector with sacB counter-selection; Gm	(Hoang et al., 1998)
pJN105	Broad host range, Pbad promoter; Gm	(Newman and Fuqua, 1999)
pJH1	Broad host range, const. PlacZ promoter; Gm	(Lee et al., 2006)
pHRP309	Broad host range, promoter-lacZ fusions; Gm	(Parales and Harwood, 1993)
pSUP5011	Descendent of pBR325; Km	(Simon et al., 1983)
pMO75	<i>P. putida</i> suicide vector; Km	(Nordeen and Holloway, 1990)
pG59	Derived from pACYC184; Km	
Cosmid 1 through 5	Descendent of cosmid pMMB33-7, containing 9A1 cbb region; Km	(Caspi, 1996)
Primer:		
9A1 Rubisco F	5'-ATC AGG GTG GTG TAG CGC T-3'	Provided by Rick Davis
9A1 Rubisco R	5'-ATG TCG ATT ACG CTT GAG CGC-3'	Provided by Rick Davis
27F	5'-AGA GTT TGA TCM TGG CTC AG-3'	Provided by Rick Davis
1492R	5'-RGY TAC CTT GTT ACG ACT T-3'	Provided by Rick Davis

Growth Curve

A. manganoxydans SI85-9A1 was grown in a 250 ml baffled flask with 50 ml K or M-medium at room temperature. Growth was started from an overnight culture at $OD_{600} \sim 0.1$ and followed for 48 hours. A blank measurement was made immediately prior to inoculation with sterile media and subtracted from each measurement at each time point. For each time point, 1 ml of culture was withdrawn and analyzed at OD_{600} in a 1.5 ml polystyrene cuvette (Fisherbrand, USA) in the spectrophotometer (Molecular Devices SpectraMax M2 UV-Vis microplate spectrophotometer).

Antibiotic Susceptibility

Tube cultures (5 ml) of either M or K-medium were allowed to grow in triplicate overnight at six different concentrations: 5, 25, 50, 100, 150, and 200 $\mu\text{g ml}^{-1}$. Five antibiotics were used to determine the antibiotic susceptibility of *A. manganoxydans* SI85-9A1. Kanamycin (Km, 25 mg ml^{-1}), and gentamicin (Gm, 25 mg ml^{-1}) were prepared in 18 Ω MilliQ water, filter sterilized (0.2 μm), and stored at 4°C. Ampicillin (Ap, 25 mg ml^{-1}) was prepared in water, filter sterilized (0.2 μm), and stored at -20°C. Tetracycline (Tc, 15 mg ml^{-1}) was prepared in 50% ethanol, filter sterilized (0.2 μm), and stored at -20°C. Chloramphenicol (Cm, 25 mg ml^{-1}) was prepared in 100% ethanol, filter sterilized (0.2 μm), and stored at -20°C.

Plasmid Transformation

Chemical competency and transformation

A low efficiency, fast transformation procedure was developed using CaCl_2 , based upon (Sambrook and Russel, 2001). A 5 ml overnight culture of *A. manganoxydans* SI85-9A1 or *E. coli* was pelleted in a in an Eppendorf centrifuge (either model 5417C or

5424) at 13,000 RPM at room temperature for 5 minutes and resuspended with 1 ml of ice cold 20 mM HEPES pH 7.8 buffered 100 mM CaCl₂ in a 1.5 ml Eppendorf tube. This was allowed to sit on ice for 5 minutes and then pelleted again at 13,000 RPM for 5 minutes. This pellet was then resuspended in 200 µl ice-cold buffered 100 mM CaCl₂ and 100 µl was used for transformation. Generally, 2 to 5 µl of Miniprep plasmid DNA (100-500 ng µl⁻¹) was added to the competent cells, mixed with the pipette tip, and allowed to sit on ice. After 30 minutes, the tubes were placed into the 42°C water bath for 30 seconds. They were then placed back onto ice for 2 minutes and 0.4 ml of room temperature LB medium was added. LB medium was used for *E. coli* transformants and K-medium for *A. manganoxydans* SI85-9A1 transformants. This suspension was then placed either into a 37°C water bath for 60 minutes for *E. coli* or room temperature overnight for *A. manganoxydans* SI85-9A1. After the recovery period, 50 µl and 200 µl were spread using sterile glass beads onto selection medium containing antibiotics necessary for the transformed plasmid (LB for *E. coli* and K for *A. manganoxydans* SI85-9A1). The LB plates were placed in the 37°C incubator overnight and K-medium plates incubated at room temperature until growth is seen.

Tribos Transformation

Tribos transformation utilizes the Yoshida effect (Yoshida, 2007). This method involves the use of nano-sized needle-like crystalline material (acicular) mixed with plasmid DNA and bacterial cells. When mixed, the acicular material binds the DNA and when spread on a solid agar plate with the cells to be transformed, the frictional force between the sterile spreader and the hydrogel agar plate force the acicular material into the cells. At this point, a DNA transfer event happens between small cellular DNA and

the plasmid DNA, transforming the cell with the plasmid (Yoshida et al., 2007). A more detailed schematic diagram can be found in Wilharm et al. (2010). Solid media formulations for Tribos transformation (Wilharm et al., 2010) are the same as described previously with the exception of a higher percentage of agar for 2%, 3%, and 4% plates: 20 g L⁻¹, 30 g L⁻¹, and 40 g L⁻¹ respectively. Sepiolite (Kremer Pigmente, USA) was used in place of chrysotile, and was made as a 4% (w/v) solution. The solid was added to buffer and then autoclaved to obtain complete dissolution of sepiolite. The working concentration of sepiolite is 0.01%, dissolved in sterile buffer (5 mM HEPES pH 7.8, 200 mM KCl). The transformation protocol is essentially as described: 500 µl of bacterial cell culture was pelleted and resuspended in 100 µl sepiolite working solution. Approximately 50 to 100 ng of plasmid were added to this suspension. The suspension was then spread onto a plate with a sterile polypropylene cell spreader using a special motion until the liquid media had absorbed into the plate. The special motion included spinning the plate on a plate spinner and moving the spreader back and forth with very firm pressure until the media absorbed into the plate. At this point, friction on the plate increased and the same motion was continued for an additional 30-60 seconds. The plates were then incubated at either 37°C for *E. coli* or room temperature for *A. manganoxydans* SI85-9A1.

Freeze-Thaw Transformation

Freeze-thaw transformation utilizes the sheering forces that occur on the cell membrane upon freezing to force DNA into the cell and was performed essentially as described (Zibat, 2001). Briefly, an overnight culture was pelleted and washed in 1ml of 20 mM HEPES pH 7.8 (HEPES buffered ASW for *A. manganoxydans* SI85-9A1) and

repeated for a total of three washes. The cells were then resuspended in 100 μ l of cold buffer, approximately 500 ng of plasmid were added, and the tubes were flicked to mix cells and plasmid. These tubes were then placed onto ice for 15 minutes to completely chill the suspension and then placed into the freezer for 30-45 minutes (-80°C). After this period in the freezer, the tubes were removed and placed onto the bench top to thaw, a process that usually took around 2 minutes. LB medium was then added (900 μ l) and the cells were allowed to recover (LB and 1 hour at 37°C for *E. coli*; K-media and overnight at room temperature for *A. manganoxydans* SI85-9A1). After recovery, the cells were plated (50 and 200 μ l) and allowed to grow as described earlier.

Triparental Conjugation

Plasmids used for conjugation are listed in Table 6. Conjugation of *A. manganoxydans* SI85-9A1 is performed with three separate strains: an *E. coli* donor strain carrying the desired plasmid (see Table 6), an *E. coli* helper strain carrying pRK2013 (Figurski and Helinski, 1979), and the *A. manganoxydans* SI85-9A1 acceptor strain. pRK2013 contains genes necessary for conjugation to occur, including those necessary for pili assembly and production (*tra* genes) and an origin of replication (*mob* genes) (Figurski and Helinski, 1979). Overnight cultures of the donor and helper strain were subcultured (100 μ l into 5 ml LB) and allowed to grow for 3-4 hours. An overnight culture of *A. manganoxydans* SI85-9A1 was used (started from $\text{OD}_{600} \sim 0.1$ in K-medium, 24 hour growth) as the acceptor strain. In a 1.6 ml Eppendorf tube, 600 μ l acceptor strain, 600 μ l donor strain, and 300 μ l helper strain were mixed and pelleted at 13,000 RPM for 5 minutes. The medium was mostly removed, leaving less than 20 μ l of medium in the tube. The pellet was resuspended in this volume and spotted onto a K-medium plate

without antibiotics. This plate was then allowed to sit at room temperature for 24-48 hours, after which the cells were scraped off the plate and resuspended in K-medium. Dilutions were made (10^0 , 10^{-2} , 10^{-4} , 10^{-6}) and approximately 100 μl were spread using glass beads onto a K-medium plate containing dual selection antibiotics. The first antibiotic used was to select for the plasmid that was being conjugated and the second antibiotic was ampicillin to select against *E. coli* but still allow *A. manganoxydans* SI85-9A1 to grow ($100 \mu\text{g ml}^{-1}$). These plates were then allowed to grow at room temperature until colonies were obtained. Once colonies were obtained, they were picked from the original plate and replica plated onto several plates. One K-medium plate was incubated at room temperature to obtain total growth, another at 37°C to kill *A. manganoxydans* SI85-9A1 and allow *E. coli* to grow, and finally a third M-medium plate containing the same antibiotics to allow only *A. manganoxydans* SI85-9A1 growth and inhibit *E. coli* growth. These plates were necessary to differentiate the colonies from resistant *E. coli* contaminants and truly conjugated *A. manganoxydans* SI85-9A1.

DNA Handling

DNA Isolation

Plasmid and genomic DNA from *E. coli* and *A. manganoxydans* SI85-9A1 were isolated using standard kits and protocols contained in those kits. Plasmid DNA was prepared using the QIAprep Spin Miniprep Kit (Qiagen, USA) and genomic DNA was prepared using the Wizard Genomic DNA Purification Kit (Promega, USA). DNA quantification was performed using a ND-1000 Spectrophotometer (Nanodrop, USA) set to the nucleic acid detection mode.

PCR

Primers used for polymerase chain reactions (PCR) can be found in Table 6. PCR to amplify the genes of interest from *A. manganoxydans* SI85-9A1 was performed in an Applied Biosystems GeneAmp PCR System 2700 or 9700. DyNAzyme II (Finnzymes, FI) DNA Polymerase was used in 50 μl reaction volumes. Reaction mixtures consisted of 50 $\text{ng } \mu\text{l}^{-1}$ genomic DNA, 1x DyNAzyme II reaction buffer (1.5 mM MgCl_2) 200 μM dNTPs, 0.5 μM forward primer, 0.5 μM reverse primer, and 0.02 U μl^{-1} DyNAzyme II polymerase. A three-step protocol was followed and reaction conditions can be found in Table 7.

Table 7: PCR reaction conditions.

Reaction conditions	Primer Set				Cycles
	27F, 1492R		9A1 RuBisCO F, R		
	Temp ($^{\circ}\text{C}$)	Time (sec)	Temp ($^{\circ}\text{C}$)	Time (sec)	
Initial Denaturation	94	120	94	120	1
Denaturation	94	30	94	30	
Hybridization	55	30	60	30	30
Elongation	72	60	72	20	
Final Elongation	72	300	72	300	1
	4	∞	4	∞	

Electrophoresis

DNA was analyzed in 1% agarose (Fisher Scientific, USA) Tris-Borate-EDTA (TBE; 8.3 mM Tris base, 89 mM boric acid, and 3.2 mM ethylenediaminetetraacetic acid (EDTA)) gels stained with GelRed (Biotium, CA, USA) using an OWL gel electrophoresis gel box. Gels were run at 100 V in TBE buffer and imaged using UV transillumination.

Computer Database Searching

The *A. manganoxydans* SI85-9A1 genome was accessed using the Integrated Microbial Genomes (IMG) web interface (<http://img.jgi.doe.gov/>; Taxon Object ID:

638341009) and through the National Center for Biotechnology Information Genome viewer (<http://www.ncbi.nlm.nih.gov/genome/>; Refseq: NZ_AAPJ000000000).

Transporter Classification Database (<http://www.tcdb.org/>) was also used to analyze protein families. Structural prediction: tools on ExPASy Proteomics Server (<http://www.expasy.ch/>).

Results and Discussion

Antibiotic Minimum Inhibitory Concentration (MIC)

A. manganoxydans SI85-9A1 is able to grow in a variety of concentrations of antibiotics in solid and liquid media, summarized in Table 8. An important observation is the fact that oxidation and growth are both limited when grown with these antibiotics. At the upper limit of growth in tetracycline, growth was only 60% of normal. Growth in ampicillin seems to not be affected, although Mn(II) oxidation was delayed in both M and K-media. The fact that *A. manganoxydans* SI85-9A1 is so resistant to ampicillin was utilized in growth of overnight cultures to eliminate contamination; 100 $\mu\text{g ml}^{-1}$ of ampicillin was used to select against *E. coli* or Gram-positive contamination (Ashour and El-Sharif, 2007). Since the plasmids that were being used to insert into *A. manganoxydans* SI85-9A1 were either kanamycin or gentamicin resistant, higher concentrations than those listed below for solid media were used. In solid media, 50 $\mu\text{g ml}^{-1}$ was used to inhibit growth of cells that did not contain the appropriate plasmid. Tetracycline cannot be easily used in M and K-media since tetracycline chelates magnesium ions and becomes inactivated, a fact brought about by the high levels of Mg^{2+} in M and K-medium (100 mM Mg^{2+}).

Table 8: Antibiotic MIC for *A. manganoxydans* SI85-9A1

Antibiotic	K ($\mu\text{g ml}^{-1}$)		M ($\mu\text{g ml}^{-1}$)	
	Liquid	Solid*	Liquid	Solid*
Tetracycline	<25	--	25	>60
Ampicillin	>200	>100	200	>200
Kanamycin	5	--	5	<25
Chloramphenicol	--	--	--	--
Gentamicin	--	<20	5	<20

* indicates data from (Caspi, 1996)

Growth Curves

Figure 6 depicts growth of *A. manganoxydans* SI85-9A1 in various media under various conditions. *A. manganoxydans* SI85-9A1 grows very differently between K and M-media with highest density growth in K-medium. *A. manganoxydans* SI85-9A1 usually reached logarithmic phase growth within 72 hours when inoculated from a single, oxidizing colony (diamonds in Figure 6). When M-medium is inoculated with a single colony, logarithmic growth never reaches >15% of growth in K-medium (squares in Figure 6). Since K-medium is the richer medium of the two, it was used for overnight cultures and for when exponential growth phase is needed. *A. manganoxydans* SI85-9A1 will reach logarithmic growth in K-medium within 48 hours (triangles in Figure 6), and exponential growth was seen after only ~24 hours when inoculated from an actively growing liquid pre-culture of *A. manganoxydans* SI85-9A1 (0.01 starting OD₆₀₀).

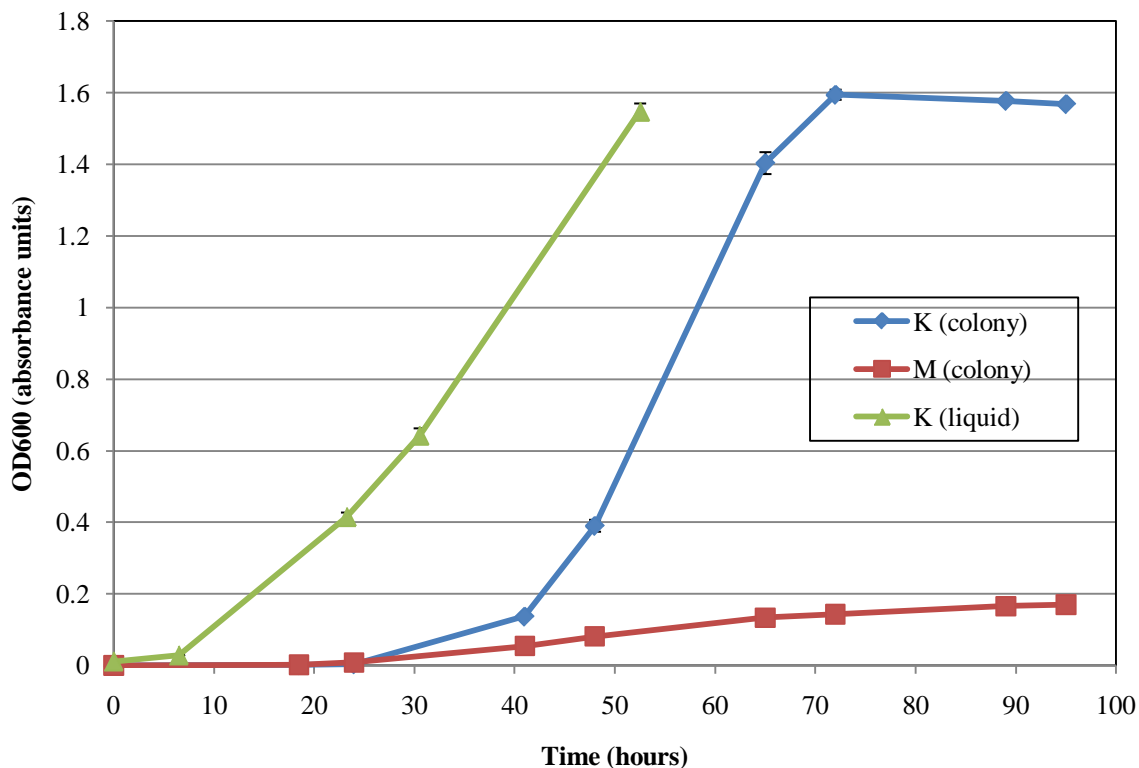


Figure 6: Growth of *A. manganoxydans* SI85-9A1 in M and K-media.
Colony: experiment started from single colony
Liquid: experiment started from actively growing liquid culture

Transformation

As a control for all transformation experiments, different strains of *E. coli* were used with various genetic backgrounds in order to test the widest spread of *E. coli* genetic types. Normal transformation methods may not work on *A. manganoxydans* SI85-9A1 due to the robustness of the cell. Electroporation has been tried on *A. manganoxydans* SI85-9A1 with limited success (Caspi, 1996). Only two electrotransformed colonies appeared, neither of which was stable upon restreaking. It is thought that the need for high salt by *A. manganoxydans* SI85-9A1 for structural integrity would cause electrical arcing, thus electroporation was not repeated. As described in the previous section, a method for chemical transformation was tried that had low efficiency, but still worked for

E. coli cultures. This method did not work for *A. manganoxydans* SI85-9A1 under the conditions tested, although optimization was not attempted. The concentration of CaCl₂ used was 100 mM, only 10-fold higher than the concentration of CaCl₂ in 1x ASW used in M- and K-medium. Generally, for *E. coli* this concentration is sufficient since it is much higher than normal growth conditions, but for halotolerant *A. manganoxydans* SI85-9A1, a higher concentration of salt may be needed or else different salts may produce different results. Incubation times may also be optimized, as well as temperatures.

Since the common methods of chemical and electrical transformation seemed to be inadequate for *A. manganoxydans* SI85-9A1, several exotic methods were tried. Freeze-thaw transformation (Zibat, 2001) has shown to be useful in transforming another halotolerant organism, *Halobacterium salinarum*. This method is simple in that a culture is mixed with plasmid in a buffer and frozen for a period-of-time. This causes sheering forces that disrupt cell walls and allow the possible transfer of plasmid DNA from the suspension into the cell. The cells were still viable afterwards (both *E. coli* and *A. manganoxydans* SI85-9A1), as shown by plating a portion onto non-selective K-media, although nothing ever grew on selective media. The addition of glycerol as a cryoprotectant did not help in transformation efficiency. This method may prove to be more useful after optimization, but the simple method carried out for *A. manganoxydans* SI85-9A1 yielded no transformants.

Tribos transformation (as described in the previous section) is another exotic transformation method that was unsuccessful for *A. manganoxydans* SI85-9A1 under the conditions tested. It has been successfully used to transform *Acinetobacter baumannii*,

Yersinia enterocolitica, and *Bacillus subtilis* with transformation efficiencies comparable to chemical competency ($10^5 - 10^6$ transformants per μg plasmid DNA) (Wilharm et al., 2010). This transformation utilizes nanofibers and specific plating conditions to help drive circular DNA into the cell (Yoshida and Sato, 2009). The firmness of the media was the main variable tested for these experiments. For both *A. manganoxydans* SI85-9A1 and *E. coli*, growth was seen in non-selective media but never in selective media. The original published description (Yoshida and Saeki, 2004) for this technique describes a much more complicated mechanical set-up involving specified rotation speeds and higher spreader pressure compared to what was performed. The necessity for consistent pressure and speeds may be more important than stated by Wilharm et al. (2010). Despite the failure of Tribos transformation to produce transformed *A. manganoxydans* SI85-9A1, it is still believed that further work examining the different variables may allow this technique to work.

Triparental Conjugation with pJH1

Triparental conjugation takes advantage of natural genetic exchange that occurs between organisms of similar and different origins. It was previously tried in *A. manganoxydans* SI85-9A1 with only a few plasmids (pSUP5011, pSUP10220, and pSUP10221 (Simon et al., 1983)) with no success (Caspi, 1996). It was repeated using a suite of plasmids that have been shown to be broad host range and/or able to conjugate within *Pseudomonas* strains. The plasmids that were used conferred resistance to Gm and Km. Since *A. manganoxydans* SI85-9A1 is sensitive to Tc, several plasmids were chosen carrying Tc^R. These turned out to be unusable because the carrier cell (Tam1 *E. coli*) is also resistant to Tc. This produced too much contamination after conjugation that

overgrew possible *A. manganoxydans* SI85-9A1 conjugant growth. Of the plasmids listed in Table 6, only pJH1 conjugated into *A. manganoxydans* SI85-9A1. Conjugation for this plasmid took place over a 48-hour period and transformant colonies were seen in the 10^{-6} dilution after 10-14 days of growth. A major problem that was consistently encountered was the growth of *E. coli* on the plates. This was presumably due to inactivation of the selection antibiotics over the period-of-time tested. In an effort to dilute contaminating *E. coli* cells, high dilutions were plated to give *A. manganoxydans* SI85-9A1 the greatest chance of growth. After 10-14 days of growth, there were two separate types of colonies growing on the plate, one non-Mn(II) oxidizing colony similar to *E. coli* colonies with one colony type much smaller and Mn(II) oxidizing. As shown in Figure 7, upon restreaking of these colonies onto freshly prepared plates (1.5 % agar K with $50 \mu\text{g ml}^{-1}$ Gm and $100 \mu\text{g ml}^{-1}$ Ap; denoted as K/Gm/AP) both colony types still grew.

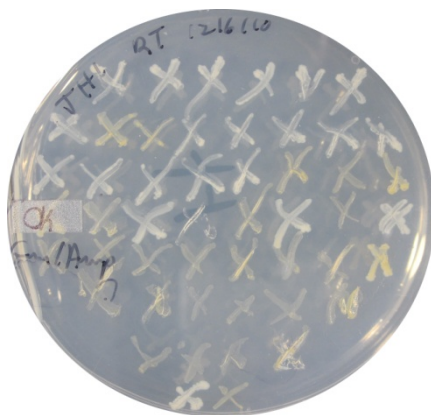
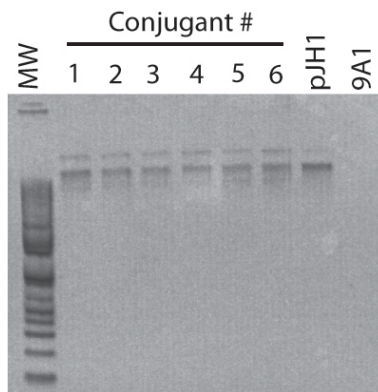


Figure 7: Restreak plate of pJH1 conjugants and contaminant (K/Gm/AP); Oxidizing (orange) and non-oxidizing (white) streaks can be seen

In order to differentiate between the colonies, three different growth conditions were tested. A K/Gm/AP incubated at room temperature will allow growth of all colony types for use as a comparison. A K/Gm/AP plate incubated at 37°C for a week will allow *E. coli* to grow and inhibit *A. manganoxydans* SI85-9A1 growth since it will not grow at

that temperature. An M/Gm/Ap plate incubated at room temperature allows *A. manganoxydans* SI85-9A1 to grow while *E. coli* will not since M-media is too nutrient limited for *E. coli*. The K/Gm/Ap plate incubated at 37°C did not show any growth of the Mn(II) oxidizing colonies and the M/Gm/Ap plate did not show any growth of the non-Mn(II) oxidizing colonies.

In order to confirm that these colonies were indeed *A. manganoxydans* SI85-9A1 and contain the plasmid of interest, the presence of the plasmid and the identity of the organism needed to be confirmed. Six random, oxidizing colonies were selected and grown in a 5 ml culture on K-medium supplemented with 50 µg ml⁻¹ Gm and 100 µg ml⁻¹ Ap. After they had grown to high cell density, a standard miniprep procedure (QIAprep Spin Miniprep Kit) was performed using 4 ml of the actively growing culture. This DNA was collected alongside two controls: an *E. coli* carrying pJH1 and a blank *A. manganoxydans* SI85-9A1 culture. Figure 8 shows that the six randomly selected, oxidizing colonies did indeed contain the plasmid of interest when compared to the pJH1 positive control (labeled pJH1), while *A. manganoxydans* SI85-9A1 contained no isolatable plasmid (labeled 9A1). The presence of the double band is likely associated with super-coiled DNA.



**Figure 8: Plasmid DNA isolated from the six conjugants
1% TBE agarose gel run as described in materials and methods**

In order to confirm the identity of the oxidizing colonies, genomic DNA was purified (Wizard Genomic DNA Purification Kit) from the same conjugants as above and subjected to a PCR screen using primers to test for the presence of the *A. manganoxydans* SI85-9A1 RuBisCO gene. Figure 9 shows that the six conjugants did indeed contain the *A. manganoxydans* SI85-9A1 specific gene, while a general bacterial control (*Pseudomonas putida* GB-1, also a Mn(II) oxidizing strain) did not contain these genes.

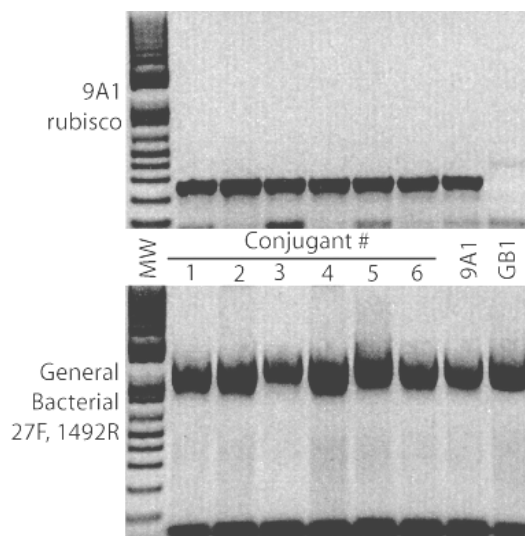


**Figure 9: PCR screen to prove the identity of conjugants.
9A1 rubisco (top gel) denotes PCR screen looking for the presence of *A. Manganoxydans* SI85-9A1 RuBisCO gene. General bacterial (bottom gel) is PCR screen to make sure all isolates were bacteria. *P. putida* GB-1 is used as a negative control for 9A1 rubisco, *A. manganoxydans* SI85-9A1 used as positive control.**

Plasmid pJH1 is simply an *E. coli*-*Pseudomonas* shuttle vector based off pUC18. It contains a pRO1614 *Pseudomonas* replication origin, a ColE1 *E. coli* replication origin a multiple cloning site, and a lacZ' gene for blue/white screening (Lee et al., 2006).

The “Moperon”

The identity of the genes surrounding *mopA* was examined using IMG genome viewer (<http://img.jgi.doe.gov/>) to get a sense of what other possible proteins may work cooperatively with MopA for possible maturation and secretion. As stated in Chapter 2, MopA is likely secreted from the cell through a C-terminal type 1 secretion signal, thus there may be other proteins that are nearby in the genome that assist in type 1 secretion. Below, these proteins are referred to through their locus tag numbers. Figure 10 displays the genes surrounding *mopA*. It should be be noted that 2120 and 2121 overlap by three nucleotides, 2122 is separated on its front and backend by four amino acids from 2121 and 2123, and there is a 77 nucleotide space between 2123 and 2124. This strongly suggests that they are all part of the same regulon.

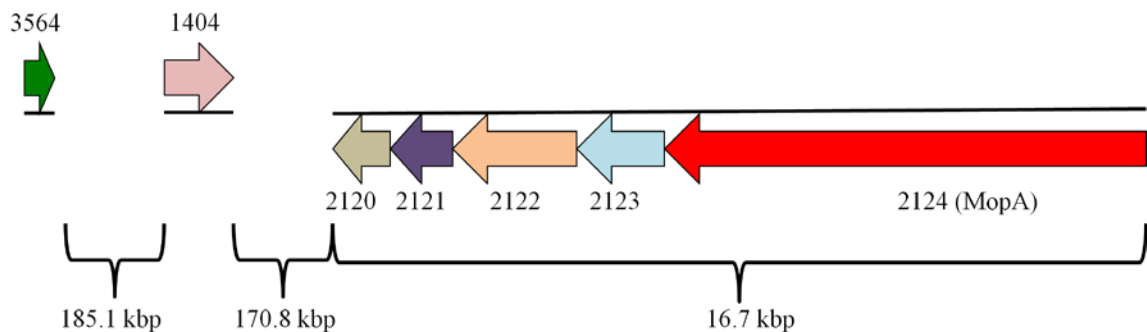


Figure 10: Putative ‘Moperon’
 Numbers refer to locus tag, with full accession SI859A1_0xxxx, where xxxx are the four digits from figure

The predicted properties of all proteins can be found in Table 9. These properties were found in the Joint Genome Institute Integrated Microbial Genome (JGI-IMG) database (<http://img.jgi.doe.gov/cgi-bin/pub/main.cgi>). Including MopA, there are five

total genes that are grouped together. This represents ~16.7kbp of DNA, with MopA (accession no. 2124) the largest at 9894 bp. Two secretion proteins are present (accession no. 2123 and 2121) that are part of the type 1 secretion family of proteins. 2123 is an inner-membrane bound ATP binding cassette (ABC) type transporter protein that uses the energy from ATP to drive transport of unfolded proteins across the cell membrane. 2121 is an adaptor or a membrane fusion protein (MFP) that bridges the periplasmic gap between the ABC transporter protein and the outer membrane transporter. The outer membrane transporter protein is a TolC multi-drug transporter like protein. This gene (1404) is not found close to 2121 and 2123, but is found ~170kbp upstream. This gene has been annotated as a type 1 secretion protein from the TolC family of proteins and is probably used by multiple complexes to transport protein or other chemicals across the membrane. A chaperone protein (SecB) that has been found to be essential for type 1 secretion is also found elsewhere in the *A. manganoxydans* SI85-9A1 genome. SecB protein escorts type 1 secreted protein to their transport protein in the unfolded state. Other proteins found nearby MopA include a related Ca²⁺ binding domain with unknown function (2122) and another protein that has been identified to be related to metalloendopeptidases (2120). These proteins may be involved in proper maturation of MopA to be a fully functional protein.

All proteins necessary for type 1 secretion of MopA (Delepelaire, 2004) appear to be present in the *A. manganoxydans* SI85-9A1 genome. The probable pathway of MopA maturation goes as follows. The ABC transporter is bound to the inner-membrane and is responsible for recognizing the secretion signal of MopA as it has been made but still unfolded. After MopA has been translated by the ribosome, the unfolded protein is

chaperoned through the cell by SecB (3564). SecB keeps MopA in the unfolded state until it reaches the ABC transporter (2123). This protein then dimerizes, recruiting both the adapter protein (2121) and TolC-like protein (1404). This complex spans the periplasm and secretes the protein directly into the extracellular space. MopA is secreted in an unfolded form until it reaches the extracellular space, where it proceeds to fold. It is unknown at this time whether folding requires a chaperone or not. Localization of MopA to the LBOM fraction suggests it may be associated with a membrane-anchored protein; thus, its secretion is most likely near the complex that helps anchor MopA to the extracellular surface.

Table 9: Properties of proteins found near MopA and other accessory proteins

Locus Tag	Name	COG	Family	Length	Notes
'Moperon' genes					
SI859A1_02124	putative hemolysin-type calcium-binding peroxidase protein	RTX toxins and related Ca ²⁺ -binding proteins		3297 aa 9894 bp	MopA
SI859A1_02123	ATP-binding transmembrane ABC transporter protein	ABC-type protease/lipase transport system, ATPase and permease components	type 1 secretion system ABC transporter, PrtD family	589 aa 1770 bp	transmembrane, MopB
SI859A1_02122	possible hemolysin-type calcium-binding region	RTX toxins and related Ca ²⁺ -binding proteins	Hemolysin-type calcium-binding region; Serralysin-like metalloprotease, C-terminal	845 aa 2538 bp	MopC
SI859A1_02121	possible secretion membrane fusion protein	Multidrug resistance efflux pump	Gram-negative bacterial RTX secretion protein D; Type 1 hemolysin secretion membrane fusion protein, HlyD; Single hybrid motif	445 aa 1338 bp	MopD
SI859A1_02120	conserved hypothetical protein	Membrane proteins related to metalloendopeptidase		350 aa 1053 bp	transmembrane, MopE
Other possibly involved genes					
SI859A1_01404	type I secretion outer membrane family protein	Outer membrane protein	type 1 secretion outer membrane protein, TolC family	454 aa 1365 bp	transmembrane,
SI859A1_03564	protein export chaperone SecB	Preprotein translocase subunit SecB	protein-export chaperone SecB	172 aa 519 bp	

This region of the genome could be considered the Mn(II) oxidizing peroxidase operon, or Moperon. The proteins have been renamed in Table 9 to reflect their involvement with MopA secretion and maturation. Their direct activities have not yet been probed due to the lack of a complete genetic system for *A. manganoxydans* SI85-9A1. When a more complete one does become available, these genes should be examined through directed mutagenesis to determine whether these proteins are necessary for MopA secretion, activation, or folding.

Progress on Complementation

Previous work on *A. manganoxydans* SI85-9A1 mutagenesis centered on chemical mutagenesis using ethylmethane sulfonate (EMS) (Caspi, 1996). EMS mutants were prepared and stored at -80°C for further testing when a genetic system for *A. manganoxydans* SI85-9A1 could be developed. Forty such mutants have been recovered, 34 stored in the 1980s by an unknown person, and 7 in the 1990s by a former student (Caspi, 1996). When grown on M-medium, these mutants display varying phenotypes and growth characteristics. These EMS mutants are alive and grew on solid and liquid M and K-medium, though at varying growth rates. Their Mn(II) oxidation phenotype was varied as well, some oxidized faster and some slower or not at all. Table 10 summarizes the growth and Mn(II) oxidizing potential. Identifying the genes disrupted in these mutants will be an invaluable aid to determining what other proteins and regulators are involved in Mn(II) oxidation in this organism.

Table 10: Qualitative Mn(II) oxidation and cell density of EMS mutants
 + : More than wild type; - : less than wild type; o : similar to wild type

STRAIN	Mn(II) oxidation	Cell Density	STRAIN	Mn(II) oxidation	Cell Density
SI85-9A1-EMS 1	--	o	SI85-9A1-EMS 18b	-	+
SI85-9A1-EMS 2	--	o	SI85-9A1-EMS 19a	+++	-
SI85-9A1-EMS 3	o	o	SI85-9A1-EMS 1X	-	o
SI85-9A1-EMS 4A	--	-	SI85-9A1-EMS 2X	-	o
SI85-9A1-EMS 4B	-	-	SI85-9A1-EMS 3X	--	o
SI85-9A1-EMS 5	++	o	SI85-9A1-EMS 4AX	-	+
SI85-9A1-EMS 6	--	+	SI85-9A1-EMS 4BX	-	o
SI85-9A1-EMS 7	-	o	SI85-9A1-EMS 5X	o	o
SI85-9A1-EMS 8	o	o	SI85-9A1-EMS 6X	o	+
SI85-9A1-EMS 9	-	o	SI85-9A1-EMS 7X	--	o
SI85-9A1-EMS 10a	-	o	SI85-9A1-EMS 8X	-	o
SI85-9A1-EMS 10b	-	o	SI85-9A1-EMS 9X	--	+
SI85-9A1-EMS 11	--	+	9A1 EMS 1R	++	o
SI85-9A1-EMS 12	-	o	9A1 EMS 2R	+	-
SI85-9A1-EMS 13	--	o	9A1 EMS 3R	-	-
SI85-9A1-EMS 14	-	-	9A1 EMS 4R	-	-
SI85-9A1-EMS 15	-	o	9A1 EMS 5R	--	-
SI85-9A1-EMS 16	--	o	9A1 EMS 6R	-	--
SI85-9A1-EMS 17	+	+	9A1 EMS 9R	--	-
SI85-9A1-EMS 18a	o	+	WT 9A1	o	o

A second important tool that was previously prepared is a cosmid library containing parts of the *A. manganoxydans* SI85-9A1 genome. This library has previously been screened (Caspi, 1996) to verify that it contains the *A. manganoxydans* SI85-9A1 genome on cosmids and was stored in *E. coli* at -80°C. The library still grows on LB/Ap plates very well, showing that the strain still carries the cosmids. The ultimate goal for these cosmids was to place them into the EMS mutants to try to complement the mutations. Conjugation was tried between the cosmid library and a wild type *A. manganoxydans* SI85-9A1 strain, but no conjugation occurred. If more robust methods of plasmid uptake by *A. manganoxydans* SI85-9A1 are ever found, this should be the first step repeated in order to screen for more proteins involved in Mn(II) oxidation.

Summary

The development of a genetic system in *A. manganoxydans* SI85-9A1 would be beneficial for many reasons. It would allow identification of more proteins within the cell that play a direct role in Mn(II) oxidation and allow us to see how Mn(II) oxidation may play a role in the metabolism of the cell. The fact that both the *A. manganoxydans* SI85-9A1 genome and a partial Mn(II) oxidizing proteome is known, we can directly relate mutagenic studies to known features. This would allow us to gain a greater understanding of Mn(II) oxidation in bacteria. The development of the genetic system is the first step to achieving this goal because not all techniques work for all organisms.

It has been shown above that out of a dozen plasmids tested, *A. manganoxydans* SI85-9A1 will conjugate plasmid pJH1. All other attempts at plasmid transfer have failed, including both traditional and non-traditional methods. This work leads to the following future directions: 1) a framework to refine the conjugation conditions because different methods and vectors have been tried and tested, 2) ideas to try more exotic conditions of plasmid transfer since their initial tests have already been performed, 3) a reference plasmid in pJH1 with which to compare other plasmids in further conjugation studies, and 4) alteration of pJH1 in some way to allow for random/directed mutagenesis. Once a consistent method of transfer of genetic material has been found, complementation studies can be performed with the EMS mutants and the cosmid library. These mutants have the potential to give a lot of information quickly and greatly expand our knowledge of Mn(II) oxidation in *A. manganoxydans* SI85-9A1. Finally, genome mining into the probable route of MopA maturation gives an idea of how MopA is transported to the extracellular space and gives targets for directed mutagenesis studies. These chaperones

and transport proteins could also be useful in the overexpression of MopA; by coexpressing them, we may be able to get higher yields of soluble protein for structural and mechanistic studies.

Whatever the next path in *A. manganoxydans* SI85-9A1 genetics, patience is needed as well as an active imagination.

Chapter 4: The Mechanism of Mn(II) oxidation *in vivo* and *in vitro*

Introduction

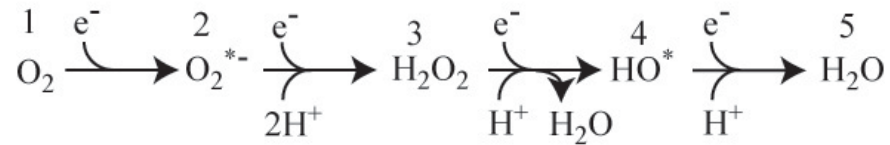
It is not known how oxygen and Mn(II) react to form Mn oxides. Reactive oxygen species (ROS) are an important group of radical species that have been implicated in Mn(II) oxidation (Hansard et al., 2011; Learman et al., 2011). Thus, in order to fully understand the mechanism of Mn(II) oxidation, the role of ROS must be studied. The interplay between Mn and oxygen is well documented in enzymology (Sigel and Sigel, 1999). In terms of manganese utilizing enzymes, there are several very important proteins. Manganese superoxide dismutases react with superoxide, catalyzing the disproportionation of superoxide to dioxygen and hydrogen peroxide. This helps protect the cell from oxidative stress such as DNA double stranded breaks and inactivation of metalloenzymes (Imlay, 2008). Manganese catalases perform a similar oxygen detoxification function, but with hydrogen peroxide as a reactant forming dioxygen and water. The oxygen-evolving complex of the photosynthetic electron transport chain

contains a tetranuclear manganese cluster that performs a four-electron oxidation of two molecules of water to form one molecule of dioxygen. Without the tetranuclear manganese complex producing oxygen, aerobic life as we know it would not have been able to evolve (Yocum and Pecoraro, 1999).

ROS have been well studied for their roles in cell damage, signaling, and other processes (Imlay, 2008). In respiration, dioxygen is used as a terminal electron acceptor by the cellular electron transport chain. It is reduced to water in four sequential one-electron reductions by complex IV of the electron transport chain in Eukarya, Archaea, and Bacteria. Since the cell membrane is highly permeable to dioxygen, the ubiquity of it both inside and outside of the cell leads to problems as well. Dioxygen is a ready electron acceptor, even without its reduction coupled to proteins. This means that it is able to accept electrons from various other sources within a cell, with superoxide being formed. The sources of electrons leading to superoxide production can include exposed redox centers of proteins (particularly flavoenzymes) and free conjugated organic molecules. Hydrogen peroxide can also be formed within the cell through an additional reduction of superoxide or through photochemical oxidation of water (Imlay, 2008). The rate at which superoxide and hydrogen peroxide can be produced in the cell has been measured at $5 \mu\text{M s}^{-1}$ and $15 \mu\text{M s}^{-1}$ respectively (Korshunov and Imlay, 2006). In addition to superoxide and hydrogen peroxide, the hydroxyl radical can form from hydrogen peroxide through the Fenton reaction. This is one of the more toxic ROS and reacts with any biomolecules within the cell, including DNA and protein catalytic centers such as iron sulfur clusters (Imlay, 2008).

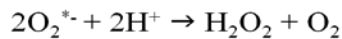
Equation 3 displays the sequential one electron reduction of dioxygen to two molecules of water:

Equation 3: Sequential one electron reductions forming reactive oxygen species
1: dioxygen; 2: superoxide; 3: hydrogen peroxide; 4: hydroxyl radical; 5: water
 adapted from Imlay (2008)



With all these ROS formed within the cell through the processes listed above and the resulting damage they can cause, there needs to be a mechanism to protect the cell from ROS. Superoxide dismutases (SOD, discussed previously in this chapter), catalases (Cat, discussed previously in this chapter), and peroxidases (discussed previously in Chapter 2) are metalloenzymes that have evolved to help the cell fight ROS. SOD catalyzes the disproportionation of superoxide to dioxygen and hydrogen peroxide in a two-electron transfer reaction, seen in Equation 4:

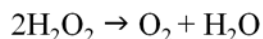
Equation 4: Reaction catalyzed by superoxide dismutases



The mechanism of SOD catalysis consists first of a reduction of the metal center with the release of dioxygen followed by an oxidation of the metal center back to its resting state and the release of hydrogen peroxide. SOD has various isoforms containing different catalytic metals such as Mn, Fe, Ni, and Cu/Zn. MnSOD is found in Eukarya, Archaea, and Bacteria, which shows the ubiquity of organisms that carry out extensive reactions between manganese and dioxygen (Valentine, 2007).

Catalase catalyzes the heterolytic cleavage of hydrogen peroxide to dioxygen and water in the following two-electron transfer reaction (Valentine, 2007), seen in Equation 5:

Equation 5: Reaction catalyzed by catalases



Catalases have two different types that belong to two different protein families but perform the same chemistry. Type I catalases are heme dependent and exhibit a reaction mechanism similar to peroxidases. Type II catalases utilize a dimanganese core that acts in a similar manner to Type I catalases and peroxidases with a two electron catalytic cycle.

Reactive oxygen species have been implicated to play a role in Mn(II) oxidation. Specifically, superoxide (O_2^-) has been found to react with Mn(II), producing Mn(III) and hydrogen peroxide (H_2O_2) in the presence of Mn(III) chelators such as pyrophosphate (PP_i) and other organic acid chelators (Learman et al., 2011). This work was performed using SOD as well as other ROS scavenging molecules and metals to inhibit Mn(II) oxidation (Learman et al., 2011). Equation 1 can be broken down into component reactions, with the initial formation of Mn(III) as an intermediate through reaction with superoxide shown in Equation 6 (Höfer and Schlosser, 1999; Learman et al., 2011):

Equation 6: Possible Mn(II→III) oxidation



Other work has shown that in the open ocean, superoxide and Mn(II) can react abiotically at nanomolar concentrations of Mn(II) (Hansard et al., 2011). This can occur

with high amounts of PP_i or other Mn(III) chelators and free Mn(II) in the open oceans was shown to be a large potential sink for O_2^- (Hansard et al., 2011).

The subsequent reaction between Mn(III) and oxygen (as O_2 , O_2^- or H_2O_2) is unknown and it is not known whether this reaction occurs with hydrogen peroxide. In *A. manganoxydans* SI85-9A1, the mechanism of Mn(II) oxidation is not known and can only be speculated about from the information presented in Chapter 2. Since MopA is a peroxidase, hydrogen peroxide would play a role somehow although possibly not in the same way as in MnPs. In order to test the different forms of oxygen that may play a role in Mn(II) oxidation, various antioxidant enzymes were added to the Mn(II) oxidation assay to see how their addition affected Mn(II) oxidation. The use of SOD and/or catalase in Mn(II) oxidation assays would allow the observation of how the removal of superoxide and/or hydrogen peroxide from the reaction assay affects the resulting Mn(II) oxidation. We would then be able to deduce how superoxide and hydrogen peroxide might fit into the overall reaction scheme. To determine if Mn(II) oxidation is a two-step process, the reaction needs to be split up into its component parts. By using pyrophosphate (PP_i) to trap Mn(III) and utilizing Mn(III) PP_i as a starting material, the Mn(II \rightarrow III) and Mn(III \rightarrow IV) reactions can be observed on their own. The purified LBOM proteins may not contain all of the necessary components for Mn(II) oxidation to occur and may be different than what is found *in vivo*. By combining observations from *in vitro* and *in vivo* experiments using SOD and catalase, we may be able to begin to assign specific roles for superoxide and hydrogen peroxide.

Methods and Materials

Cultivation

A. manganoxydans SI85-9A1 was grown in six 1 L batches in 2.8 L baffled Fernbach flasks at room temperature at 150-200 RPM in M-medium (Tebo et al., 2007). M-medium is a minimal nutrient medium made with autoclaved 1x artificial seawater (ASW; 100 mM MgSO₄, 20 mM CaCl₂, 600 mM NaCl, 20 mM KCl), 0.05 g L⁻¹ Bacto yeast extract and 0.05 g L⁻¹ Bacto peptone (Fisher Scientific, USA). The following are added to the above post autoclaving and are filter sterilized (0.2 μm) immediately prior to addition to the medium: 20 mM HEPES pH 7.8 (1 M initial), 2 mM KHCO₃ (1 M initial), 100 μM MnCl₂ (1 M initial), and 3 mg ml⁻¹ ferric ammonium citrate (15 mg ml⁻¹ initial). Both MnCl₂ and ferric ammonium citrate were freshly prepared prior to addition. As carbon sources, 10 mM glycerol (5 M initial) and 10 mM sodium formate (5 M initial) were added to the base M-medium, both filter sterilized (0.2 μm) immediately prior to addition. As an inoculum, a 5 ml overnight K-medium (see Chapter 3) culture is prepared from a single Mn(II) oxidizing colony grown on an M-media plate. From this overnight culture, 100 μl, is used to inoculate each flask. For solid M-medium, 15 g L⁻¹ noble agar is used.

In vitro assays

Reagents

A 1 mM Mn(II) was prepared from solid MnCl₂ tetrahydrate (Fisher, USA) prepared in 18 Ω milliQ water. A 5 mM pyrophosphate (PP_i) solution was prepared by dissolving NaPP_i decahydrate (Sigma-Aldrich, USA) into 18 Ω milliQ water. To prepare Mn(III)PP_i, Mn(III) ion must be dissolved in a 5X molar excess of PP_i to ensure complete

dissolution, therefore Mn(III) acetate dihydrate (Sigma-Aldrich, USA) was added to a concentration of 1 mM into the above 5 mM PP_i solution and allowed agitate on the rotary shaker at 35 RPM until all solids were visibly dissolved. This solution was then filtered (0.2 µm) and stored at 4°C until use. Leucoberbelin Blue reagent (LBB: 0.4% w/v LBB solid, 45 mM acetic acid) was prepared ahead of time and stored at 4°C shielded from light. Hydrogen peroxide (50% stock solution, Fisher, USA) was freshly prepared by dilution of stock hydrogen peroxide to 100 µM via serial dilutions in 18 Ω milliQ water. Two different batches of CuZnSOD were used (S5395 and S7571, Sigma, USA). A stock solution was prepared at 500 µM (58 kU ml⁻¹) in 18 Ω milliQ water and frozen at -20°C until use. A stock solution of catalase (C1345, Sigma, USA) was prepared at 1.8 µM (2 kU ml⁻¹) in 18 Ω milliQ water and frozen at -20°C until use.

Protein Isolation

Mn(II) oxidation activity has been localized to loosely bound outer membrane proteins (LBOM). To obtain this protein fraction, 6 L of actively oxidizing *A. manganoxydans* SI85-9A1 was collected into one pellet (approximately 4-6 g) at 8,000 rotations per minute (RPM) for 10 minutes using a Sorvall RC5-B centrifuge with a Fiberlite F10-6x500y fixed angle rotor at 4°C. Once all of the *A. manganoxydans* SI85-9A1 was collected into one pellet, it was resuspended in 100 ml of a high salt Tris buffer (100 mM Tris pH 7.5, 1 M KCl) and ascorbate was added to 200 µM in order to reduce all Mn oxides. This salt/cell solution was stirred vigorously for 4 hours at 4°C. The cells were pelleted again and the supernatant was collected and filtered to remove residual cells. The supernatant was then concentrated to a volume of 5-15 ml using a 400 ml Amicon stirred ultraconcentration cell fitted with a 10 kDa MWCO membrane (Millipore

Ultrafiltration membranes, Millipore, USA). This ultraconcentrated fraction is considered the loosely bound outer membrane (LBOM) protein fraction. The LBOM fraction was dialyzed in 20 mM HEPES buffer pH 7.8 using 10 kDa MWCO dialysis membranes. Dialysis proceeded in three phases of 4 L in 20 mM 4-(2-hydroxyethyl)-1-piperazineethanesulfonic acid (HEPES) dialysis buffer as follows: overnight at 4°C, 2 hours at room temperature, and 3 hours at room temperature; all with ~25 RPM stirring. The final, dialyzed fraction was concentrated using a 10 kDa cutoff spin column (Amicon Ultra-4 or -15) to ~1 ml and stored at 4°C until use. Protein concentration was measured using the standard Bradford Assay (Pierce, USA).

Assay Conditions

LBOM protein concentration for all assays was fixed at 100 $\mu\text{g ml}^{-1}$, the reactions were performed in 20 mM HEPES pH 7.8, and 100 $\mu\text{M Mn(II)}$ was used. For these assays, 10 $\mu\text{M H}_2\text{O}_2$, 5 $\mu\text{M SOD}$ (580 U ml^{-1}), and either 92 or 9.2 nM catalase (described below; 100 or 10 U ml^{-1}) were used. Assays were performed in triplicate in flat-bottomed 96-well microtiter plates (Fisher, USA) with a volume of 200 μl at room temperature. In order to test for abiotic Mn(II) oxidation or other interferences, blanks were made that either had no Mn(II) or no LBOM. LBB measurements for each time point were made by mixing 50 μl of sample with 250 μl of LBB. This was allowed to react for 15 minutes in the dark and measured on a Molecular Devices SpectraMax M2 UV-Vis microplate spectrophotometer at 618 nm. The absorbance measurements were converted to a relative concentration of Mn oxides through a KMnO_4 standard curve (Tebo et al., 2007).

***In vivo* Assays**

Reagents

Mn(II), LBB, superoxide dismutase, and catalase solutions were prepared as described for the *in vitro* assays. A xanthine (Sigma, USA) stock solution was freshly prepared by dissolving 15.2 mg of solid in 10 ml of 25 mM NaOH (10 mM xanthine). After the solid had fully dissolved, it was further diluted to 150 μ M in 20 mM HEPES pH 7.8 buffer.

Ascorbate washed whole cells

To obtain ascorbate-washed whole cells for use in Mn(II) oxidation experiments, 2 L of actively oxidizing *A. manganoxydans* SI85-9A1 were collected via centrifugation by an RC5-B centrifuge with a Fiberlite F10-6x500y fixed angle rotor. The cell pellet was resuspended in 100 ml of 20 mM HEPES pH 7.8 buffered artificial seawater (BASW). In order to remove the Mn oxides, ascorbic acid (Acros, USA) was added to a final concentration of 200 μ M and allowed to sit on ice or at 4°C for at least 30 minutes, or until all oxides were reduced. The suspension was pelleted, supernatant discarded, and the cell pellet was resuspended in 100 ml BASW to dilute residual ascorbic acid. This was repeated four more times for a total of five times and the cells were finally resuspended in 100 ml BASW. OD₆₀₀ was measured in a 1.5 ml polystyrene cuvette (Fisherbrand, USA) in the spectrophotometer (Molecular Devices SpectraMax M2 UV-Vis microplate spectrophotometer).

Assay conditions

For all assays, cell density was fixed at an OD₆₀₀ of approximately 1 by diluting the ascorbate washed cells in BASW. The assays were performed while shaking (~200

RPM), in triplicate, at room temperature in a volume of 2 ml. In order to test for abiotic Mn(II) oxidation or other interferences, two sets of blanks were made: one with no Mn(II) but with ascorbate washed cells and another without ascorbate washed cells but with Mn(II). LBB measurements for each time point were made by mixing 30 μ l or 60 μ l of sample with 300 μ l of LBB. The ratio of sample:LBB changed based upon the intensity of Mn(II) oxidation seen in each tube. This was allowed to incubate in the dark. After 15 minutes, the cells were removed by centrifugation and 300 μ l of each sample was measured in a microtiter plate on a Molecular Devices SpectraMax M2 UV-Vis microplate spectrophotometer at 618 nm. The absorbance measurements were converted to a relative concentration of Mn oxides through a KMnO_4 standard curve (Tebo et al., 2007).

Results and Discussion

Disruption of *in vitro* Mn(II) oxidation

It has been shown in *Roseobacter* AZWK-3b that Mn(II) oxidation is decreased as more and more superoxide is removed from the system (by increasing SOD concentration). In addition, the reaction between superoxide and Mn(II) may be an abiotic process with the superoxide produced by the organism (Learman et al., 2011). An initial experiment was performed where SOD and catalase (loss of superoxide and loss of hydrogen peroxide respectively) were added to the standard Mn(II \rightarrow IV) oxidation assay as seen in Figure 11. The loss of superoxide seems to reduce Mn(II) oxidation, suggesting that the reaction is requires superoxide. When the concentration of hydrogen peroxide was reduced using catalase, overall Mn(II) oxidation was not affected. This suggests that Mn(II \rightarrow IV) oxidation is more sensitive to superoxide than hydrogen peroxide. Since

Mn(II→IV) oxidation may occur in two steps as described earlier, it is necessary to determine at which step superoxide and hydrogen peroxide affect Mn(II) oxidation.

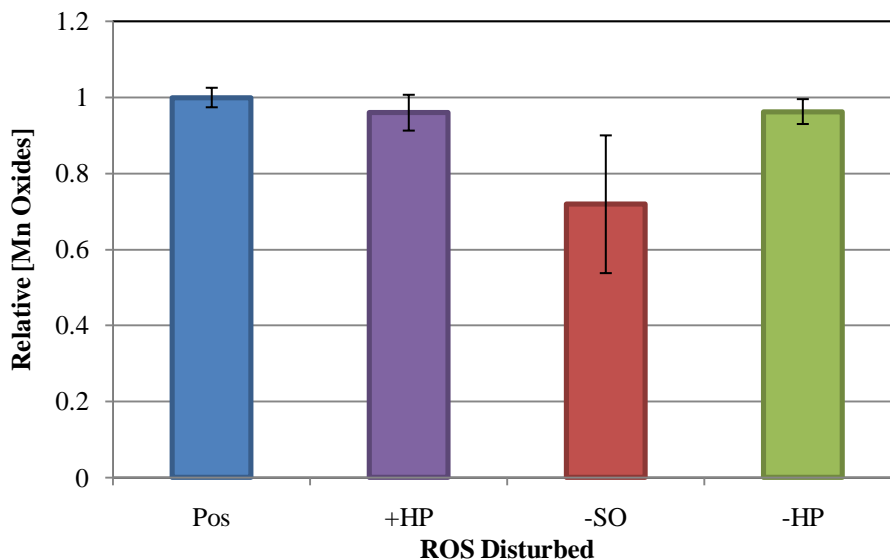


Figure 11: *In vitro* Mn(II→IV) oxidation disruption
Perturbation of superoxide and hydrogen peroxide separately
Pos: Mn Oxidation with no additions; +HP: 10 μ M hydrogen peroxide; -SO: 5 μ M superoxide dismutase; -HP: 9.2 nM Catalase

Figures 12, 13, 14, and 15 show what happens when superoxide and hydrogen peroxide are removed from Mn oxidation assays containing the LBOM proteins and Mn(II) or Mn(III). The oxidation of Mn(II→IV) (Figure 11) was reduced markedly by the loss of superoxide in the system and was unaffected by the loss of hydrogen peroxide (HP). The changes are not very large though, indicating that the particular LBOM protein preparation may have been able to overcome the loss of superoxide. This experiment has been repeated several times and each time SOD always decreases oxidation, although to varying degrees. This variability is presumed to be due to different concentration of the Mn(II) oxidase in solution since the LBOM protein composition varies for each preparation. The fact that addition of hydrogen peroxide (+HP column) showed no additional Mn oxidation for Mn(II→IV), Mn(II→III), or Mn(III→IV) oxidation is not

surprising. The system may already be saturated with enough hydrogen peroxide for catalysis to occur so additional hydrogen peroxide will not have an effect.

Figure 12 displays Mn(II) oxidation disruption performed in the presence of pyrophosphate (PP_i), a Mn(III) chelating molecule that will trap Mn(III) at Mn(III)PP_i and only allow Mn(II→III) oxidation to occur. Addition of a 5-fold higher concentration of PP_i over Mn(II) (500 μM PP_i compared to 100 μM Mn(II)) traps Mn(II) oxidation at the middle step and stops formation of Mn oxides. The loss of superoxide in the system stops formation of Mn(III). This may indicate that superoxide indeed plays a role in Mn(II→III) oxidation *in vitro*. Additionally, the loss of hydrogen peroxide from the system seems to play no role for this half of Mn(II) oxidation. Taken together, this could mean that superoxide is the key molecule responsible for this chemistry, rather than hydrogen peroxide or hydroxyl radical formed by reduction of superoxide.

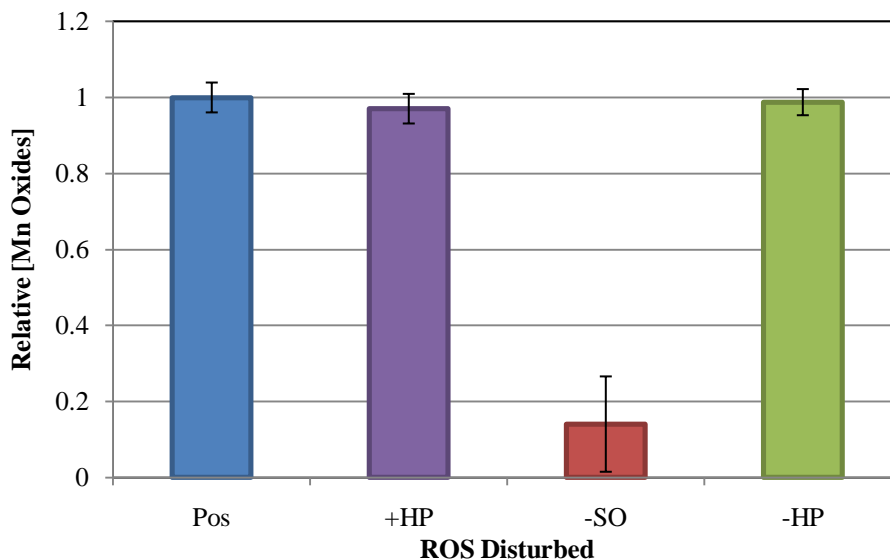


Figure 12: *In vitro* Mn(II→III) oxidation disruption
Perturbation of superoxide and hydrogen peroxide separately
Pos: Mn Oxidation with no additions; +HP: 10 μM hydrogen peroxide; -SO: 5 μM superoxide dismutase; -HP: 9.2 nM Catalase

Figure 13 displays Mn(III→IV) oxidation disruption. Mn(III) is completely unstable in aqueous solutions without stabilization by a chelating molecule. PP_i was used here to stabilize Mn(III) so it could be oxidized, although without the 5-fold excess of added PP_i as in the Mn(III) trapping experiments. The loss of superoxide again reduces this reaction, meaning that superoxide may be important for this half reaction although may play a different role as discussed below. The loss of hydrogen peroxide reduces overall Mn(III) oxidation as well. Since this was such a minor reduction in overall Mn(III) oxidation for that particular experiment, it was repeated, this time with 10-times more catalase added to the assay (92 nM compared to 9.2 nM).

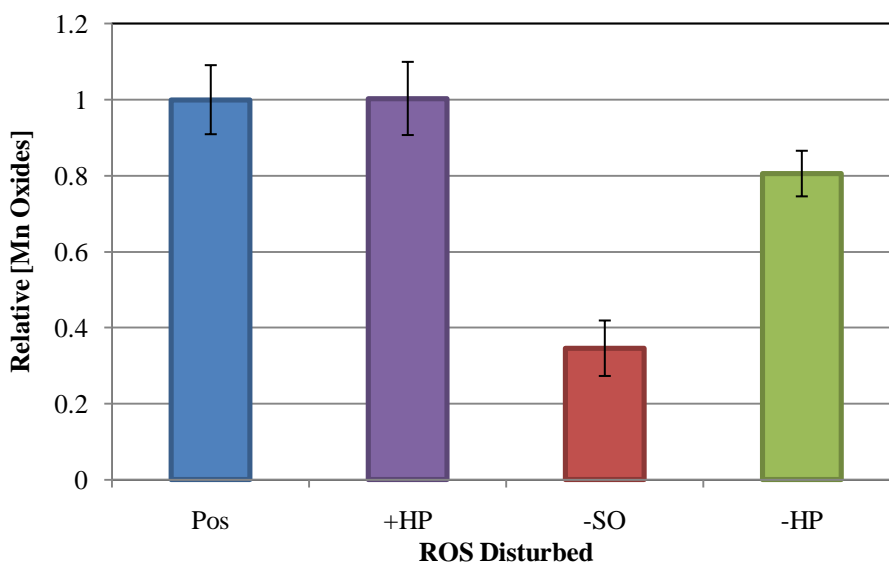


Figure 13: *In vitro* Mn(III→IV) oxidation disruption
Perturbation of superoxide and hydrogen peroxide separately
Pos: Mn Oxidation with no additions; +HP: 10 μM hydrogen peroxide; -SO: 5 μM superoxide dismutase; -HP: 9.2 nM Catalase

Figure 14 shows that when additional catalase was added, which should cause an even greater loss of hydrogen peroxide, Mn(III) oxidation was decreased to almost zero and on par with the loss of superoxide. Taken together, this data may implicate hydrogen peroxide as being important for Mn(III→IV) oxidation. Hydrogen peroxide may be

produced endogenously by the cell through enzymatic processes (possibly from oxidation of Mn(II→III)), or by other unknown means.

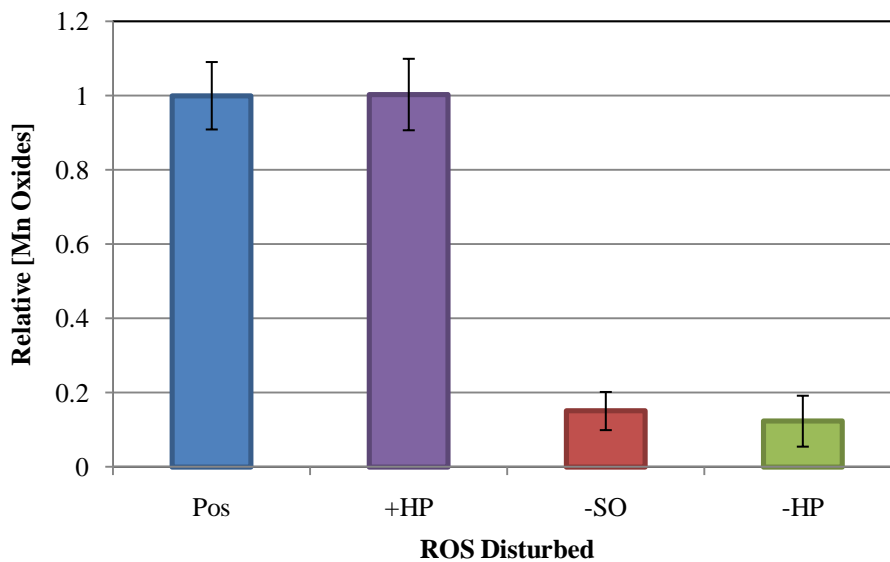


Figure 14: *In vitro* Mn(III→IV) oxidation disruption; 10x [Cat] over Figure 13
Perturbation of superoxide and hydrogen peroxide separately
Pos: Mn Oxidation with no additions; +HP: 10 μ M hydrogen peroxide; -SO: 5 μ M superoxide
dismutase; -HP: 92 nM Catalase

As seen in Figure 15, when both superoxide and hydrogen peroxide were disturbed in the assays, no Mn(II→IV) oxidation occurred. This was not performed with Mn(III→IV) though so nothing can be said about what happens when all ROS are removed from that half reaction.

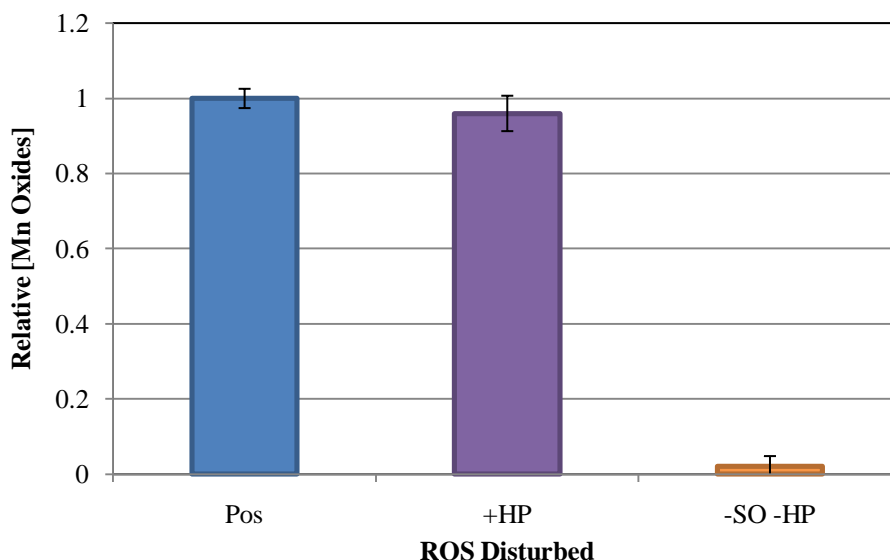


Figure 15: *In vitro* Mn(II→IV) oxidation disruption
Perturbation of superoxide and hydrogen peroxide combined
Pos: Mn Oxidation with no additions; +HP: 10 μ M hydrogen peroxide; -SO: 5 μ M superoxide dismutase; -HP: 92 nM Catalase

It should be noted that the individual LBOM protein preparations have a lot of variability among them. Each preparation will have varying amounts of active protein. Every effort was taken to produce consistent LBOM preparations, but variability in the original culture in terms of amount of Mn(II) oxidation and growth stage may play a role in final protein isolation. These assays were meant to be a bulk approach that should potentially destroy all ROS in the system with observation of the resulting Mn(II) oxidation. The same type of CuZnSOD was used on all the above experiments, as well as the same batch of catalase, so the variability in the experiments are not due to these additions

Disruption of *in vivo* Mn(II) oxidation

In order to study the effect of Mn(II) oxidation with intact *A. manganoxydans* SI85-9A1 cells, an ascorbate washed protocol was developed. This protocol removes Mn oxides with 200 μ M ascorbate, followed by four washing steps using BASW. The cells

were then added to the standard Mn(II) oxidation assay as if they were a reagent. This was then allowed to react with Mn(II) and either SOD or catalase, at which point LBB was added and the overall level of Mn(II) oxidation was measured.

Figure 16 displays how high levels of SOD and catalase effect Mn(II) oxidation over time. High levels of SOD and catalase were necessary to cause any changes in Mn(II) oxidation because the cells most likely have the ability to overcome the effects of SOD and catalase by making its own ROS for use in Mn(II) oxidation.

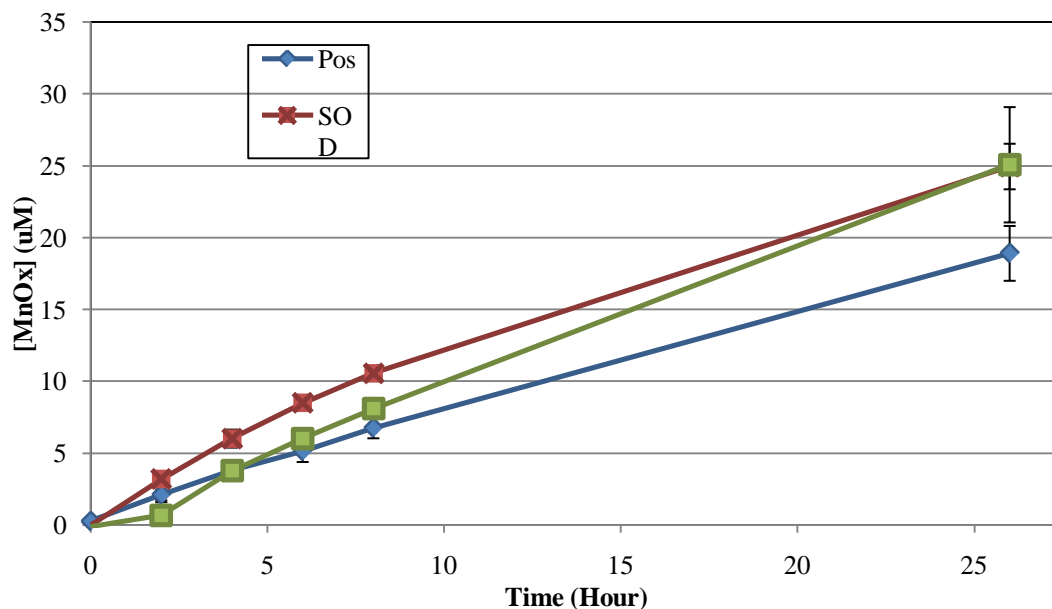


Figure 16: Time course of Mn(II) oxidation *in vivo* 50 μ M SOD or 92 nM catalase

The cause of increased Mn(II) oxidation at high levels of SOD is interesting since it goes against what was found *in vitro*. As superoxide concentration is decreased (increasing SOD), the reaction equilibrium may be shifted. It would initially go down since superoxide is predicted to react with Mn(II) to form Mn(III) and hydrogen peroxide: Le Chatelier's Principle would predict that the loss of a reactant would shift the equilibrium to the reactants. With excess SOD present, there may be a role for the hydrogen peroxide produced by SOD in its reaction with superoxide (Equation 4). If

hydrogen peroxide is utilized to oxidize Mn(III→IV) then increasing hydrogen peroxide concentration may drive the rate of that reaction forward and more Mn oxides would be produced. This would reduce the overall concentration of Mn(III), which would in turn drive the first step forward using whatever superoxide was produced by the cells naturally.

The effect of reduced hydrogen peroxide concentration (high catalase) causing an increase in overall Mn(II) oxidation is puzzling. This too can be explained by using Le Chatelier's principle. According to Equation 6, hydrogen peroxide is a product of the reaction of Mn(II) with superoxide. If this is removed, then the equilibrium of the Mn(II→III) reaction shifts towards the products. This would produce more Mn(III) and Mn oxides can form from Mn(III) both biotically and abiotically. This could increase the rate of oxidation for Mn(II) since more of it is being oxidized to Mn(III).

An interesting phenomenon was discovered while trying to produce superoxide using the xanthine oxidase *in vitro* assay. When xanthine is oxidized by xanthine oxidase, ROS are formed. This reaction produces both hydrogen peroxide and superoxide. It is used as a standard superoxide generation assay for *in vitro* assays (Galbusera et al., 2006). It was used here to produce superoxide to see if an increase in oxidation occurred. The results were variable, presumably due to possible inactivation of xanthine oxidase multiple from freeze-thaw cycles of the stock solution. In spite of this, the addition of xanthine alone produced surprising results *in vivo*. Figure 17 displays how increasing levels of xanthine cause increasing Mn(II) oxidation compared to abiotic controls. The reason for this increase of oxidation may be as follows: *A. manganoxydans* SI85-9A1 contains a copy of the gene encoding xanthine oxidase which is most likely expressed

within the cell in nucleotide biosynthesis. Thus, *A. manganoxydans* SI85-9A1 may be able to use xanthine to produce ROS and increase Mn(II) oxidation on its own. Therefore, *A. manganoxydans* SI85-9A1 may have other systems to produce ROS either specifically or non-specifically.

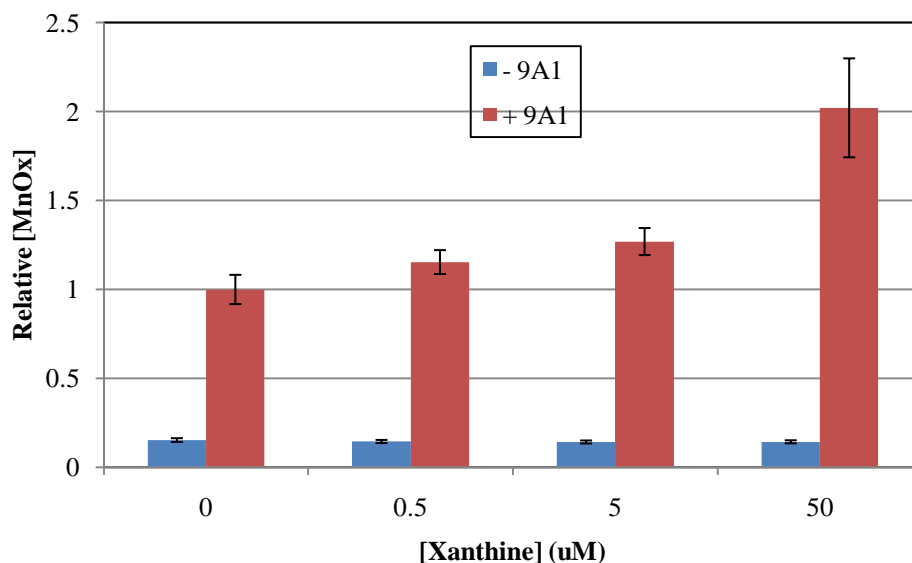


Figure 17: Effect of xanthine concentration on *in vivo* Mn(II) oxidation

Summary

The effect of antioxidant enzymes on Mn(II) oxidation has been investigated and several important clues have been found as to the mechanism of Mn(II) oxidation. It has been shown that superoxide seems to be essential for Mn(II→III) oxidation while hydrogen peroxide may be necessary for Mn(III→IV) oxidation *in vitro*. This would corroborate previous reports that Mn(II) can react with superoxide (Learman et al., 2011), although abiotic oxidation has never been seen by this author even though it has been reported in the literature (Hansard et al., 2011; Learman et al., 2011). The fact that hydrogen peroxide is necessary for Mn(II→IV) oxidation goes along with MopA being necessary for overall Mn(II) oxidation. Since MopA is a peroxidase protein, it would need hydrogen peroxide in order to perform its chemistry to oxidize Mn(III). This

hydrogen peroxide may be made by the cell through a complex of proteins, similar to what has been found in fungi (Schlosser and Hofer, 2002). The loss of superoxide by addition of superoxide dismutase reduces Mn(II) oxidation in all cases tested.

Another observation on the role of ROS in Mn(II) oxidation comes from *in vivo* disruption of the oxygen equilibrium within the systems tested. Addition of high amounts of SOD and catalase disrupt Mn(II) oxidation, causing more oxidation to occur. This seems to be counter to the *in vitro* results, where SOD and catalase decrease oxidation. A possible explanation for the discrepancies could be that the cell is able to ramp up its own production of these ROS proportional to the amount of ROS that is removed by SOD and catalase. This may set off catalytic reaction that increase the overall Mn oxides within the culture compared to the control. The *in vivo* results are much more complicated due to the fact that the cell are still living and actively oxidizing, with all cellular processes active. The *in vitro* system does not have ways to overcome the loss of ROS and therefore may provide a better picture of what is happening within the cell.

If hydrogen peroxide is truly the reactant for Mn(III) oxidation, the possible reaction would be simply the addition of Mn(III) to Equation 2, as seen below in Equation 7:

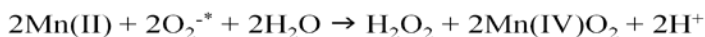
Equation 7: Possible reaction catalyzed by MopA for Mn(III→IV) oxidation *in vitro*



This could provide the cell with energy since the electrons from this reaction may be able to be shuttled into the cell for use in metabolism. When Equation 7 is added to the equation proposed by Learman et al. (2011) for the oxidation of Mn(II→III) (Equation 6), the following reaction (Equation 8) may be the sum Mn(II→IV) oxidation containing the

ROS in place of O₂ in Equation 1. Hydrogen peroxide is a product of this overall reaction since the first reaction must turnover twice to make 2 molecules of Mn(III) for the peroxidase reaction to occur. This creates an excess of hydrogen peroxide, which may help drive the reaction forward to make Mn oxides.

**Equation 8: Possible Mn(II→IV) oxidation
containing superoxide and hydrogen peroxide**



These observations may provide a starting point for further examination of the role of ROS in Mn(II) oxidation. More work should be done with varying levels of SOD and catalase and careful preparation of the assays to perform stoichiometry analysis. This would be important in order to determine how many superoxide or hydrogen peroxide molecules are needed to oxidize Mn(II) or Mn(III). These assays must also be broken up into the component reactions and studied as described but following only the half reactions. Definitive evidence as to the nature of the reactions would be achieved with the use of O¹⁸ and Mn⁵⁴ isotope experiments that would allow us to follow the oxygen or manganese in the system and see where each isotope goes when specific reactions are allowed to occur. Finally, either purification of high levels of native protein or heterologous expression of the protein would allow us to study the reactions using more simple protein complexes under more controlled conditions. Hopefully the observations in this chapter will aid identification of the Mn(II) oxidation components in the future.

Chapter 5: Summary and Future Directions

Resolving the mechanism and reasons of Mn(II) oxidation in bacteria is a difficult task that has been explored here. The role of ROS is still uncertain and more needs to be done to figure out how ROS relates to Mn(II) oxidation. Many ideas have been presented as to the function of MopA as well as the potential use of Mn(II) oxidation by *A. manganoxydans* SI85-9A1.

MopA was identified as the major portion of all fractions from the purification strategy presented in Chapter 2. An in gel Mn(II) oxidation assay and heme activity stain correlated Mn(II) oxidation to heme activity from the LBOM proteins of *A. manganoxydans* SI85-9A1. This gave credence to the theory that MopA plays a role in Mn(II) oxidation. The MS data showed that the extracellular portion of *A. manganoxydans* SI85-9A1 is made up predominantly of MopA, with the rest being transport proteins of the ABC and TRAP families. The fact that an MCO was also found in this MS data suggests that there may be a complex of proteins including an MCO that contribute to Mn(II) oxidation. The relationship of MopA to other proteins of similar structural form and possible roles of MopA were discussed. It is clear that this is a new

type of peroxidase that performs interesting chemistry and is different from both types of previously described Mn(II) oxidases: fungal MnPs and bacterial MCOs.

The development of a genetic system is necessary to study Mn(II) oxidation from a genetic standpoint. This is the one piece missing, since the genome of *A. manganoxydans* SI85-9A1 has been published (Dick, Podell, et al., 2008) and a Mn(II) peroxidase has been identified (Anderson, Johnson, et al., 2009). Through the use of mutation analysis, other components necessary for Mn(II) oxidation can be found. This study involved initial method development for inserting plasmids into *A. manganoxydans* SI85-9A1. The MIC for various antibiotics for *A. manganoxydans* SI85-9A1 was determined and multiple methods of plasmid transfer were attempted. Success was found with conjugation and a plasmid named pJH1. This is a repeatable procedure and is the first stably incorporated plasmid into *A. manganoxydans* SI85-9A1. Further work needs to be performed to adapt this plasmid or find other plasmids for future genetic screening and apply the *A. manganoxydans* SI85-9A1 cosmid library to screen the EMS mutants for their Mn(II) oxidation mutations.

The use of antioxidant enzymes has allowed observation of the ways in which ROS are involved with Mn(II) oxidation. *In vitro*, SOD and catalase are both able to influence Mn(II) oxidation chemistry, with SOD influencing Mn(II→III) and Mn(III→IV) oxidation and catalase specifically influencing Mn(III→IV) chemistry. This shows that superoxide is involved with the first half of Mn(II) oxidation while hydrogen peroxide is involved with the second part. *In vivo*, SOD and catalase influence Mn(II) oxidation as well, although in different ways. The rate of Mn(II) oxidation with excess SOD and catalase gave clues to the cellular response of oxygen disruption and show that

the cell may take an active role in Mn(II) oxidation since xanthine increases Mn(II) oxidation.

Overall, Mn(II) oxidation in *A. manganoxydans* SI85-9A1 has been found to be novel and possibly different than in other Mn(II) oxidizing bacteria. It will be interesting to find out whether MopA is part of a complex of proteins, including the MCO that has been found to be necessary in other Mn(II) oxidizing organisms. Determination of the structure through X-ray crystallography of MopA will also allow characterization of this new class of Mn(II) oxidizing peroxidase and give more insights into Mn(II) oxidation. The development of a genetic system will be interesting to see because it will allow identification of more factors involved with Mn(II) oxidation. Finally, figuring out the role of reactive oxygen species in the different steps of Mn(II) oxidation will allow us to find out the mechanism of oxidation and allow us to understand it more completely in *A. manganoxydans* SI85-9A1. All of these aspects of *A. manganoxydans* SI85-9A1 will help us increase our overall understanding of Mn(II) oxidation by microorganisms.

References

- Anderson, C.R., Dick, G.J., Chu, M.-L., Cho, J.-C., Davis, R.E., Bräuer, S.L., Tebo, B.M., 2009. *Aurantimonas manganooxydans*, sp. nov. and *Aurantimonas litoralis*, sp. nov.: Mn(II) oxidizing representatives of a globally distributed clade of alpha-Proteobacteria from the order Rhizobiales. *Geomicrobiol J* 26, 189-198.
- Anderson, C.R., Johnson, H.A., Caputo, N., Davis, R.E., Torpey, J.W., Tebo, B.M., 2009. Mn(II) Oxidation Is Catalyzed by Heme Peroxidases in “*Aurantimonas manganooxydans*” Strain SI85-9A1 and *Erythrobacter* sp. Strain SD-21. *Appl Environ Microbiol* 75, 4130-4138.
- Archibald, F.S., Fridovich, I., 1981. Manganese and Defenses against Oxygen Toxicity in *Lactobacillus plantarum*. *J Bacteriol* 145, 442-451.
- Archibald, F.S., Fridovich, I., 1982a. The scavenging of superoxide radical by manganous complexes: In vitro. *Arch Biochem Biophys* 214, 452-463.
- Archibald, F.S., Fridovich, I., 1982b. Investigations of the state of the manganese in *Lactobacillus plantarum*. *Arch Biochem Biophys* 215, 589-596.
- Ashour, H.M., El-Sharif, A., 2007. Microbial Spectrum and Antibiotic Susceptibility Profile of Gram-Positive Aerobic Bacteria Isolated From Cancer Patients. *J Clin Oncol* 25, 5763 -5769.
- Boardman, B.K., Meehan, B.M., Fullner Satchell, K.J., 2007. Growth Phase Regulation of *Vibrio cholerae* RTX Toxin Export. *J Bacteriol* 189, 1827-1835.
- Brahamsha, B., 1996. A genetic manipulation system for oceanic cyanobacteria of the genus *Synechococcus*. *Appl Environ Microbiol* 62, 1747-1751.
- Brouwers, G.-J., de Vrind, J.P.M., Corstjens, P.L.A.M., Cornelis, P., Baysse, C., de Vrind-de Jong, E.W., 1999. *cumA*, a Gene Encoding a Multicopper Oxidase, Is Involved in Mn²⁺ Oxidation in *Pseudomonas putida* GB-1. *Appl Environ Microbiol* 65, 1762-1768.
- Caspi, R., 1996. Molecular Biological Studies of Manganese Oxidizing Bacteria (Ph.D. Dissertation).
- Caspi, R., Haygood, M.G., Tebo, B.M., 1996. Unusual ribulose-1,5-bisphosphate carboxylase/oxygenase genes from a marine manganese-oxidizing bacterium. *Microbiology* 142, 2549-2559.
- Caspi, R., Tebo, B.M., Haygood, M.G., 1998. c-Type Cytochromes and Manganese Oxidation in *Pseudomonas putida* MnB1. *Appl Environ Microbiol* 64, 3549-3555.

- Cummings, T.F., 2004. The treatment of cyanide poisoning. *Occup Med* 54, 82 -85.
- Daly, M.J., Gaidamakova, E.K., Matrosova, V.Y., Vasilenko, A., Zhai, M., Venkateswaran, A., Hess, M., Omelchenko, M.V., Kostandarithes, H.M., Makarova, K.S., Wackett, L.P., Fredrickson, J.K., Ghosal, D., 2004. Accumulation of Mn(II) in *Deinococcus radiodurans* Facilitates Gamma-Radiation Resistance. *Science* 306, 1025-1028.
- Daly, M.J., Gaidamakova, E.K., Matrosova, V.Y., Kiang, J.G., Fukumoto, R., Lee, D.-Y., Wehr, N.B., Viteri, G.A., Berlett, B.S., Levine, R.L., 2010. Small-Molecule Antioxidant Proteome-Shields in *Deinococcus radiodurans*. *PLoS ONE* 5, e12570.
- Delepelaire, P., 2004. Type I secretion in gram-negative bacteria. *BBA-Mol Cell Res* 1694, 149-161.
- Dick, G.J., Podell, S., Johnson, H.A., Rivera-Espinoza, Y., Bernier-Latmani, R., McCarthy, J.K., Torpey, J.W., Clement, B.G., Gaasterland, T., Tebo, B.M., 2008. Genomic Insights into Mn(II) Oxidation by the Marine Alphaproteobacterium *Aurantimonas* sp. Strain SI85-9A1. *Appl Environ Microbiol* 74, 2646-2658.
- Dick, G.J., Torpey, J.W., Beveridge, T.J., Tebo, B.M., 2008. Direct Identification of a Bacterial Manganese(II) Oxidase, the Multicopper Oxidase MnxG, from Spores of Several Different Marine *Bacillus* Species. *Appl Environ Microbiol* 74, 1527-1534.
- Duckworth, O.W., Sposito, G., 2005. Siderophore–Manganese(III) Interactions. I. Air-Oxidation of Manganese(II) Promoted by Desferrioxamine B. *Environ Sci Technol* 39, 6037-6044.
- Eitinger, T., Rodionov, D.A., Grote, M., Schneider, E., 2011. Canonical and ECF-type ATP-binding cassette importers in prokaryotes: diversity in modular organization and cellular functions. *FEMS Microbiol Rev* 35, 3-67.
- Farazi, T.A., Waksman, G., Gordon, J.I., 2001. The Biology and Enzymology of Protein N-Myristoylation. *J Biol Chem* 276, 39501 -39504.
- Figurski, D.H., Helinski, D.R., 1979. Replication of an origin-containing derivative of plasmid RK2 dependent on a plasmid function provided in trans. *P Natl Acad Sci USA* 76, 1648 -1652.
- Galbusera, C., Orth, P., Fedida, D., Spector, T., 2006. Superoxide radical production by allopurinol and xanthine oxidase. *Biochem Pharmacol* 71, 1747-1752.
- Geszvain, K., Tebo, B.M., 2009. Identification of a two-component regulatory pathway essential for Mn(II) oxidation in *Pseudomonas putida* GB-1. *Appl Environ Microbiol* AEM.02473-09.

- Geszvain, K., Yamaguchi, A., Maybee, J., Tebo, B.M., 2011. Mn(II) oxidation in *Pseudomonas putida* GB-1 is influenced by flagella synthesis and surface substrate. *Arch Microbiol*.
- Gifford, J.L., Walsh, M.P., Vogel, H.J., 2007. Structures and metal-ion-binding properties of the Ca²⁺-binding helix–loop–helix EF-hand motifs. *Biochem J* 405, 199.
- Hagan, E.C., Mobley, H.L.T., 2009. Haem acquisition is facilitated by a novel receptor Hma and required by uropathogenic *Escherichia coli* for kidney infection. *Mol Microbiol* 71, 79-91.
- Hansard, S.P., Easter, H.D., Voelker, B.M., 2011. Rapid Reaction of Nanomolar Mn(II) with Superoxide Radical in Seawater and Simulated Freshwater. *Environ Sci Technol* 45, 2811-2817.
- Hoang, T.T., Karkhoff-Schweizer, R.R., Kutchma, A.J., Schweizer, H.P., 1998. A broad-host-range Flp-FRT recombination system for site-specific excision of chromosomally-located DNA sequences: application for isolation of unmarked *Pseudomonas aeruginosa* mutants. *Gene* 212, 77-86.
- Höfer, C., Schlosser, D., 1999. Novel enzymatic oxidation of Mn²⁺ to Mn³⁺ catalyzed by a fungal laccase. *FEBS Lett* 451, 186-190.
- Imlay, J.A., 2008. Cellular Defenses against Superoxide and Hydrogen Peroxide. *Annu Rev Biochem* 77, 755-776.
- Jung, W.K., Schweisfurth, R., 1979. Manganese oxidation by an intracellular protein of a *Pseudomonas* species. *Z Allg Mikrobiol* 19, 107-115.
- Keller, A., Nesvizhskii, A.I., Kolker, E., Aebersold, R., 2002. Empirical Statistical Model To Estimate the Accuracy of Peptide Identifications Made by MS/MS and Database Search. *Anal Chem* 74, 5383-5392.
- Korshunov, S., Imlay, J.A., 2006. Detection and Quantification of Superoxide Formed within the Periplasm of *Escherichia coli*. *J Bacteriol* 188, 6326-6334.
- Kovach, M.E., Phillips, R.W., Elzer, P.H., Roop II, R.M., Peterson, K.M., 1994. pBBR1MCS: A Broad-Host-Range Cloning Vector. *BioTechniques* 16, 800-803.
- Kovach, M.E., Elzer, P.H., Steven Hill, D., Robertson, G.T., Farris, M.A., Roop, R.M., Peterson, K.M., 1995. Four new derivatives of the broad-host-range cloning vector pBBR1MCS, carrying different antibiotic-resistance cassettes. *Gene* 166, 175-176.
- Laemmli, U.K., 1970. Cleavage of Structural Proteins during the Assembly of the Head of Bacteriophage T4. *Nature* 227, 680-685.

- Lally, E.T., Hill, R.B., Kieba, I.R., Korostoff, J., 1999. The interaction between RTX toxins and target cells. *Trends Microbiol* 7, 356-361.
- Larsen, R., Wilson, M., Guss, A., Metcalf, W., 2002. Genetic analysis of pigment biosynthesis in *Xanthobacter autotrophicus* Py2 using a new, highly efficient transposon mutagenesis system that is functional in a wide variety of bacteria. *Archives of Microbiology* 178, 193-201.
- Learman, D.R., Voelker, B.M., Vazquez-Rodriguez, A.I., Hansel, C.M., 2011. Formation of manganese oxides by bacterially generated superoxide. *Nat Geosci* 4, 95-98.
- Lee, B.-U., Hong, J.-H., Kahng, H.-Y., Oh, K.-H., 2006. Construction of an *Escherichia-Pseudomonas* Shuttle Vector Containing an Aminoglycoside Phosphotransferase Gene and a lacZ' Gene for α -Complementation. *J Microbiol* 44, 671-673.
- Linhartová, I., Bumba, L., Mašín, J., Basler, M., Osička, R., Kamanová, J., Procházková, K., Adkins, I., Hejnová-Holubová, J., Sadílková, L., Morová, J., Šebo, P., 2010. RTX proteins: a highly diverse family secreted by a common mechanism. *FEMS Microbiol Rev* 34, 1076-1112.
- de Lorenzo, V., Herrero, M., Jakubzik, U., Timmis, K.N., 1990. Mini-Tn5 transposon derivatives for insertion mutagenesis, promoter probing, and chromosomal insertion of cloned DNA in gram-negative eubacteria. *J Bacteriol* 172, 6568-6572.
- Loughran, N., O'Connor, B., O'Fagain, C., O'Connell, M., 2008. The phylogeny of the mammalian heme peroxidases and the evolution of their diverse functions. *BMC Evol Biol* 8, 101.
- Macnab, R.M., 2003. How Bacteria Assemble Flagella. *Annu Rev Microbiol* 57, 77-100.
- Madison, A.S., Tebo, B.M., Luther III, G.W., 2011. Simultaneous determination of soluble manganese(III), manganese(II) and total manganese in natural (pore)waters. *Talanta* 84, 374-381.
- Mulligan, C., Fischer, M., Thomas, G.H., 2011. Tripartite ATP-independent periplasmic (TRAP) transporters in bacteria and archaea. *FEMS Microbiol Rev* 35, 68-86.
- Nealson, K.H., Tebo, B.M., Rosson, R.A., 1988. Occurrence and Mechanisms of Microbial Oxidation of Manganese. Academic Press, pp. 279-318.
- Neidhardt, F.C., Bloch, P.L., Smith, D.F., 1974. Culture Medium for Enterobacteria. *J Bacteriol* 119, 736-747.
- Nesvizhskii, A.I., Vitek, O., Aebersold, R., 2007. Analysis and validation of proteomic data generated by tandem mass spectrometry. *Nat Meth* 4, 787-797.

- Newman, J.R., Fuqua, C., 1999. Broad-host-range expression vectors that carry the - arabinose-inducible Escherichia coli araBAD promoter and the araC regulator. *Gene* 227, 197-203.
- Nordeen, R.O., Holloway, B.W., 1990. Chromosome mapping in *Pseudomonas syringae* pv. *syringae* strain PS224. *J Gen Microbiol* 136, 1231-1239.
- Okazaki, M., Sugita, T., Shimizu, M., Ohode, Y., Iwamoto, K., de Vrind-de Jong, E., de Vrind, J., Corstjens, P., 1997. Partial purification and characterization of manganese-oxidizing factors of *Pseudomonas fluorescens* GB-1. *Appl Environ Microbiol* 63, 4793-4799.
- Parales, R.E., Harwood, C.S., 1993. Construction and use of a new broad-host-range lacZ transcriptional fusion vector, pHRP309, for Gram - bacteria. *Gene* 133, 23-30.
- Perez, J., Jeffries, T.W., 1992. Roles of manganese and organic acid chelators in regulating lignin degradation and biosynthesis of peroxidases by *Phanerochaete chrysosporium*. *Appl Environ Microbiol* 58, 2402-2409.
- Piekarski, T., Buchholz, I., Drepper, T., Schobert, M., Wagner-Doebler, I., Tielen, P., Jahn, D., 2009. Genetic tools for the investigation of *Roseobacter* clade bacteria. *BMC Microbiol* 9, 265.
- Reading, N.S., Aust, S.D., 2001. Role of Disulfide Bonds in the Stability of Recombinant Manganese Peroxidase†. *Biochemistry-US* 40, 8161-8168.
- Ridge, J.P., Lin, M., Larsen, E.I., Fegan, M., McEwan, A.G., Sly, L.I., 2007. A multicopper oxidase is essential for manganese oxidation and laccase-like activity in *Pedomicrobium* sp. ACM 3067. *Environmental Microbiology* 9, 944-953.
- Sambrook, J., Russel, D.W., 2001. *Molecular cloning* □: a laboratory manual. Cold Spring Harbor Laboratory Press, Cold Spring Harbor, NY.
- Satchell, K.J.F., 2007. MARTX, Multifunctional Autoprocessing Repeats-in-Toxin Toxins. *Infect Immun* 75, 5079-5084.
- Schlosser, D., Hofer, C., 2002. Laccase-Catalyzed Oxidation of Mn²⁺ in the Presence of Natural Mn³⁺ Chelators as a Novel Source of Extracellular H₂O₂ Production and Its Impact on Manganese Peroxidase. *Appl Environ Microbiol* 68, 3514-3521.
- Sigel, A., Sigel, H., 1999. *Manganese and its Role in Biological Processes*, 1st ed, Metal Ions in Biological Systems. Marcel Dekker, Inc., New York.
- Simon, R., Priefer, U., Puhler, A., 1983. A Broad Host Range Mobilization System for In Vivo Genetic Engineering: Transposon Mutagenesis in Gram Negative Bacteria. *Nat Biotechnol* 1, 784-791.

- Slade, D., Radman, M., 2011. Oxidative Stress Resistance in *Deinococcus radiodurans*. *Microbiol Mol Biol R* 75, 133-191.
- Studier, F.W., 2005. Protein production by auto-induction in high-density shaking cultures. *Protein Express Purif* 41, 207-234.
- Sundaramoorthy, M., Gold, M.H., Poulos, T.L., 2010. Ultrahigh (0.93 Å) Resolution Structure of Manganese Peroxidase from *Phanerochaete chrysosporium*: Implications for the Catalytic Mechanism†. *J Inorg Biochem* 104, 683-690.
- Sundaramoorthy, M., Youngs, H.L., Gold, M.H., Poulos, T.L., 2005. High-Resolution Crystal Structure of Manganese Peroxidase: Substrate and Inhibitor Complexes†,‡. *Biochemistry-US* 44, 6463-6470.
- Sutherland, G.R.J., Zapanta, L.S., Tien, M., Aust, S.D., 1997. Role of Calcium in Maintaining the Heme Environment of Manganese Peroxidase†. *Biochemistry-US* 36, 3654-3662.
- Taurog, A., 1999. Molecular evolution of thyroid peroxidase. *Biochimie* 81, 557-562.
- Tebo, B.M., Bargar, J.R., Clement, B.G., Dick, G.J., Murray, K.J., Parker, D., Verity, R., Webb, S.M., 2004. BIOGENIC MANGANESE OXIDES: Properties and Mechanisms of Formation. *Annu Rev Earth Planet Sci* 32, 287-328.
- Tebo, B.M., Clement, B.G., Dick, G.J., 2007. Biotransformations of Manganese, in: *Manual of Environmental Microbiology*. ASM Press, United States of America, pp. 1223-1238.
- Tebo, B.M., Johnson, H.A., McCarthy, J.K., Templeton, A.S., 2005. Geomicrobiology of manganese(II) oxidation. *Trends Microbiol* 13, 421-428.
- Thomas, P.E., Ryan, D., Levin, W., 1976. An improved staining procedure for the detection of the peroxidase activity of cytochrome P-450 on sodium dodecyl sulfate polyacrylamide gels. *Anal Biochem* 75, 168-176.
- Valentine, J.S., 2007. Superoxide Dismutases and Reductases, in: *Biological Inorganic Chemistry: Structure & Reactivity*. University Science Books, Sausalito, California, pp. 331-342.
- De Vrind, J., De Groot, A., Brouwers, G.J., Tommassen, J., De Vrind-de Jong, E., 2003. Identification of a novel Gsp-related pathway required for secretion of the manganese-oxidizing factor of *Pseudomonas putida* strain GB-1. *Mol Microbiol* 47, 993-1006.
- van Waasbergen, L., Hildebrand, M., Tebo, B., 1996. Identification and characterization of a gene cluster involved in manganese oxidation by spores of the marine *Bacillus* sp. strain SG-1. *J Bacteriol* 178, 3517-3530.

- Webb, S.M., Dick, G.J., Bargar, J.R., Tebo, B.M., 2005. Evidence for the presence of Mn(III) intermediates in the bacterial oxidation of Mn(II). *P Natl Acad Sci-USA* 102, 5558-5563.
- West, S.E.H., Schweizer, H.P., Dall, C., Sample, A.K., Runyen-Janecky, L.J., 1994. Construction of improved Escherichia-Pseudomonas shuttle vectors derived from pUC18/19 and sequence of the region required for their replication in Pseudomonas aeruginosa. *Gene* 148, 81-86.
- Wilharm, G., Lepka, D., Faber, F., Hofmann, J., Kerrinnes, T., Skiebe, E., 2010. A simple and rapid method of bacterial transformation. *J Microbiol Meth* 80, 215-216.
- Yocum, C.F., Pecoraro, V.L., 1999. Recent advances in the understanding of the biological chemistry of manganese. *Curr Opin Chem Biol* 3, 182-187.
- Yoshida, N., 2007. Discovery and application of the Yoshida effect: nano-sized acicular materials enable penetration of bacterial cells by sliding friction force. *Recent Patents on Biotechnology* 1, 194-201.
- Yoshida, N., Nakajima-Kambe, T., Matsuki, K., Shigeno, T., 2007. Novel Plasmid Transformation Method Mediated by Chrysotile, Sliding Friction, and Elastic Body Exposure. *Anal Chem Insights* 2, 9-15.
- Yoshida, N., Saeki, Y., 2004. Chrysotile fibers penetrate Escherichia coli cell membrane and cause cell bursting by sliding friction force on agar plates. *Journal of Bioscience and Bioengineering* 97, 162-168.
- Yoshida, N., Sato, M., 2009. Plasmid uptake by bacteria: a comparison of methods and efficiencies. *Appl Microbiol Biotechnol* 83, 791-798.
- Zibat, A., 2001. Efficient Transformation of Halobacterium salinarum by a "Freeze and Thaw" Technique. *BioTechniques* 31, 1010-1012.

Appendix A: Expression of Mn(II) oxidizing Proteins

Introduction

Purified proteins allow for detailed study of the mechanism of proteins. When proteins are purified from complex systems such as cellular proteins, there can be accessory proteins that may interfere with activity or alter activity. By isolating the main protein of interest from contaminant proteins, a more detailed description of the reaction mechanism can be found. This chapter details work leading to potential expression and isolation of MopA, MopA domains, and MoxA in order to perform more detailed study of Mn(II) oxidation.

Methods and Materials

Growth conditions, strains, and plasmids

Strains, plasmids, and primers are listed in Table 11. *A. manganoxydans* SI85-9A1 was grown as written in Chapter 3. *Escherichia coli* is grown in Luria Broth (LB; 10

g L⁻¹ Bacto Tryptone, 5 g L⁻¹ Bacto yeast extract, 10 g L⁻¹ NaCl (Fisher, US)) or in MOPS Minimal Medium (Neidhardt et al., 1974) at 37°C supplemented with antibiotics as necessary. MOPS minimal medium consists of 40 mM 3-(N-morpholino)propanesulfonic acid (MOPS), 4 mM Tricine, 10 µM FeSO₄, 9.52 mM NH₄Cl, 276 µM K₂SO₄, 0.5 µM CaCl₂, 523 µM MgCl₂, 50 mM NaCl and 1x nutrient stock (see reference for nutrient stock formulation).

Table 11: Strains, plasmids and primers used in Appendix A

Strain, plasmid, or primer	Description	Reference
Strain		
A manganoxydans SI85-9A1 Escherichia coli:	Mn(II) oxidizing α -proteobacterium	(Anderson, Dick, et al., 2009)
Tam1	General cloning strain: mcrA Δ (mrr-hsdRMS-mcrBC) Φ 80lacZ Δ M15 Δ lacX74 recA1 araD139 Δ (ara-leu)7697 galU galK rpsL endA1 nupG General expression strain: F' proA+B+ lacIqzzf::Tn10(TetR)/ fhuA2 lacZ::T7 gene1 [lon] ompT gal sulA11 R(mcr-73::miniTn10--TetS)2 [dcm] R(zgb-210::Tn10--TetS) endA1 Δ (mcrC-mrr)114::IS10	RapidTrans, Activ Motif, USA
ER2566		NEB, USA
Plasmid		
pJet1.2	General PCR cloning vector; blunt end	Fermentas, USA
pTXB1	N-terminal CBD tagged expression vector	NEB, USA
pET23a	C-terminal histidine tagged vector	Provided by Dr. Jim Whittaker
pProEX-1	C-terminal TEV cleavable histidine tagged vector	Provided by Dr. Michiko Nakano
Primer		
MopD1 F*	5'-CATATGGCTGGCGCCGACCTCAATGATCT-3'	This Work
MopD1 R^	5'-ACTAGTTTACTCGATCAGCTGATTGGATTTGTTGACCTCGAGAAC-3'	This Work
MopD2 F*	5'-CATATGCAAGCTTTCGAGGACGATGACGATACCGC-3'	This Work
MopD2 R^	5'-ACTAGTTTAGTTGTTGTCTTCGCCAACTGTGTCGCTG-3'	This Work
pPro F	5'-TTGTGAGCGGATAACAATTCA-3'	This Work
pPro R	5'-ATCAGACCGCTTCTGCGTTC-3'	This Work

*: **Italics indicate NdeI restriction site added.** ^: **Italics indicate SpeI restriction site added.**

DNA Handling

Isolation

Plasmid and genomic DNA from *E. coli* and *A. manganoxydans* SI85-9A1 were isolated using standard kits and protocols contained in those kits. Plasmid DNA was prepared using the QIAprep Spin Miniprep Kit (Qiagen, USA) and genomic DNA was prepared using the Wizard Genomic DNA Purification Kit (Promega, USA). DNA

quantification was performed using a ND-1000 Spectrophotometer (Nanodrop, USA) set to the nucleic acid detection mode.

Gel Electrophoresis

DNA was analyzed in 1% agarose (Fisher Scientific, USA) TBE (; 8.3 mM Tris base, 89 mM boric acid, and 3.2 mM ethylenediaminetetraacetic acid (EDTA)) gels stained with GelRed (Biotium, CA, USA) using an OWL gel electrophoresis gel box. Gels were run at 100V and imaged using UV transillumination.

Gel purification

Gels were examined under low power UV transillumination and gel slices were excised using a scalpel and forceps. Gel purification of DNA fragments from agarose gels was performed using the QIAquick Gel Extraction Kit (Qiagen, USA). DNA quantification was performed using a ND-1000 Spectrophotometer (Nanodrop, USA) set to the nucleic acid detection mode.

Construction of Histidine Tagged Protein

The peroxidase domains from MopA were amplified from *A. manganoxydans* SI85-9A1 genomic DNA (gDNA) using Phusion High-Fidelity DNA Polymerase (Fermentas, USA) according to the PCR conditions are found in

Table 12. The blunt end PCR products were gel purified and ligated into pJet1.2 using the Clonejet kit (Fermentas, USA). Briefly, 10 μ l of 2x reaction buffer, 2 μ l gel purified PCR product, 1 μ l pJet1.2 blunt end vector, 6 μ l water, and 1 μ l T4 DNA ligase were mixed in a tube. After a period of ligation at room temperature for 5-10 minutes, 2-5 μ l of DNA were placed into one tube of chemically competent Tam1 *E. coli* cells (RapidTrans, Active Motif, USA). The cell/DNA mixture was incubated on ice for 30 minutes, then heat shocked at 42°C for 30 seconds, followed by a 2 minute incubation on

ice. At this point, 250 μl of manufacturer supplied SOC medium was added to each tube and they were placed into a 37°C water bath for 1 hour to allow the cells to recover. After the period of recovery, 50 and 200 μl were spread plated onto LB plates containing ampicillin (100 $\mu\text{g ml}^{-1}$). These plates were incubated overnight at 37°C.

The following morning, 4-6 colonies were picked and placed into 5 ml culture tubes containing LB and ampicillin, and allowed to grow overnight. After growth had occurred, 2-4 ml of each culture would be pelleted and plasmids isolated using QIAprep Spin Miniprep Kit (Qiagen, USA). These plasmids were then analyzed for correct fragment length using NdeI and SpeI (NEB, USA) restriction enzymes. Each individual digestion consisted of 0.1 μl bovine serum albumin (BSA), 0.3 μl NdeI, 0.3 μl SpeI, 1 μl vector DNA, and water to make a total volume of 10 μl . The correct size band was excised, gel purified and ligated into NdeI/SpeI digested pProEX-1 using the Quick Ligation Kit (NEB, USA). Briefly, 7.5 μl purified fragment, 2.5 μl vector, 10 μl Quick Ligation Buffer Mix, and 1 μl T4 DNA ligase were mixed in a tube and allowed to react at room temperature for 5-10 minutes. These were then transformed, grown, and reisolated using the above procedures. The same restriction digest was performed and sequencing of the plasmids was performed at the OHSU Molecular and Cell Biology core on a 96-capillary ABI 3700 XL DNA sequencer to confirm that the insert was in-frame and the junctions were correct. The correct plasmid was then transformed into ER2566 (NEB, USA) cells using the CaCl_2 procedure described in Chapter 3.

Table 12: PCR conditions used in Appendix A

<u>Reaction conditions</u>	<u>Primer Set</u>	
	<u>MopD1 & D2 F, R</u>	<u>Cycles</u>

	Temp (°C)	Time (sec)	
Initial Denaturation	98	30	1
Denaturation	98	10	
Hybridization	68	30	30
Elongation	72	75	
Final Elongation	72	300	1
	4	∞	

Expression and Crude Extract Preparation

IMPACT

C-terminally tagged Mop (pTXB1 MopCBD) was expressed in *E. coli* using isopropyl β -D-1-thiogalactopyranoside (IPTG). Initially, an overnight culture was grown in 100 ml of LB with ampicillin from a single colony. In the morning, 50 ml of this overnight culture was added to 1 L of LB with ampicillin supplemented with 5 mg L⁻¹ ferric ammonium citrate and allowed to grow until an OD₆₀₀ 0.5. IPTG was then added to a concentration of 400 μ M and incubated for 5 hours at room temperature. The entire culture was then collected by centrifugation and frozen until use. Isolation of soluble proteins was performed by sonication using a Branson Digital Sonifier fitted with a microtip. The cell pellet was resuspended in 50 ml sonication buffer. The power was set to 50% and was performed for 8x10 second pulses with 10 second rests between each pulse. Soluble proteins were removed from insoluble proteins by centrifugation, the sample was filter sterilized, and was not pre-concentrated prior to loading.

MopA Domains

C-terminally tagged Mop (pTXB1 MopCBD) was expressed in *E. coli* ER2566 cells using isopropyl β -D-1-thiogalactopyranoside (IPTG). Only small-scale studies have been performed to optimize expression. A 5 ml overnight culture is grown in LB with ampicillin at 37°C, from a single colony. In the morning, 5 ml is inoculated to and OD₆₀₀ ~0.1 and allowed to grow at 37°C until the OD₆₀₀ reaches 0.5-0.7. IPTG is added to a

concentration of 300 μM and the culture is allowed to grow for 4-5 hours at 37°C. These growth conditions yielded the best protein expression levels, although further optimization is necessary.

MoxA

MoxA is an MCO that has been implicated in *Pedomicrobium* ACM 3067 to be essential for Mn(II) oxidation (Ridge et al., 2007) and was studied to ascertain whether *A. manganoxydans* SI85-9A1 utilizes its own MoxA homologue in Mn(II) oxidation. Expression of MoxA was performed using an autoinduction medium (Studier, 2005). This medium consisted of MOPS Minimal Medium supplemented with 50x 5052, 20x NPS, 1,000x MgSO_4 , and the trace metals as outlined in Studier (2005).

Purification

MoxA

MoxA purification was performed using immobilized metal affinity chromatography (IMAC). Talon Cobalt Metal Affinity resin (Clontech, USA) was used for this purification to get highest purity, although yield is reduced. Batch/gravity style purification was used for this purification. The standard Clontech purification protocol was followed for purification using a 5 ml bed volume. All samples were analyzed by SDS-PAGE.

MopCBD

MopCBD purification was performed using Chitin affinity chromatography as outlined by the Impact Kit instruction manual (NEB, USA). Gravity style purification was used and a 5 ml column volume of immobilized Chitin resin was used. All samples were then analyzed by SDS-PAGE.

Antibody Production

MoxA polyclonal antibodies were produced by the Proteintech Group (Chicago, IL, USA). Rabbits were immunized with purified histidine tagged MoxA and allowed to produce antibodies for 102 days. Blood serum was received from Proteintech and antibodies were isolated from the serum using column chromatography. The first set of antibodies were isolated using DEAE sepharose (Bio-Rad, USA) and the second was isolated using a Thiophilic adsorbent resin (Pierce, USA). Protocols for purification were provided in the accompanying manuals and were followed as written.

SDS-PAGE

Reducing Conditions

SDS-PAGE was performed as in Chapter 2 under the Reducing Conditions heading.

Western Blotting

Western blotting was performed using the SuperSignal West Pico Complete Rabbit IgG Detection Kit (Pierce, USA) according to the manufacturers protocol. Anti-rabbit secondary antibodies were used to conjugate to the rabbit primary antibodies from Proteintech. After the proteins were separated using 1-D electrophoresis, they were transferred to a nitrocellulose membrane using a Mini Trans-Blot cell (BioRad, USA). The optimized concentrations of antibodies are 1:25,000 for primary and 1:100,000 for the secondary antibodies. Imaging was performed using a standard X-Ray film developer.

Results and Discussion

Construction, Expression, Purification and Analysis of MoxA

MoxA was cloned into pET23a by Dr. James W. Whittaker. It was kindly provided for expression, purification, and analysis work. Rosetta 2(DE3) cells (Novagen, USA) were used for expression. These cells contain an accessory plasmid that supplies unusual transfer RNAs (tRNA) for unusual codons for enhancement of hard to express proteins. This made it necessary to use chloramphenicol ($34 \mu\text{g ml}^{-1}$) to keep the tRNA plasmid within the cell.

Optimal expression of the MoxA-histidine fusion protein occurred using an autoinduction protocol. Overnight cultures were made from individual colonies and 500 ml flasks were allowed to grow overnight at 37°C to achieve high-level expression.

Purification proceeded as normal and gave a nearly pure protein, as shown in Figure 18. This protein was quantified using the UV absorbance at 280 nm (assuming A_{280} of 1 = 1 mg ml^{-1}), and concentrated to the smallest possible volume using 0.5 ml Amicon spin concentration tubes (Millipore, USA).

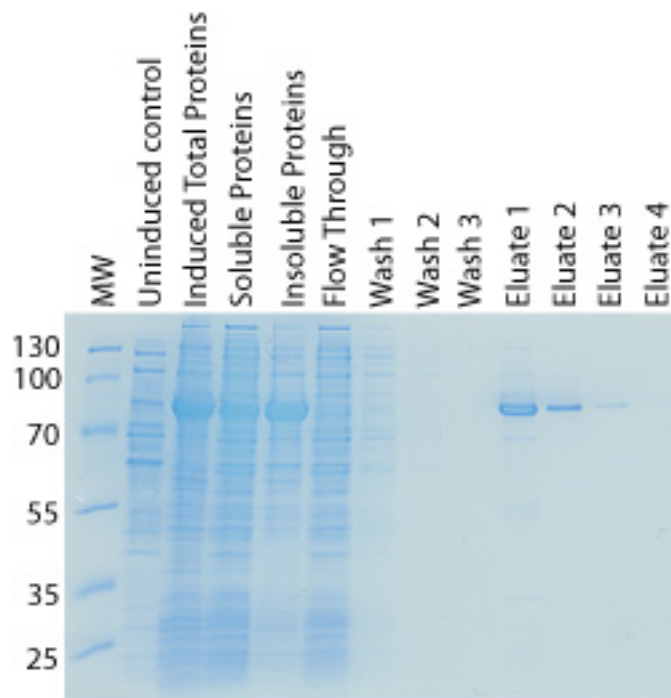


Figure 18: Purification of MoxA using immobilized metal affinity chromatography

Purified MoxA was sent to the Proteintech Group for antibody production using rabbits. Antibodies were purified using thiophilic adsorbent (Pierce, USA) and used for Western blotting experiments. As can be seen in Figure 19, when the purified MoxA (denoted as rMox for recombinant MoxA) was placed next to actively Mn(II) oxidizing LBOM proteins (as shown by an *in vitro* Mn(II) oxidation assay) from *A. manganoxydans* SI85-9A1, no MoxA can be found in the LBOM proteins. This may go to show that MoxA is not expressed into the LBOM proteins and not involved with Mn(II) oxidation in *A. manganoxydans* SI85-9A1.

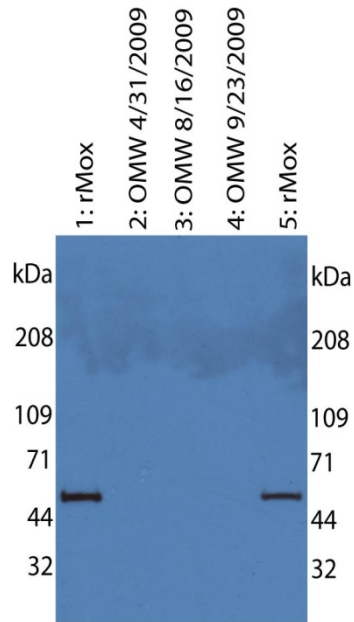


Figure 19: Western blot of purified MoxA compared to active LBOM proteins from *A. manganoxydans* SI85-9A1

Construction, Expression, Purification and Analysis of MopCBD

Construction of the C-terminally tagged MopA with a chitin binding domain (CBD) for chitin affinity chromatography through the Impact kit (NEB, USA) was performed by Rick Davis. This is denoted as MopCBD and is found in the pTXB1 plasmid. Expression yielded low levels of MopCBD, but was enough to proceed to purification experiments. Multiple variables were tweaked in order to elute the protein from the column but Mop never came off the column. The variables tested can be found below in Table 13. In spite of variation of these aspects of elution, no MopA ever eluted from the column and purified, full-length MopA was never achieved.

Table 13: Variables tested for elution of Mop from chitin resin

Condition Tested	Variable
Temperature (°C)	4, 20, 28
Elution Time (hrs)	2, 20, 48
Agitation	none, gentle side-to-side, vigorous rotation
Adjunct	Ca ²⁺ , 1% SDS

Construction, Expression, Purification and Analysis of the Mop domains

In order to gain an understanding of how the individual peroxidase domains of MopA may function on Mn(II) oxidation, the domains were cloned from MopA and placed into expression plasmids. The cloning proceeded as normal (described in methods above). These domains were cloned with 5 amino acid overhangs from before and after the domain predicted start sites. pPROEX-1 was used as the expression plasmid because it has a cleavable histidine affinity tag. The cleavable region consists of a highly specific Tobacco Etch Virus (TEV) protease cleavage region that leaves a native protein after cleavage has occurred. Six clones each of the first and second domains were made (MopD1 and MopD2). These were confirmed by digestion with NdeI/SpeI as well as junction sequencing at each end of the insert.

Initial experiments were performed to see how well these clones expressed the Mop domains. One clone of each was taken from each domain and subjected to varying expression conditions such as concentration of IPTG, expression time and expression temperature. It was found that maximal expression occurred for both MopD1 and MopD2 using 0.3 mM IPTG expressed for 5 hours at room temperature in LB. This information will be useful for future studies using these constructs.

Summary

The expression of MopA proved to be harder than originally thought. The elution of MopA from the resin-bound MopCBD through intein cleavage did not occur. This may be due to blockage of the cleavage site by the bulky Mop protein. The protein may also not be folding correctly since *A. manganoxydans* SI85-9A1 folding chaperones were not

present to help MopA fold correctly. This would make it hard for E. coli to deal with high level expression of MopA and the protein may have settled into inclusion bodies.

Appendix B: Tandem MS Data

Introduction

Mn(II) oxidizing fractions of the purification scheme were taken and analyzed at the OHSU Proteomics Shared Resource (PSR) as described in Chapter 2. The amount of protein analyzed for each fraction was 10 µg and the resulting data can be found below. Electronic files of all tandem MS data can be found in the data DVD accompanying this thesis.

Results

The tables below show what proteins were identified after each purification stage (Table 14), and then the top five proteins after each purification stage based on the number of individual peptides identified with sequences and molecular weights of the peptides (Table 15, Table 16, Table 17, and Table 18).

Table 14: Proteins identified after each stage of purification
LBOM: loosely bound outer membrane proteins; IEX: ion exchange chromatography; HIC: hydrophobic interaction chromatography; SEC: size-exclusion chromatography

Identified Proteins	Accession Number	LBOM	IEX	HIC	SEC
putative hemolysin-type calcium-binding peroxidase protein	gi 90417986	x	x	x	x
glutamine synthetase I	gi 90419644	x	x	x	x
ABC-type branched-chain amino acid transport systems	gi 90420909	x	x		
lysine-arginine-ornithine-binding periplasmic protein	gi 90419549	x	x		
periplasmic phosphate-binding protein, ABC-type transporter	gi 90418936	x	x		
flagellin protein	gi 90418385	x	x	x	x
ABC-type sugar transport system, periplasmic component	gi 90420899	x	x		
putative multicopper oxidase	gi 90417997	x	x	x	
possible hemolysin-type calcium-binding region	gi 90417984	x		x	
flagellin protein	gi 90418382	x	x	x	
twin-arginine translocation pathway signal	gi 90420836	x	x	x	
periplasmic substrate-binding protein, ABC-type proline/glycine betaine transporter	gi 90418106	x	x	x	
putative flagellin protein	gi 90418259	x	x	x	
flagellin protein	gi 90418380	x	x	x	x
putative IMP dehydrogenase/GMP reductase	gi 90420304	x	x	x	
flagellin protein	gi 90418379	x	x	x	
putative extracellular solute-binding protein, TRAP-type dicarboxylate transporter, DctP subunit	gi 90418556	x	x		
putative flagellar hook-associated protein FlgK	gi 90418364	x	x		
putative flagellar hook protein FlgE	gi 90418365	x	x	x	
periplasmic substrate-binding protein, ABC-type glycerol-3-phosphate transporter	gi 90420718	x	x		
periplasmic substrate-binding protein, ABC-type peptide transporter	gi 90418335	x	x		
periplasmic substrate binding protein, TRAP-T Family	gi 90417888	x		x	
ABC transporter periplasmic binding protein	gi 90420323	x	x	x	
basic membrane lipoprotein	gi 90417812	x		x	
periplasmic substrate-binding protein, ABC-type amino acid transporter	gi 90418079	x	x		
TRAP transporter solute receptor, DctP family	gi 90419689	x			
putative gluconolactonase	gi 90419705			x	x
periplasmic substrate-binding protein, ABC-type nitrate/sulfonate/bicarbonate transporter	gi 90419877	x	x		
periplasmic component, TRAP dicarboxylate transporter	gi 90418731		x		
periplasmic substrate-binding protein ABC-type glycine/betaine/proline transporter	gi 90418328	x			
TRAP-type dicarboxylate transporter, DctP subunit	gi 90420639	x	x		
conserved hypothetical protein, Bordetella uptake gene (bug) product family	gi 90419835	x			
5'-nucleotidase	gi 90421245	x			
O-acetylhomoserine sulfhydrylase	gi 90418045	x		x	
putative periplasmic substrate-binding protein, ABC-type sugar transporter	gi 90420078	x	x		
substrate binding protein, ABC-type nitrate/sulfonate/taurine/bicarbonate transporter	gi 90418404	x			
polyribonucleotide nucleotidyltransferase	gi 90420519	x			
Enolase	gi 90419619	x			
glycine dehydrogenase (glycine cleavage system P-protein)	gi 90419836			x	

ABC type amino acid transporter	gi 90417954		x		
glyceraldehyde-3-phosphate dehydrogenase	gi 90418732			x	
acetyl-CoA C-acyltransferase	gi 90420301	x			x
carbon monoxide dehydrogenase, large subunit	gi 90420001			x	x
carbon monoxide dehydrogenase, medium subunit	gi 90420002				x
chaperonin groEL	gi 90419968			x	
putative periplasmic substrate-binding protein, ABC-type spermidine/putrescine transporter	gi 90419921	x			
periplasmic solute receptor, TRAP-type transporter	gi 90420747			x	
periplasmic substrate-binding protein, ABC-type transporter	gi 90419702	x			
putative basic membrane protein	gi 90419746			x	
periplasmic substrate-binding protein, ABC-type sulfate/tungstate transporter	gi 90418451			x	
TRAP transporter solute receptor, TAXI family	gi 90420958			x	
dihydrodipicolinate synthetase	gi 90419351	x			
conserved hypothetical protein	gi 90419561	x			
catalase	gi 90418682				x
putative flagellar hook-associated protein	gi 90418363	x			
urease alpha subunit, UreC	gi 90420342	x			x
branched-chain amino acid ABC transporter, periplasmic substrate-binding protein	gi 90419104	x			
sugar ABC transporter permease protein	gi 90417908	x			
putative TRAP-type transport system, periplasmic component	gi 90419348	x			
adenosylhomocysteinase	gi 90420580			x	
flagellin protein	gi 90418383	x			
possible extracellular solute-binding protein, TRAP-type dicarboxylate transporter, DctP subunit	gi 90418437			x	
possible metallo-beta-lactamase	gi 90418080				x
oxidoreductase	gi 90420666	x			
putative substrate-binding protein, ABC-type sugar transporter	gi 90420826	x			
ABC transporter, substrate-binding protein	gi 90418529			x	
putative high affinity urea/thiourea/hydroxyurea porter	gi 90420355	x			
periplasmic substrate-binding component, ABC-type ferric iron transporter	gi 90419930	x			
1,4-alpha-glucan branching enzyme 1	gi 90420317				x
periplasmic substrate-binding protein, ABC-type iron transporter	gi 90418323			x	
Holliday junction specific DNA helicase, subunit RuvA	gi 90418966	x			
malate/lactate dehydrogenase	gi 90421031			x	
malate synthase G	gi 90420748			x	
periplasmic component, ABC-type sugar transporter	gi 90418635	x			
2-hydroxyacid dehydrogenase	gi 90418740			x	
periplasmic substrate-binding protein, ABC-type xylose transporter	gi 90419814	x			
cold-shock protein	gi 90420715			x	
putative oxidoreductase	gi 90418083			x	
possible transport system, periplasmic component	gi 90419338			x	

Table 15: Peptide sequences top five identified proteins from LBOM protein matrix

Peptide sequence	Previous Amino Acid	Peptide Mass (Da)
putative hemolysin-type calcium-binding peroxidase protein (gi 90417986)		
AAAAAANINPGGPNNEIVTR	R	2076
AINPIFAGLDAR	R	1258
ANENFALTSMHTIWAR	R	1861
APGVDPADLTR	R	1227
ASGDPYIQEAVGFAGNLDPYASWADFQAR	K	3118
ASPFVDQNAAYGSNALVGQFLR	K	2383
AVIRFTDANGVR	R	1319
DADGNVLR	R	860
DLAGLK	R	615
DLLGDDGGSDTLNGDEDDDILAGGR	R	2505
DMIFGGAGDDVVLGGADNDMIFGDAGDDR	R	2946
DSVNGGGGTDTLSSINGDEGVAETFR	R	2470
DTGMPTLNTR	R	1234
ELIAHHWENDTIFVDPSLPGGVSFR	R	2924
ENAEHLGILTDEDLANAPVLK	R	2377
EQLYQATGSSFLKPYDSWVDFEANLK	R	2980
EQWGAADTVMPR	R	1360
ESGDQGVGMR	R	1150
EYKFNADGEPVSTGR	R	1671
FDKVEALSGWNGNDQLFGDDR	R	2385
FDNFDYDNFIDGQEFSDIAR	R	2691
FGHSMILTETVAR	R	1348
FGTEMQYQHLVFEFAR	R	2133
FILDQIK	R	876
FNADGEPVSTGR	K	1249
FTDANGVR	R	879
GDAGRDMIFGGAGDDVVLGGADNDMIFGDAGDDR	K	3387
GEDGDDVIANSAGPFDILMGGR	K	2205
GEGDHGFNDYNPNADAR	R	1849
GEVYTIDENGVPQHLNK	R	1914
GIDRVDLWVGGLAEK	K	1628
GLNGNDTISGGDGR	R	1334
GNDTVNGGAGDDTVFWFTGDGR	R	2259
GNENIALTAVHHVFHSEHNR	R	2283
GNGQDNIINGDLDGVVADDTIR	R	2270
GRDTGMPTLNTR	R	1449
GTGDDVIAR	R	903
GTNGTVYIPLQPDDPLYVPGGFTNFMVLTR	K	3285
GWDVGLGTLNQVR	R	1415
HIGVDAFGQYDYVLEVNK	R	2067
HLDPLVADGVTLGIDGVDYLK	R	2211
HVFDGISGPAEWAGK	R	1572
HVLGGMVGGQTFWVVLHEQFDR	K	2472
HYITGDGR	R	918
IAEAHAAGADLNDLVPDPHPVWGLR	K	2637
IFTTEQQDILR	K	1363
IISNLIVDMSVDNPAAVLAFLNNELAVETFK	R	3362
IKIFTTEQQDILR	R	1606
INADLFAFNVAR	R	1351
IQNGGGNDIISGDHWLHVR	R	2090
IQPAIDPFVFNSSDIDPSIFSEFANVVYR	K	3388
ISHEFASAVYR	R	1279
ISISDPDSGGEIATVTTLR	R	1934
LGIALDDQDALNIPLLR	K	1850

LIANTDLSDPGPDGIR	K	1766
LIANTDLSDPGPDGIRGTGDDVIAR	K	2652
LLDGLEGLLATWGQIK	R	1670
LLDGLEGLLATWGQIKAEAAK	R	2213
LLSGATDPSTPDFNLLPTLR	R	2130
LNENDLR	K	873
LNPDGTLR	K	885
MFGDDGDDMLEGGGGFDTVYGGAGNDR	R	2741
NAAMALVFNTEGAPADR	R	1748
NDLVR	R	616
NEGMFGFDWATFQGNLSDAYADMR	R	2743
NGLSDTIMDQMK	R	1370
NHNFHVEMLLEAGFEGTEEEVFQAAK	R	2977
NIEELEINTR	R	1230
NIEELEINTRPIGGATVAR	R	2054
NLVNGHQAFEDDDDTAGAGGVR	K	2260
NNLLGLPLDLAAINIAR	R	1793
NNNESHPEYGAADDEVFIR	R	2064
NPMSVVNFIAAYGTHETIVAAGNNLQER	K	3017
NRFDKVEALSGWNGNDQLFGDDR	R	2655
NSANGVLAIGGPGTSR	K	1473
NTGESAVAGAVYTLSFDIGDR	R	2144
NTGESAVAGAVYTLSFDIGDRTDHPWPGGQVR	R	3375
NTGLTGLPEEIFR	R	1446
PAQMEIVR	K	943
QYDASGTPTGILIDGSENVIPGITVGDRL	K	2958
RNAAMALVFNTEGAPADR	R	1904
SLFELLVER	K	1105
SNQLIEDPTGVDPVLEALGLGK	K	2266
TDHPWPGGQVR	R	1252
TDPYGEFIR	R	1098
TGQAIVDGPATNETVIDPVGLAQAYTPGSYLR	R	3276
TNIHDGSADNIGLIQAFLNPEVFTK	R	2714
TPQDESAVSGYVASINALVK	R	2050
TQGLNLLNELENNAFSK	R	1906
TVDGAPDSNADR	R	1217
TVDGTYNLVDGR	R	1424
TVKPAQMEIVR	R	1274
VDLWVGGLAEK	R	1187
VEALSGWNGNDQLFGDDR	K	1992
VFQAAR	R	691
VGHSLVGQTMTVIGPDGQPR	R	2065
VVFTEFADMLIGGIR	R	1666
YGEYDGTNNR	R	1290

lysine-arginine-ornithine-binding periplasmic protein (gi|90419549)

AIAAAVFGDPSK	K	1146
AIAAAVFGDPSKVEYSPLSAVQR	K	2377
AVGNYGEIFER	K	1255
CDVLTTDASGLAASR	R	1537
CGVNTGLPGFASQNDQGAWQGLDIDYCK	R	3074
EPLGPAVR	K	838
FPALQNNNEVDVLAR	R	1586
GGLQYGMPPIR	K	1091
GQNALWTK	R	917
LEMGNADEHTILPEIISK	R	2008
LLGEDK	R	673
LLGEDKNFGESIGLSQDWAVNIIK	R	2647
NFGESIGLSQDWAVNIIK	K	1992

NIGVDTPLEIAR	R	1297
NTTWTMDR	R	1024
QGDTEWFNVVK	R	1323
TNNMEYNPVVIESQSDVNSAYDSGR	R	2792
TSENPEIR	K	944
VEYSPLSAVQR	K	1249
WTHNALLNAEELGVTQENVEDMK	K	2641

ABC-type sugar transport system, periplasmic component (gi|90420899)

AGIQGDIGPK	R	955
APELGGLVEFYR	R	1350
AQAAWLYAQFVGSK	R	1542
EEQEKELQWFVDAAEPYQGMEIK	R	2798
EGLPVVNEEDGTPK	K	1354
ELQWFVDAAEPYQGMEIK	K	2153
ESTIRDESFTER	R	1470
EVTNPGLDLDYIGTSFTTAPDGK	K	2526
FLDAEIGDLSTLSR	K	1536
GGDTNGPASVYAIEK	R	1479
GIPNGVPVDEWGIR	K	1508
KEDEKEQPITVNYDELVK	K	2178
KQWSPTGTNVPDYPK	R	1719
LGYQDVGSWTLMK	K	1497
LNEEQDMEYWVEQAK	K	1913
LQTQMOSGENIYDAYINDSDLIGHTHR	K	3171
NLTDWMEGEGK	R	1279
VLAPAFTAITGIK	K	1302
VSHDLIGEGDVVEK	K	1496
VVSETITTHEYESK	K	1623

glutamine synthetase I (gi|90419644)

ADPYNTGFK	K	1012
AGGVFDDDDQIDAFIDLK	K	1837
ALNAFTNPSTNSFK	K	1511
DLYDLPPEELK	K	1332
EAMEALDTDR	R	1150
EAMEALDTRDFLK	R	1669
FEMTPHPVEFDMYYSV	R	2009
GGYFPLPIDSCQDMR	K	1852
IHPGSAMDKLDLYDLPPEELK	K	2270
IPFGQSPK	R	873
KAEAYLTQSGTGDTAFFGPEAEFFIFDDVR	K	3331
LDSTELPSNDDAEYETGNLGHHR	K	2434
LDSTELPSNDDAEYETGNLGHHRPR	K	2687
LVPGYEAPVLLAYSAR	R	1719
PVFGDNGSGMHVHQSIVK	K	1997
SEMLTVMAEMGVAVEK	R	1724
SQHVTMDVTLVDEDLFSEGTMFDGSSIAGWK	K	3418
YKADPYNTGFK	R	1304
YVIHQVANAYGK	K	1363

putative multicopper oxidase (gi|90417997)

ASDPDKSQIPPLLTEQIPIVAPVR	R	2584
ASGPDGNGGLNLVPGDFR	R	1743
AVPVHFIANDGNLVVSPLQIPTLGPQGMGER	R	3242
CQLQAPIPLR	R	1195
FDIIVDFSQFR	R	1387
FPNELGELPGR	K	1228
FPNELGELPGRR	K	1384
GDDKDPVVGAFMEFR	R	1684

GNEEMDDGVNLR	R	1364
GPIEGRPPGEIFAHQR	R	1762
IGLADQQGR	K	956
IVNKVESVDVPGVFHR	R	1797
IYLVNQALHR	R	1227
MKEELSLK	R	993
SAVGSMPPFLIK	R	1262
SQIPLLTEQPIVAPVR	K	1971
VESVDVPGVFHR	K	1341
VYNNMPVDRSQNAGFGR	R	1939
YSEPLTR	R	996

Table 16: Peptide sequences top five identified proteins after IEX purification stage

Peptide sequence	Previous Amino Acid	Peptide Mass (Da)
putative hemolysin-type calcium-binding peroxidase protein (gi 90417986)		
AINPIFAGLDAR	R	1,257
APGVDNPADLTR	R	1,225
ASPFVDQNQAYGSNALVGQFLR	K	2,382
DADGNVLR	R	859
DLLLGDDGSDTLNGDEDDDILAGGR	R	2,505
DMIFGGAGDDVVLGGADNDMIFGDAGDDR	R	2,918
DSVNGGGGTDTLSINGDEGVAETFR	R	2,470
DTGMPTLNTR	R	1,234
ENAEHLGIILTDEDLANAPVLK	R	2,377
EQLYQATGSSFLKPYDSWVDFEANLK	R	2,980
EQWGAADTVMPR	R	1,360
ESDGDQGVGMR	R	1,149
EYKFNADGEPVSTGR	R	1,670
FGHSMLTETVAR	R	1,348
FILDQIK	R	876
FNADGEPVSTGR	K	1,249
GEDGDDVIANSAGPFDILMGR	K	2,206
GEGDHGFNDYNPNADAR	R	1,849
GEVYTIDENGVPQHNLK	R	1,915
GLNGNDTISGGDGR	R	1,333
GNDTVNNGGAGDDTVFWFTGDGR	R	2,258
GNGQDNIINGDLGVAADDTIR	R	2,271
GRDTGMPTLNTR	R	1,447
GTGDDVIAR	R	904
GTNGTVYIPLQPDDPLYVPGGFTNFMVLTR	K	3,283
HIGVDAFGQYDYVLEVNK	R	2,065
HLDPLVADGVTLGIDGVDYLK	R	2,210
HVFDGISGPAEWAGK	R	1,569
IAEAHAAGADLNDLVPDPHPVWGLR	K	2,636
IFTTEQQDILR	K	1,363
IQGNGGNDIISGDHWLHVR	R	2,090
IQPAIDPFVFNSSSTDIDPSIFSEFANVVYR	K	3,389

ISHEFASAVYR	R	1,280
ISISDPDSGGEIATVTTLR	R	1,933
LIANTDLSDPGPDGIR	K	1,767
LIANTDLSDPGPDGIRGTGDDVIAR	K	2,651
LLDGLEGLLATWGQIK	R	1,671
LLSGATDPSTPDFNLLPTLR	R	2,128
LNENDLR	K	873
LNPDGTLR	K	885
MFGDDGDDMLEGGGGFDTVYGGAGNDR	R	2,743
NAAMALVFENTEAPADR	R	1,763
NDLVR	R	616
NEGMFGFDWATFQNSLADYADMAR	R	2,761
NGLSDTIMDQMK	R	1,353
NIEELEINTRPIGGATVAR	R	2,052
NLVNGHQAFEDDDDTAGAGGVR	K	2,258
NNLLGLPLDLAAINIAR	R	1,791
NNNESHPEYGADEVFIR	R	2,061
NPMSVVNFIAAYGTHETIVAAGNNLQER	K	3,017
NSANGVLAIGGPGTSR	K	1,472
NTGLTGLPEEIFR	R	1,447
PQDVIELAPGATLADYQTSMNGMTK	R	2,768
QYDASGTPGTGILIDGSENVIPGITVGDLR	K	2,959
SLFELLVER	K	1,105
SNQLIEDPTGVDPVLEALGLGK	K	2,266
TDHPWPGGQVR	R	1,249
TDPYGEFIR	R	1,097
TGQAIVDGPATNETVIDPVGLAQAYTPGSYLR	R	3,274
TNIHDGSADNIGLIQAFLNPVEFTK	R	2,715
TQGLNLLNELENNAFSK	R	1,906
TVDGAPDSNADR	R	1,217
TVDGTYNLVDGR	R	1,425
TVKPAQMEIVR	R	1,271
VDLWVGGLAEK	R	1,186
VEALSGWNGNDQLFGDDR	K	1,995
VGHSLVGQTMTVIGPDGQPR	R	2,066
VVFTEFADMLIGGIR	R	1,684

ABC-type sugar transport system, periplasmic component (gi|90420899)

AGIQGDIGPK	R	955
APELGGLVEFYR	R	1,350
EGLPVVNEDGTPK	K	1,356
ELQWFVDAAEPYQGMEIK	K	2,155
ESTIRDESFTER	R	1,469
EVTNPGLDLDYIGTSFTTAPDGK	K	2,526
GGDTNGPASVYAIK	R	1,478
GIPNGVPVDEWGIR	K	1,509
KEDEKEQPITVNYDELVK	K	2,178
KQWSPTGTNVPDYPK	R	1,718
LNEEQDMEYWVEQAK	K	1,929
LQTQMOSGENIYDAYINDSDLIGHTWR	K	3,168

MAPSPHGVYWVDGMK	R	1,677
NLTDWMEGEGK	R	1,280
QWSPTGTNVPDYPK	K	1,588
SAQEAMDSLCAEQEK	K	1,696
VSHDLIGEGDVVEK	K	1,497
VVSETITTHEYESK	K	1,625

ABC-type branched-chain amino acid transport systems (gi|90420909)

AGSTDFDPVVAALNDGDYTTVIGDLSFDDK	K	3,118
DDQQGEVAGK	R	1,046
DGKYDYVDGAAQ	K	1,301
DYTALVTK	K	910
GDVTLPGYVVYEWK	K	1,625
GLADQTQK	K	859
KNEAAPVVAELEK	R	1,468
KPALVEAYTAGEK	K	1,377
LSVGDDACDPK	K	1,176
NEAAPVVAELEK	K	1,340
RPGDGVFR	K	905
TGAEQAVADINAAGGVNGEMLK	R	2,115
YISDNFPDANVAIINDK	K	1,909

twin-arginine translocation pathway signal (gi|90420836)

AADLLEATK	R	931
AANMDLLDEGTLVAK	R	1,741
DNMPVRPSVVAITK	K	1,527
EEADAANPR	R	972
FDVSKEPNEPNR	R	1,431
FKHEGAESIVAPDGR	R	1,613
MDRPEDIQNETNGR	K	1,771
NAFGHIIIEAEDGGFAATK	K	2,089
NGWFGMPDNCAVDAEGR	K	1,896
RAADLLEATK	R	1,086
REEADAANPR	K	1,128
TDGLFAVDTEGAAR	R	1,424
WGDPLFADSPFDPANQTPEAQR	R	2,659

putative flagellar hook-associated protein FlgK (gi|90418364)

AALSQFAVSPENGQTAEAAVNAAR	K	2,374
DADDQLDLAAK	K	1,174
DQIVR	R	630
EVIGDVDSPTSPAATLSSLK	R	1,987
GLAGTIQIAAGVDPTKPGGEPAR	K	2,177
IDGVVVAGASSMPIK	K	1,557
IMAGSASGSDVTDVDR	K	1,667
IMAGSASGSDVTDVDRR	K	1,825
KDADDQLDLAAK	R	1,302
SVEFTPQPAYDATVAGNSFK	R	2,129
TQETLSDATGINIDDEMTR	R	2,111

Table 17: Peptide sequences top five identified proteins after HIC purification stage

Peptide sequence	Previous Amino Acid	Peptide Mass (Da)
putative hemolysin-type calcium-binding peroxidase protein (gi 90417986)		
AINPIFAGLDAR	R	1,257
APGVDNPADLTR	R	1,225
ASPFVDQNAAYGSNALVGQFLR	K	2,382
DADGNVLR	R	859
DLLLGDDGGSDTLNGDEDDDILAGGR	R	2,505
DMIFGGAGDDVVLGGADNDMIFGDAGDDR	R	2,918
DSVNGGGGTDLSINGDEGVAETFR	R	2,470
DTGMPTLNETR	R	1,234
ENAEHLGIILTDEDLANAPVLK	R	2,377
EQLYQATGSSFLKPYDSWVDFAAANLK	R	2,980
EQWGAADTVMPR	R	1,360
ESDGDQGVGMR	R	1,149
EYKFNADGEPVSTGR	R	1,670
FGHSMLTETVAR	R	1,348
FILDQIK	R	876
FNADGEPVSTGR	K	1,249
GEDGDDVIANSAGPFDILMGGGR	K	2,206
GEGDHGFNDYNPADAR	R	1,849
GEVYTIIDENGVPQHNLK	R	1,915
GLNGNDTISGGDGR	R	1,333
GNDTVNGGAGDDTVFWFTGDGR	R	2,258
GNGQDNIINGDLGCVVADDTIR	R	2,271
GRDTGMPTLNETR	R	1,447
GTGDDVIAR	R	904
GTNGTVYIPLQPDDPLYVPGGFTNFMVLTR	K	3,283
HIGVDAFGQYDYVLEVNK	R	2,065
HLDPLVADGVTLGIDGVDYLK	R	2,210
HVFDGISGPAEWAGK	R	1,569
IAEAHAAGADLNDLVDPDPHVPWGLR	K	2,636
IFTTEQQDILR	K	1,363
IQNGGNDIISGDHWLHVR	R	2,090
IQPAIDPFVFNSTIDPSIFSEFANVVYR	K	3,389
ISHEFASAVYR	R	1,280
ISISDPDSGGEIATVTTLR	R	1,933
LIANTDLSDPGPDGIR	K	1,767
LIANTDLSDPGPDGIRGTGDDVIAR	K	2,651
LLDGLEGGLATWGQIK	R	1,671
LLSGATDPSTPDFNLLPTLR	R	2,128
LNENDLR	K	873
LNPDGTLR	K	885
MFGDDGDDMLEGGGGFDTVYGGAGNDR	R	2,743
NAAMALVFENTEAPADR	R	1,763
NDLVR	R	616

NEGMFGFDWATFQNSLDAYADMR	R	2,761
NGLSDTIMDQMK	R	1,353
NIEELEINTRPIGGATVAR	R	2,052
NLVNGHQAFEDDDDTAGAGGVR	K	2,258
NNLLGLPLDLAAINIAR	R	1,791
NNNESHPEYGAADDEVFIR	R	2,061
NPMSVVNFIAAYGTHETIVAAGNNLQER	K	3,017
NSANGVLAIGGPGTSR	K	1,472
NTGLTGLPEEIFR	R	1,447
PQDVIELAPGATLADYQTSMNGMTK	R	2,768
QYDASGTPTGILIDGSENVIPGITVGDLR	K	2,959
SLFELLVER	K	1,105
SNQLIEDPTGVDPVLEALGLGK	K	2,266
TDHPWPGGQVR	R	1,249
TDPYGEFIR	R	1,097
TGQAIVDGPATNETVIDPVGLAQAYTPGSYLR	R	3,274
TNIHDGSADNIGLIQAFLNPVEFTK	R	2,715
TQGLNLLNELENNAFSK	R	1,906
TVDGAPDSNADR	R	1,217
TVDGTYNLVDGR	R	1,425
TVKPAQMEIVR	R	1,271
VDLWVGGLAEK	R	1,186
VEALSGWNGNDQLFGDDR	K	1,995
VGHSLVGQTMTVIGPDGQPR	R	2,066
VVFTEFADMLIGGIR	R	1,684

ABC-type sugar transport system, periplasmic component (gi|90420899)

AGIQGDIGPK	R	955
APELGGLVEFYR	R	1,350
EGLPVVNEDGTPK	K	1,356
ELQWFVDAAEPYQGMEIK	K	2,155
ESTIRDESFTER	R	1,469
EVTNPGLDLDYIGTSFTTAPDGK	K	2,526
GGDTNGPASVYAIEK	R	1,478
GIPNGVPVDEWGIR	K	1,509
KEDEKEQPITVNYDELVK	K	2,178
KQWSPTGTNVPDYPK	R	1,718
LNEEQDMEYWVEQAK	K	1,929
LQTQMQSGENIYDAYINDSDLIGTHWR	K	3,168
MAPSPHGVYWVDGMK	R	1,677
NLTDWMEGEGK	R	1,280
QWSPTGTNVPDYPK	K	1,588
SAQEAMDSLCAEQEK	K	1,696
VSHDLIGEDVVEK	K	1,497
VVSETITTHEYESK	K	1,625

ABC-type branched-chain amino acid transport systems (gi|90420909)

AGSTDFDPVVAALNDGDYTTVIGDLSFDDK	K	3,118
DDQQGEVAGK	R	1,046
DGKYDYVDGAAQ	K	1,301
DYTALVTK	K	910

GDVTLPGYVVYEWK	K	1,625
GLADQTQK	K	859
KNEAAAPVVAELEK	R	1,468
KPALVEAYTAGEK	K	1,377
LSVGDDACDPK	K	1,176
NEAAAPVVAELEK	K	1,340
RPGDGVFR	K	905
TGAEQAVADINAAGGVNGEMLK	R	2,115
YISDNFPDANVAIINDK	K	1,909
twin-arginine translocation pathway signal (gi 90420836)		
AADLLEATK	R	931
AANMDLLDEGTLYVAK	R	1,741
DNMPVRPSVVAITK	K	1,527
EEADAANPR	R	972
FDVSKEPNEPNR	R	1,431
FKHEGAESIVAPDGR	R	1,613
MDRPEDIQPNETNGR	K	1,771
NAFGHIIIEAEDGGFEAATK	K	2,089
NGWFGMPDNCAVDAEGR	K	1,896
RAADLLEATK	R	1,086
REEADAANPR	K	1,128
TDGLFAVDTEGAAR	R	1,424
WGDPLFADSPEFDPANQTPEAQR	R	2,659
putative flagellar hook-associated protein FlgK (gi 90418364)		
AALSQFAVSPENGGQTAEAAVNAAR	K	2,374
DADDQLDLAAK	K	1,174
DQIVR	R	630
EVIGDVDSPTSPAATLSSLK	R	1,987
GLAGTIQIAAGVDPTKPGGEPAR	K	2,177
IDGVVVAGASSPMPK	K	1,557
IMAGSASGSDVTDAVDR	K	1,667
IMAGSASGSDVTDAVDRR	K	1,825
KDADDQLDLAAK	R	1,302
SVEFTPQPAYDATVAGNSFK	R	2,129
TQETLSDATGINIDDEMTR	R	2,111

Table 18: Peptide sequences top five identified proteins after SEC purification stage

Peptide sequence	Previous Amino Acid	Peptide Mass (Da)
putative hemolysin-type calcium-binding peroxidase protein (gi 90417986)		
AINPIFAGLDAR	R	1,257
APGVNDNPADLTR	R	1,225
ASPFVDQNQAYGSNALVGQFLR	K	2,382
DADGNVLR	R	859
DLLLDGGSDTLNGDEDDDILAGGR	R	2,505
DMIFGGAGDDVVLGGADNDMIFGDAGDDR	R	2,918

DSVNGGGTDTLSINGDEGVAETFR	R	2,470
DTGMPTLNETR	R	1,234
ENAEHLGIILTEDLANAPVLK	R	2,377
EQLYQATGSSFLKPYDSWVDFEANLK	R	2,980
EQWGAADTVMPR	R	1,360
ESDGDQGVGMR	R	1,149
EYKFNADGEPVSTGR	R	1,670
FGHSMLTETVAR	R	1,348
FILDQIK	R	876
FNADGEPVSTGR	K	1,249
GEDGDDVIANSAGPFDILMGGGR	K	2,206
GEGDHGFNDYNPNADAR	R	1,849
GEVYTIDENGVPQHNLK	R	1,915
GLNGNDTISGGDGR	R	1,333
GNDTVNNGGAGDDTVFWFTGDGR	R	2,258
GNGQDNIINGDLGTVVADDTIR	R	2,271
GRDTGMPTLNETR	R	1,447
GTGDDVIAR	R	904
GTNGTVYIPLQPDDPLYVPGGFTNFMVLTR	K	3,283
HIGVDAFGQYDYVLEVNK	R	2,065
HLDPLVADGVTLGIDGVDYLK	R	2,210
HVFDGISGPAEWAGK	R	1,569
IAEAHAAGADLNDLVPDPHPWGLR	K	2,636
IFTTEQQDILR	K	1,363
IQNGGGNDIISGDHWLHVR	R	2,090
IQPAIDPFVFNSSDIDPSIFSEFANVVYR	K	3,389
ISHEFASAVYR	R	1,280
ISISDPDSGGEIATVTTLR	R	1,933
LIANTDLSDPGPDGIR	K	1,767
LIANTDLSDPGPDGIRGTGDDVIAR	K	2,651
LLDGLEGGLATWGQIK	R	1,671
LLSGATDPSTPDFNLLPTLR	R	2,128
LNENDLR	K	873
LNPDGTLR	K	885
MFGDDGDDMLEGGGGFDTVYGGAGNDR	R	2,743
NAAMALVFNTEGAPADR	R	1,763
NDLVR	R	616
NEGMFGFDWATFQNSLDAYADMR	R	2,761
NGLSDTIMDQMK	R	1,353
NIEELEINTRPIGGATVAR	R	2,052
NLVNGHQAFEDDDDTAGAGGVR	K	2,258
NNLLGLPLDLAAINIAR	R	1,791
NNNESHPEYGADEVFIR	R	2,061
NPMSVVNFIAAYGTHETIVAAGNNLQER	K	3,017
NSANGVLAIGGPGTSR	K	1,472
NTGLTGLPEEIFR	R	1,447
PQDVIELAPGATLADYQTSMNGMTK	R	2,768
QYDASGTPTGILIDGSENVIPGITVGDLR	K	2,959
SLFELLVER	K	1,105

SNQLIEDPTGVDPVLEALGLGK	K	2,266
TDHPWPGGQVR	R	1,249
TDPYGEFIR	R	1,097
TGQAIVDGPATNETVIDPVGLAQAYTPGSYLR	R	3,274
TNIHDGSADNIGLIQAFLNPVEFTK	R	2,715
TQGLNLLNELENNAFSK	R	1,906
TVDGAPDSNADR	R	1,217
TVDGTYNLVDGR	R	1,425
TVKPAQMEIVR	R	1,271
VDLWVGGLAEK	R	1,186
VEALSGWNGNDQLFGDDR	K	1,995
VGHSLVGQTMTVIGPDGQPR	R	2,066
VVFTEFADMLIGGIR	R	1,684

ABC-type sugar transport system, periplasmic component (gi|90420899)

AGIQGDIGPK	R	955
APELGGLVEFYR	R	1,350
EGLPVVNEDGTPK	K	1,356
ELQWFVDAAEPYQGMEIK	K	2,155
ESTIRDESFTER	R	1,469
EVTNPGLDDYIGTSFTTAPDGK	K	2,526
GGDTNGPASVYAIK	R	1,478
GIPNGVPVDEWGIR	K	1,509
KEDEKEQPITVNYDELVK	K	2,178
KQWSPTGTNVPDYPK	R	1,718
LNEEQDMEYWVEQAK	K	1,929
LQTQMQSGENIYDAYINDSDLIGTHWR	K	3,168
MAPSPHGVYWVDGMK	R	1,677
NLTDWMEGEGK	R	1,280
QWSPTGTNVPDYPK	K	1,588
SAQEAMDSLCAEQEK	K	1,696
VSHDLIGEGDVVEK	K	1,497
VVSETITTHEYESK	K	1,625

ABC-type branched-chain amino acid transport systems (gi|90420909)

AGSTDFDPVVAALNDGDYTTVIGDLSFDDK	K	3,118
DDQQGEVAGK	R	1,046
DGKYDYVDGAAQ	K	1,301
DYTALVTK	K	910
GDVTLPGYVVYEWK	K	1,625
GLADQTQK	K	859
KNEAAAPVVAELEK	R	1,468
KPALVEAYTAGEK	K	1,377
LSVGDDACDPK	K	1,176
NEAAAPVVAELEK	K	1,340
RPGDGVFR	K	905
TGAEQAVADINAAGGVNGEMLK	R	2,115
YISDNFPDANVAIINDK	K	1,909

twin-arginine translocation pathway signal (gi|90420836)

AADLLEATK	R	931
AANMDLLDEGTLYVAK	R	1,741

DNMPVRPSVVAITK	K	1,527
EEADAANPR	R	972
FDVSKEPNEPNR	R	1,431
FKHEGAESIVAPDGR	R	1,613
MDRPEDIQNETNGR	K	1,771
NAFGHIIIEIAEDGGFAATK	K	2,089
NGWFGMPDNCAVDAEGR	K	1,896
RAADLLEATK	R	1,086
REEADAANPR	K	1,128
TDGLFAVDTEGAAR	R	1,424
WGDPLFADSPEFDPANQTPEAQAR	R	2,659
putative flagellar hook-associated protein FlgK (gi 90418364)		
AALSQFAVSPENGQTAEAAVNAAR	K	2,374
DADDQLDLAAK	K	1,174
DQIVR	R	630
EVIGDVDSPTSPAATLSSLK	R	1,987
GLAGTIQIAAGVDPTKPGGEPAR	K	2,177
IDGVVVAGASSMPIK	K	1,557
IMAGSASGSDVTDVDR	K	1,667
IMAGSASGSDVTDVDRR	K	1,825
KDADDQLDLAAK	R	1,302
SVEFTPQPAYDATVAGNSFK	R	2,129
TQETLSDATGINIDEMTR	R	2,111

Biographical Sketch

I was born in Boulder, CO on February 12th, 1985 at 10:04 a.m. I lived in Boulder until the age of 19, attending Sacred Heart of Jesus School from kindergarten through 8th grade then moving to Boulder High School. During high school I played competitive baseball as a utility player, was an Environmental Club member, learned how to cook, and took part in pranks on the school (appearing on MTV for them). This is where I also developed an interest in science, with intention to go into physical or life science. I enrolled in The Colorado School of Mines where I majored in Chemistry with a minor in Life Sciences. While at CSM, I helped start the campus radio station (Mines Internet Radio), became a part of The Blue Key Honor Society, and started homebrewing. I also performed research with Dr. Kevin Mandernack studying the biological communities associated with an acid mine drainage system in Black Hawk, CO by examination of the community lipid profiles. This is where I learned how to perform high-level research and when I decided I wanted to pursue graduate school. Dr. Mandernack steered me towards the Oregon Health and Science University and Dr. Brad Tebo. At OHSU, I developed my research ability and learned what it means to be a scientist. I may not have been the best student, but I've enjoyed every moment being in the lab. Outside of the lab, I further cultivated my interests in cooking, home fermentation, music, and bicycling. In October 2011, I will be starting a temporary position with Cardno ENTRIX as an economic research technician examining aerial photography of the Gulf Coast to aid in assessment of the economic impact of the BP Deep Horizon oil spill. In the future, I hope to pursue a career in the diabetes field to help those afflicted with the disease that I have come to know very personally, with both my mother and myself having type I diabetes.